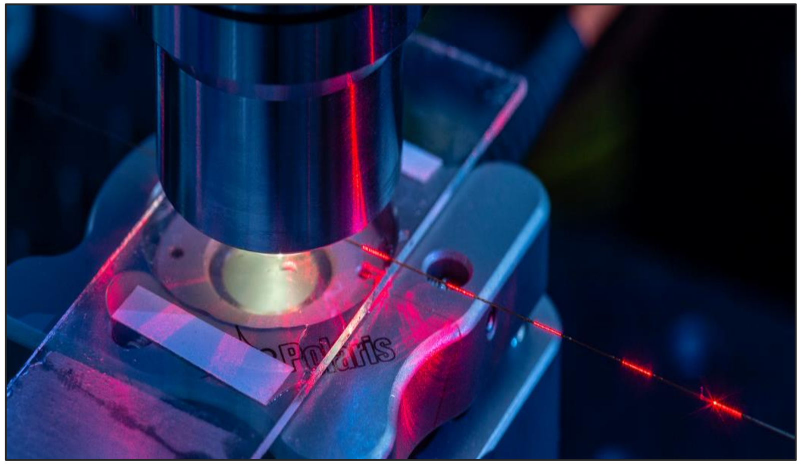

Insight on optical fiber sensing and instrumentation

CEA List LSPM *Lab. Systems and Photonics for Monitoring*

Dr Sylvain Magne

sylvain.magne@cea.fr

Training Week #1 (January 15-19, 2024)

SUMMARY

- CEA as a glance
- LIST/DIN/SMCD/LSPM
- Optical fibers : basics
- Optical fibers for telecommunications
- Optical fibers for sensing in harsh environments
- Point sensing : White-Light Interferometry (WLI)
- Quasi-distributed sensing : Fiber Bragg Gratings (FBGs)
- Truly distributed sensing : OTDR DTS, BOTDR/BOTDA, OFDR, FMCW, DAS
- MSCA USES2 DC02 : OPTICAL TIME STRETCH (OTS)

CEA at a glance ...

CEA
Atomic Energy Commission

DRF Fondamental research

DES Nuclear energy (civil)

DAM Military applications

DRT Technological research

LETI | ~~**LITEN**~~ | **LIST**

DIN

Breaking news ! …

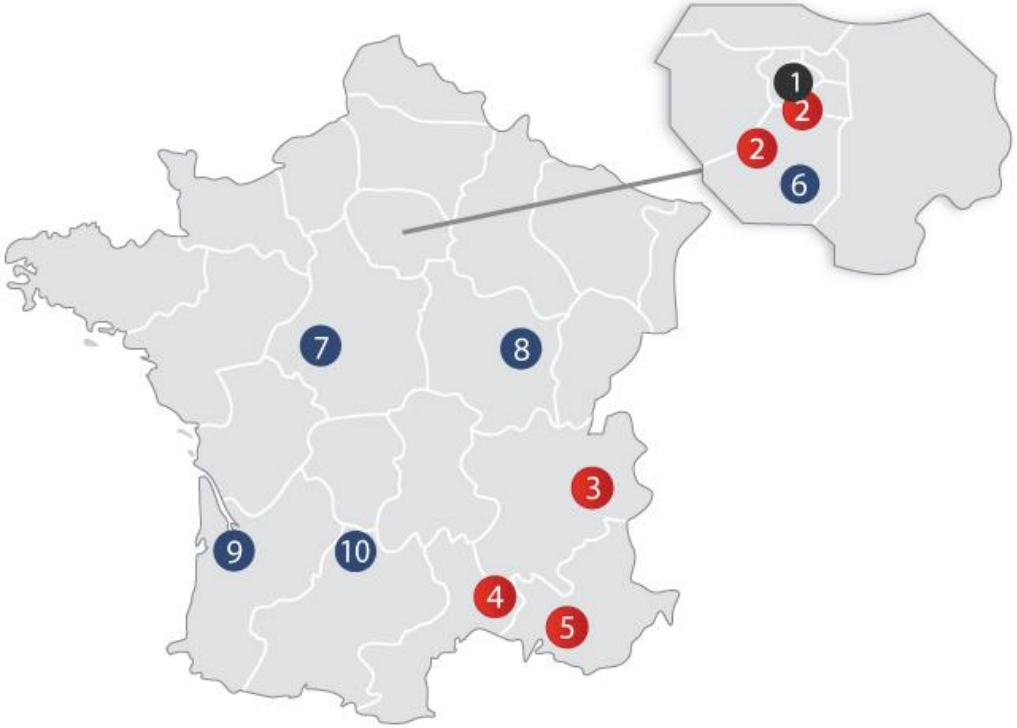

1 SIÈGE SOCIAL

CENTRES D'ÉTUDE CIVILS

2 Paris-Saclay
établissements de Fontenay-aux-Roses
et de Saclay

3 Grenoble

4 Marcoule

5 Cadarache

CENTRES POUR
LES **APPLICATIONS MILITAIRES**

6 DAM Ile-de-France

7 Le Ripault

8 Valduc

9 Cesta

10 Gramat

LSPM Lab. Systems and Photonic for Monitoring

The Team

30 Researchers

Lasers, OFS, Bragg, 3D printing for Photonic
Ultrasonic guided wave, Algorithm & Tomography
Instrumentations, Embedded Systems, SHM

Main Equipments

3 Platforms

Sachems, FemtoBragg, TowerBragg

Sachems
Acoustic Emission fiber-based system, Impact, DAQ,

FemtoBragg [3 laser Labs]
KrF, Co2, 4 femtos →1030/800/515/400/266/248 nm
Txwo Photon Polymerization 3D printing system

TowerBragg [CEA/CNRS/Univ Lille]
Draw tower, MCVD/OVD, Automated Bragg station

LSPM
Team/Equipment
Topics

Lasers Processes & Innovative Sensors

Advanced Photonic devices, Start up *Myriad4Sensing*
3D printing for photonic, Biosensing
Tranducers (PZT, Bragg, Rayleigh)

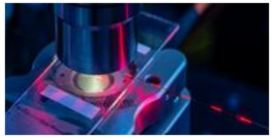

SHM for Harsh Environment

High T°, Radiations, Integration, Testing
Energies, Oil & Gas, Aero, Nuclear Energy, Defense

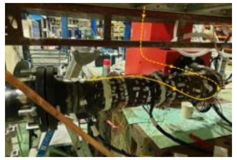

Data Processing for Monitoring/SHM

Active/Passive Tomography, Acoustic Emission
High speed optical spectrum analysis (Bragg sensors)

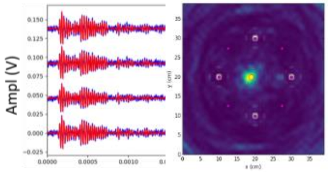

Embedded Instrumentations

Electronic and Embedded IA codes, Monitoring systems
Autonomous and Communicating sensors nodes

Monitoring For Additive Manufacturing

In situ machine monitoring, SHM
Temperature/Strain/Acoustic, Metal/Ceramic/Glass

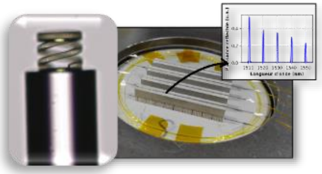

SUMMARY

- CEA as a glance
- LIST/DIN/SMCD/LSPM
- Optical fibers : basics
- Optical fibers for telecommunications
- Optical fibers for sensing in harsh environments
- Point sensing : White-Light Interferometry (WLI)
- Quasi-distributed sensing : Fiber Bragg Gratings (FBGs)
- Truly distributed sensing : OTDR DTS, BOTDR/BOTDA, OFDR, FMCW, DAS
- MSCA USES2 DC02 : OPTICAL TIME STRETCH (OTS)

Optical fibers : basics

Optical fibers are cylindrically-symmetric
Ultra-pure silica is the main material (refractive index (RI) ~1.46 [@1.55 µm]),

Fibers are also made from PMMA, PS, PC, fluoride, chalcogenide glasses, etc.

Waveguiding (in the core) provided by total internal reflection : Step index or Graded-Index (GRIN)

Waveguiding in Bragg photonic crystal is also possible, very exotic …

Core doped with GeO_2, P_2O_5 (RI ↗)
Cladding doped with F or B_2O_3 (RI ↘)
Buffer coating serves as protection against abrasion and shear stress

Usually in polymer (acrylate, polyimide)
Possibly carbon, metallic (copper, aluminum, gold) or ceramic (ormocer)

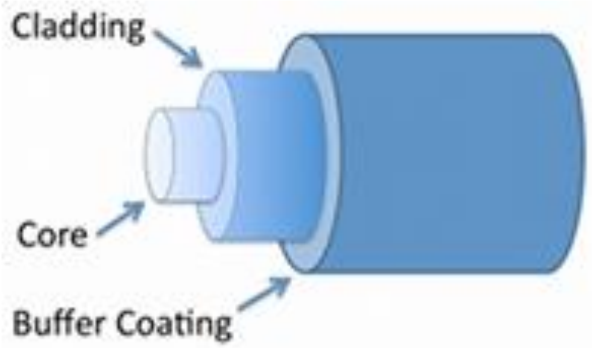

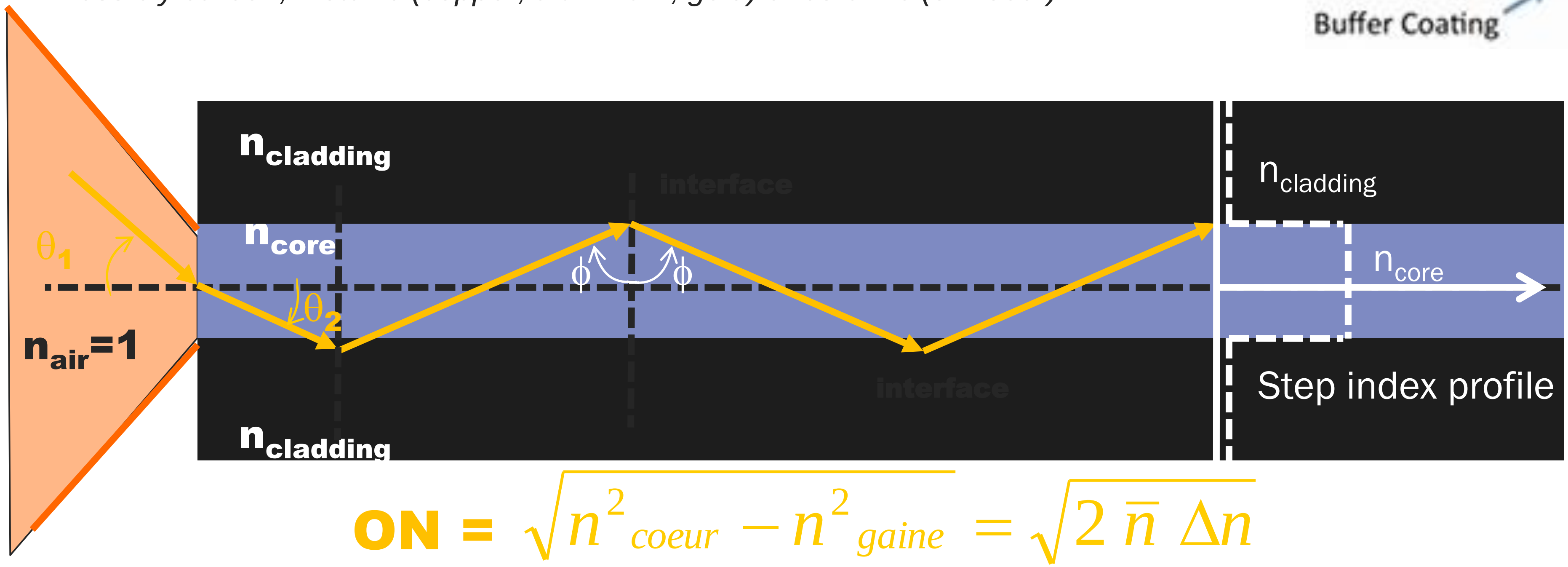

$$\text{ON} = \sqrt{n^2_{coeur} - n^2_{gaine}} = \sqrt{2\,\bar{n}\,\Delta n}$$

Brief history of optical fibers

1966	First experimental demonstration of optical fiber communication (Charles Kao, George Hockham)		
1970	20 dB/km	λ=850 nm	First manufacturing of low-loss optical fibers by Corning Glass Works using the MCVD (Modified Chemical Vapor Deposition) method (D. Keck, R. Maurer, P.C. Schultz)
Those first large-core fibers were highly multimodal, imposing a strong limitation in data rate (mode-dispersion limited) First tentative to design optical fibers in the Near Infra-Red (NIR), in order to reduce loss Singlemode fibers (1990-2000) were designed to eliminate MD and increase data rate.			
1974	2 – 3 dB/km	λ=1060 nm	ATT, Bell Labs
1976	0,47 dB/km	λ=1200 nm	NTT, Fujikura
1979	0,2 dB/km	λ=1550 nm	NTT
1986	0,15 dB/km	λ=1550 nm	Sumitomo
2002	0,148 dB/km	λ=1570 nm	Sumitomo

C. Kao, G. Hockham, Nobel prize 2009

K.C. Kao, G.A. Hockham, Dielectric-fibre surface waveguides for optical frequencies, *Proc. IEE*, 1113(7), 1966, pp. 1151-1158.
D.B. Keck, R.D. Maurer, P.C. Schultz, On the ultimate limit of attenuation in glass optical waveguides, *Appl. Phys. Lett.* 22(7), 1973, 307-309.

SingleMode Fibers (SMF)

Core diameter = 2a ~ 9.2 µm
Cladding diameter = 125 µm (± 1 µm)
NA ~ 0.1 to 0.12

N.B. : Polarization-Mode Dispersion (PMD) also plays a role (neglected at first approach)

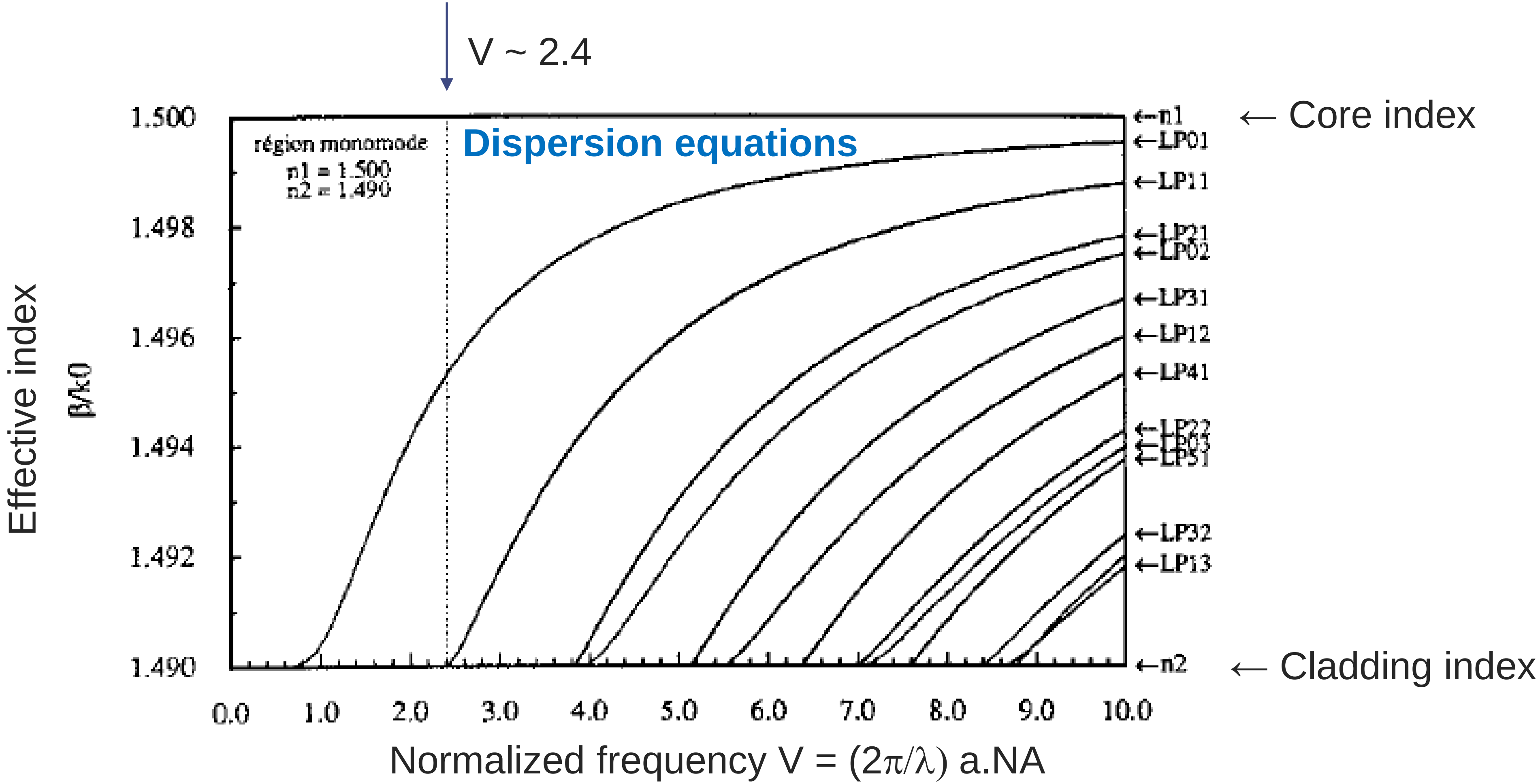

Transmission is strongly dependent on glass purity

Transmission at 1.55 µm

Matière première	VERRES	ABSORPTION en dB/km	IMPURETES Contenues dans le verre	1% d'énergie transmise (dans le proche infrarouge) sur :
Bon marché	BOUTEILLES	2.000.000	10kg/tonne	1 cm
	VITRES	200.000	1kg/tonne	10 cm
Sélection	LUNETTES	20.000	100g/tonne	1 m
Pures, traitées	OPTIQUE	2.000	10g/tonne	10 m
Ultra-pures	VERRES SODOCALCIQUES ou BOROSILICATES	20	100mg/tonne	1 km
	VERRES DE SILICE	0,2	10mg/tonne	100 km

POUR FIBRES OPTIQUES

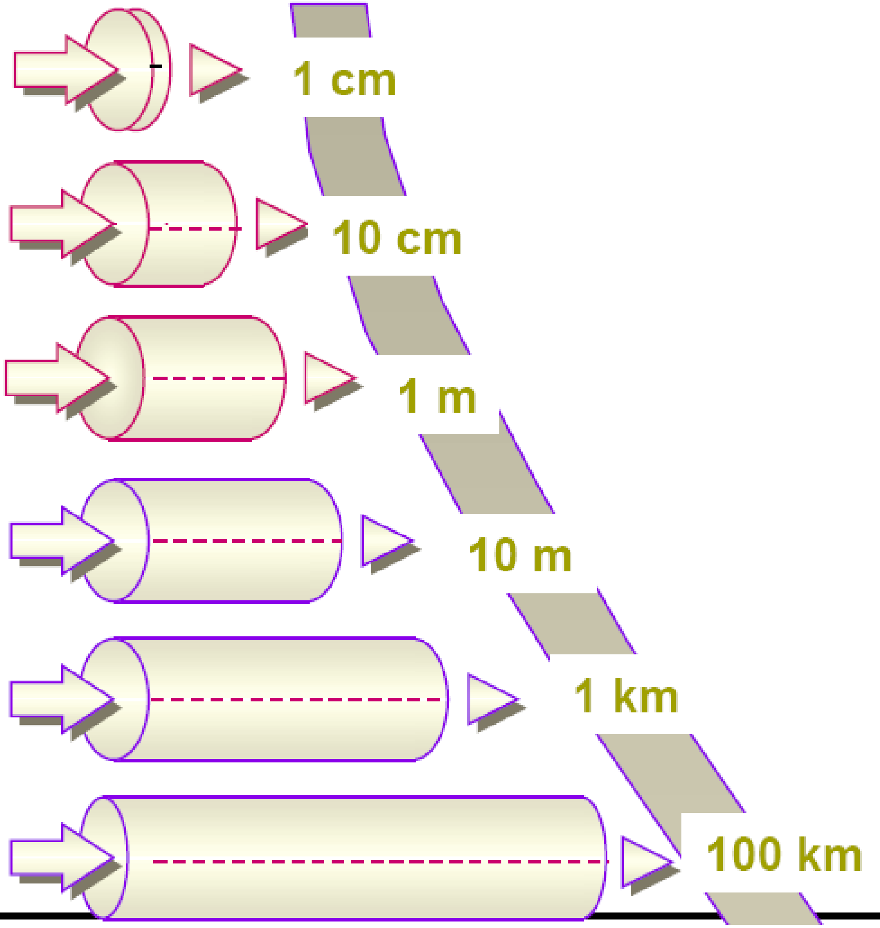

Fiber transmission is also wavelength-dependent

Light loss in fiber is due to both absorption and scattering
Minimum of attenuation ~ 0.2 dB/km (at 1.55 µm)

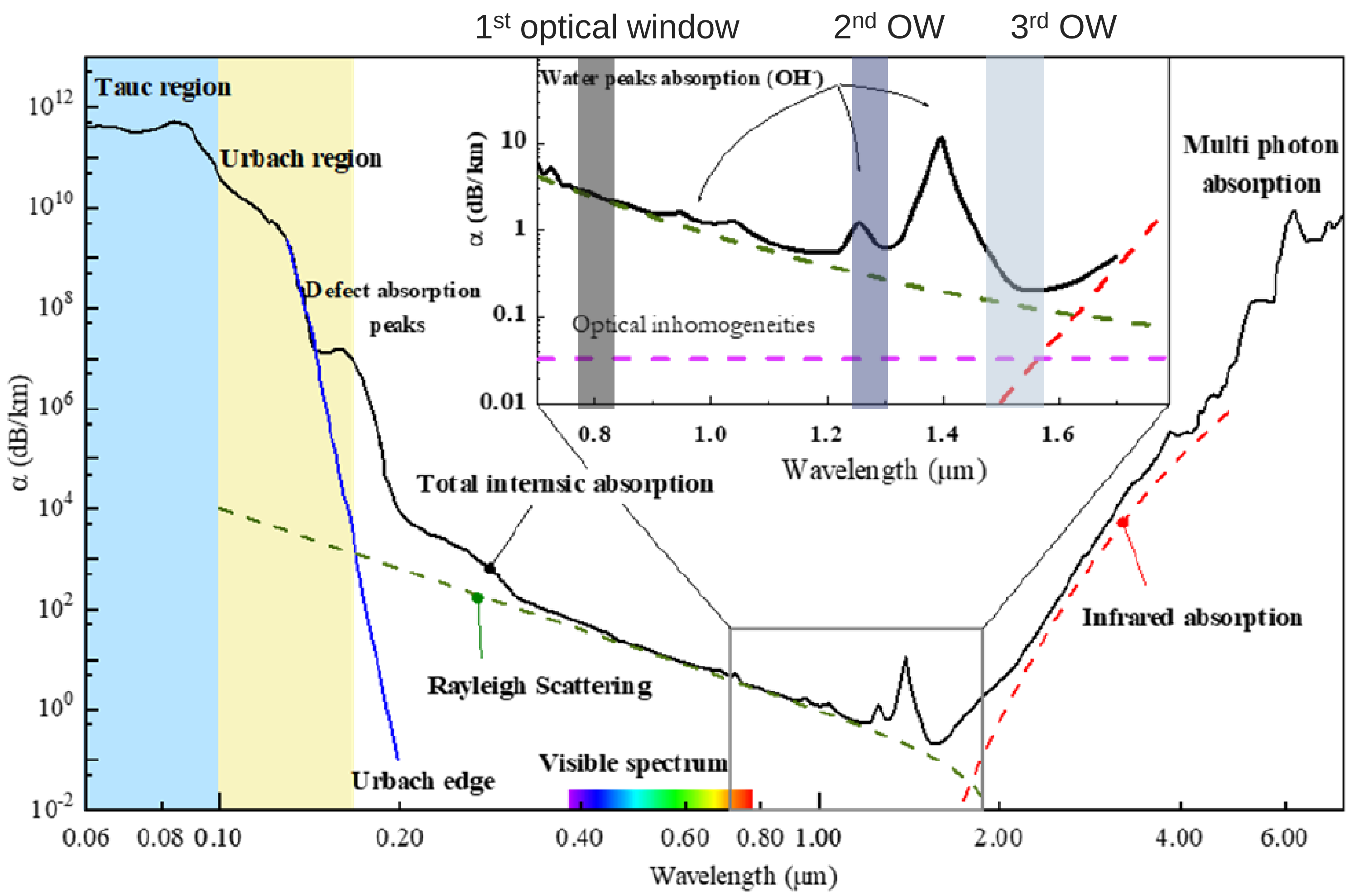

J. Hecht, the story of fiber optics, Oxford, 1999

SUMMARY

- CEA as a glance
- LIST/DIN/SMCD/LSPM
- Optical fibers : basics
- **Optical fibers for telecommunications**
- **Optical fibers for sensing in harsh environments**
- **Point sensing : White-Light Interferometry (WLI)**
- **Quasi-distributed sensing : Fiber Bragg Gratings (FBGs)**
- **Truly distributed sensing : OTDR DTS, BOTDR/BOTDA, OFDR, FMCW, DAS**
- **MSCA USES2 DC02 : OPTICAL TIME STRETCH (OTS)**

Optical fibers for telecommunications (… and sensing)

Chromatic dispersion (CD)

Two contributions : material dispersion and waveguide dispersion
Material-induced dispersion is zero at 1.3 µm (2nd OW), $\rightarrow$ 17 ps/nm.km in SMF-28 fibers (@1.55 µm)
CD may be compensated for by waveguide dispersion $\rightarrow$ dispersion-shifted (DS) fibers,
e.g. to cancel CD at 1.55 µm (3rd OW).

Standardized fibers : G651 (MM), **G652** (CD 0 @ 1,3 µm), … G655/656 (DS @1,55 µm), **G657** (*bend-insensitive*).

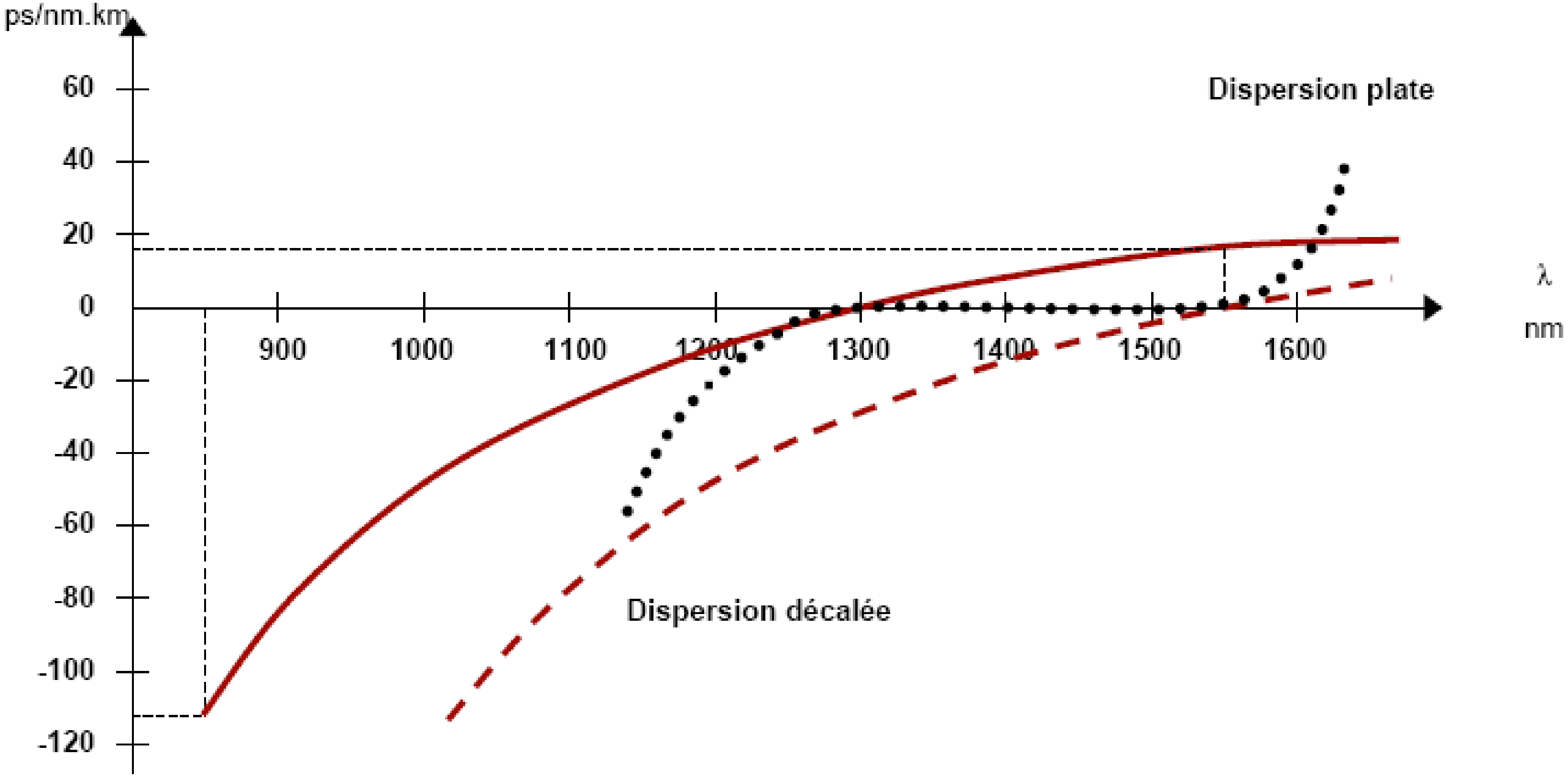

SMF made internet possible …

ITU Grid in C-band : 1520.25 nm (197.2 THz) → 1577.03 nm (190.1 THz)
Dense Wavelength-Division Multiplexing (DWDM) : 100 GHz channel spacing (~0.4 nm)
72 channels in C-band, each carrying 10 Gbits/s coded data … (720 Gbits/s)
Over a distance of 50 km or more … (between each optical amplifier)

Since then, other bands were opened : C+L-band, S-band, etc …

In fiber sensing, we use all devices and tools developped/standardized for optical telecommunications … (IEC 60793)

Initially anecdotic in the 80s, fiber sensing is now taking a significant part of the fiber market
OFS market share = 1.3 BUSD/year (continuous grow since 2000).

M.F. Bado, J.R. Casas, A review of recent distributed OFS applications for civil engineering SHM, *Sensors*, 21, 1818-1901 (2021)

(ITU : International Telecommunication Union, IEC : International Electrotechnical Commission)

SUMMARY

- CEA as a glance
- LIST/DIN/SMCD/LSPM
- Optical fibers : basics
- Optical fibers for telecommunications
- Optical fibers for sensing in harsh environments
- Point sensing : White-Light Interferometry (WLI)
- Quasi-distributed sensing : Fiber Bragg Gratings (FBGs)
- Truly distributed sensing : OTDR DTS, BOTDR/BOTDA, OFDR, FMCW, DAS
- MSCA USES2 DC02 : OPTICAL TIME STRETCH (OTS)

Optical fiber sensing – what makes them so attractive ?

Fibre

- Small volume and mass
- EM/lightning insensitive
- Low loss (~ 0,22 dB/km @ 1,55 µm),
- Remote sensing, up to tens of km (even more with EDFAs)
- Flexibility,
- Withstand high temperature, chemical & radiative environments,
- Passive sensing (no electronics in the sensor head), ATEX-compatible
- High strain/Temperature/Pressure range

Readout

- High performance
- Multi-parameter sensing
- High capacity (WDM, TDM, FMCW, …)

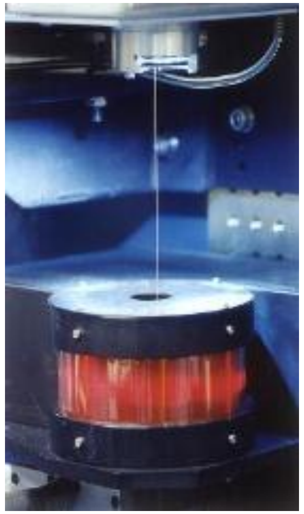

⇨ Optical sensing is used for monitoring in harsh environments, in substitution to electronic devices (*e.g.* high T°, high EM fields)

⇨ Optical sensing provides distributed monitoring (several thousands of meas^{t} points/fibre) (typical optical feature).

Optical fiber sensing for monitoring in harsh environments

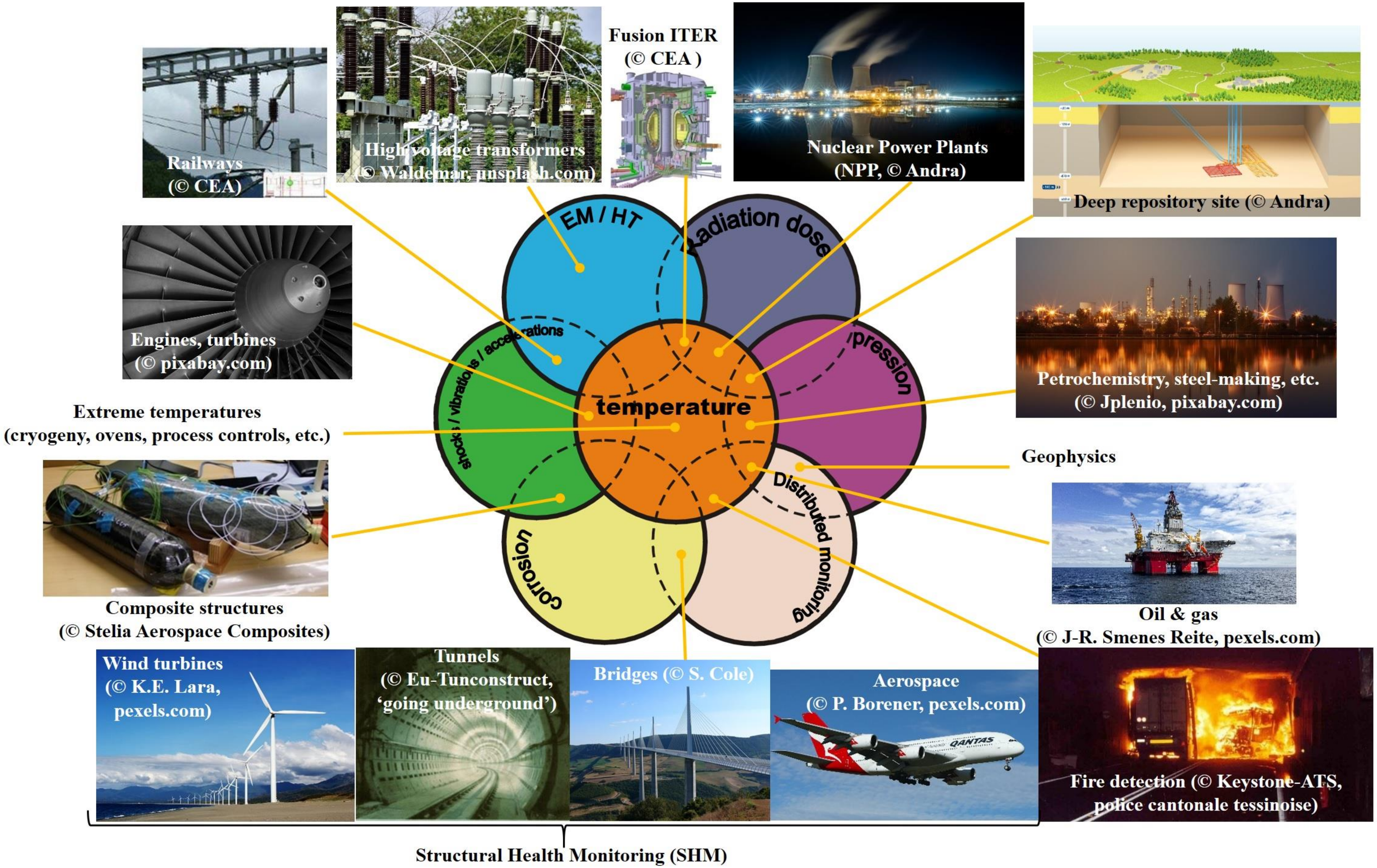

OFS may be classified into 3 categories

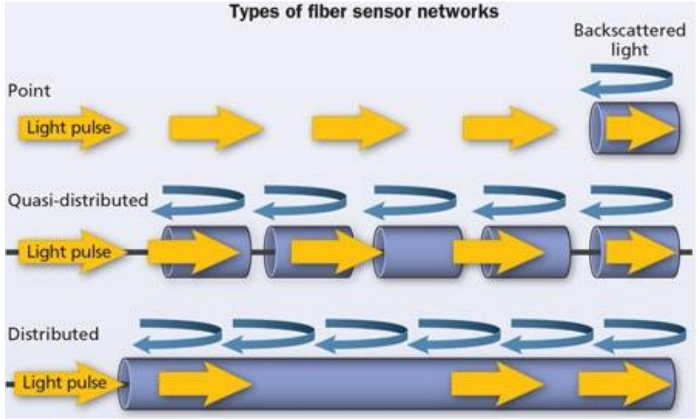

Distributed measurements

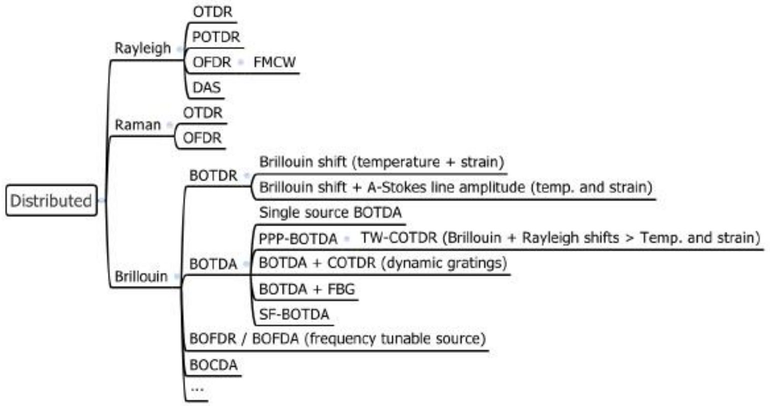

OTDR: Optical Time Domain Reflectometry; POTDR: Polarization OTDR; DAS: Distributed Acoustic Sensor; OFDR: Optical Frequency Domain Reflectometry; FWCW: Frequency Modulated Continuous Waves; BOTDR: Brillouin OTDR; BOTDA: Brillouin Optical Time Domain Analyzer; PPP-BOTDA: Pre–Pulse-Pumping-BOTDA; COTDR: Coherent OTDR; TW-COTDR: Tunable Wavelength-COTDR; SF-BOTDA: Sweep Frequency-BOTDA; BOFDR: Brillouin OFDR; BOFDA: Brillouin Optical Frequency Domain Analyzer; BOCDA: Brillouin Optical Correlation-Domain Analyzer.

TDM: Time Domain Multiplexing; PGC: Phase Generating Carrier; FBG: Fiber Bragg Grating; LPG: Long Period Grating; FP: Fabry-Perot; IPFI: Intrinsic Fabry-Perot Interferometer; EPFI: Extrinsic Fabry-Perot Interferometer; POF: Plastic Optical Fiber

Point or Quasi-distributed measurements

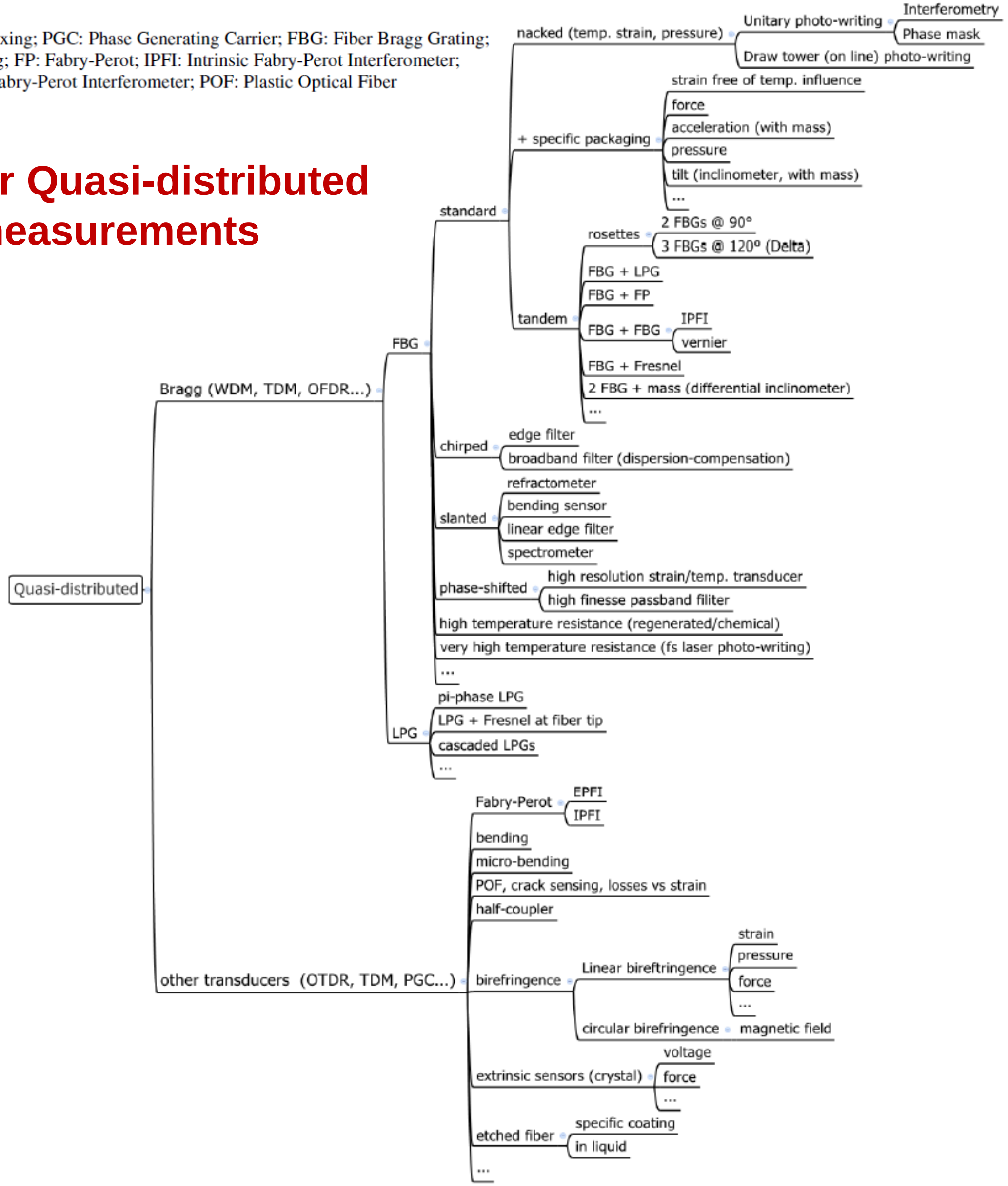

(P. Ferdinand, EWSHM 2014, Nantes, France)

SHM with OFS : Further reading

S. Abbas, F. Li, J. Qiu, A review on SHM techniques and current challenges for characteristic investigation of damage in composite material components of aviation industry, *Mater. Perf. Charact.*, 7(1), 2018, pp. 224-258.

M.F. Bado, J. R. Casas, A review of recent distributed OFS applications for civil engineering SHM, *Sensors*, 21, 2021, pp. 1818-1901.

R. Di Sante, Fiber Optic Sensors for SHM of aircraft composite structures: recent advances and applications, *Sensors* 15, 2015, pp. 18666-18713.

P. Ferdinand, The evolution of OFS technologies during the 35 last years and their applications in SHM, *7th Eur. Workshop on SHM (EWSHM),* 2014, Nantes (France).

I. Garcia, J. Zubia, G. Durana, G. Aldabaldetreku, M.A. Illarramendi, J. Villatoro, OFS for Aircraft SHM, *Sensors,* 15, 2015, pp. 15494-15519.

A. Guemes, A., Fernando-Lopez, A., Renato Pozo, J. Sierra-Pérez, J., SHM for advanced composite structures: a review, *J. Compos. Sci.* 4(13), 2020, pp. 4010013.

J.M. Lopez-Higuera, L. Rodriguez Cobo, A. Quintela Incera, A. Cobo, Fiber Optic Sensors for SHM, *J. Lightwave Technol.* 29(4), 2011, pp. 587-608.

M. Majumder, T.K. Gangopadhyay, A.K. Chakraborty, K. Dasgupta, D.K. Bhattacharya, FBGs in SHM – present status and applications, *Sens. Actuators A* **147**, 2008, pp. 150-164.

SUMMARY

- CEA as a glance
- LIST/DIN/SMCD/LSPM
- Optical fibers : basics
- Optical fibers for telecommunications
- Optical fibers for sensing in harsh environments
- **Point sensing : White-Light Interferometry (WLI)**
- **Quasi-distributed sensing : Fiber Bragg Gratings (FBGs)**
- **Truly distributed sensing : OTDR DTS, BOTDR/BOTDA, OFDR, FMCW, DAS**
- **MSCA USES2 DC02 : OPTICAL TIME STRETCH (OTS)**

White-Light Interferometry (1/2)

Broadband source → low coherence length (~ 10 µm)

Interference figure appears
where time delay is compensated.

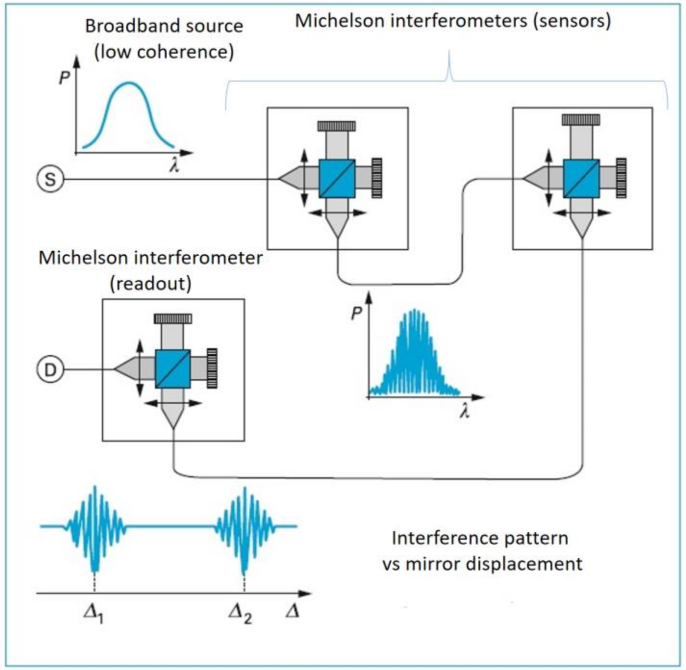

P. Ferdinand, Tech. De l'Ing., R460, 2020

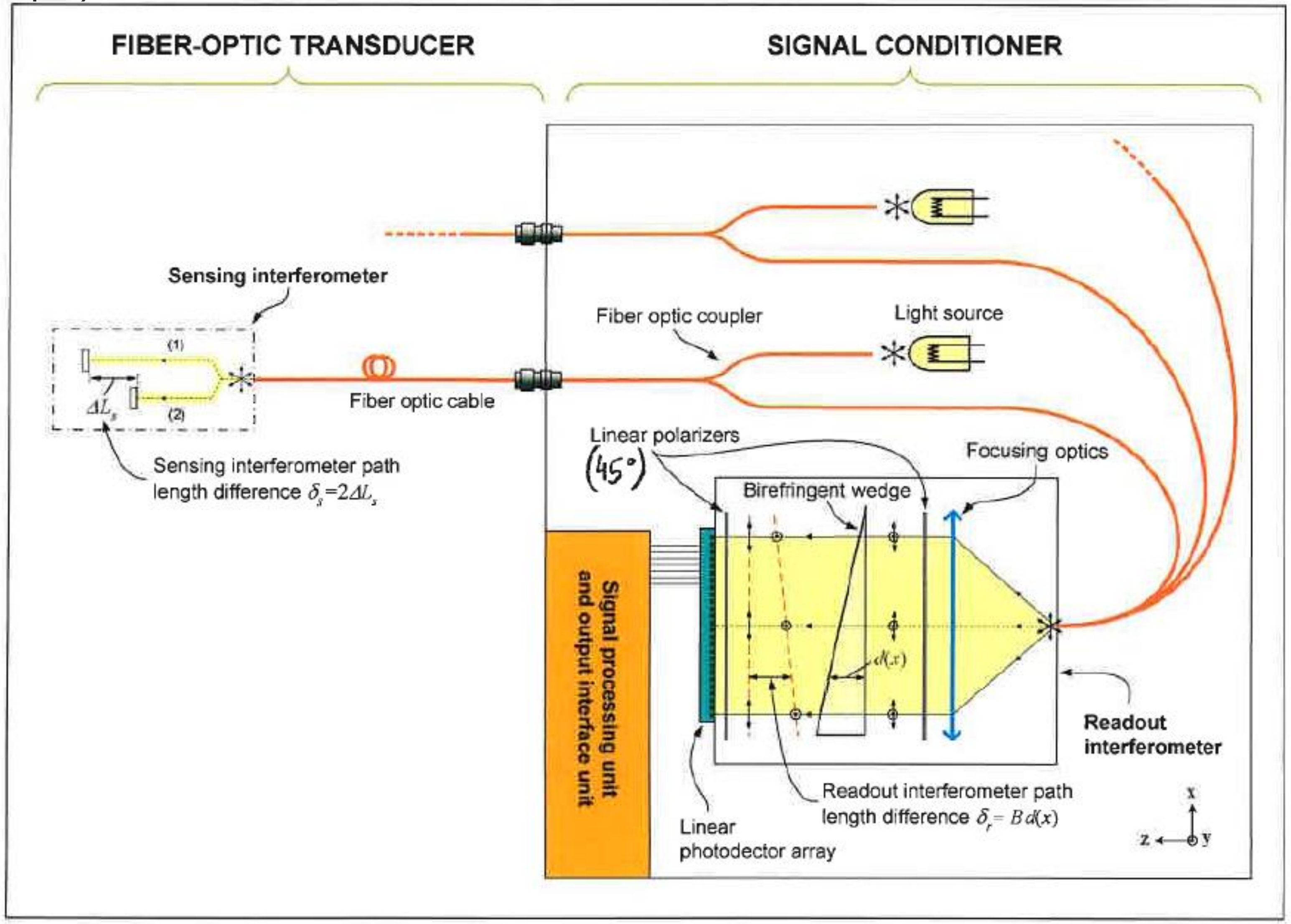

White-Light Interferometry (2/2)

SOFO long-base extensometers (Smartec, first bought by Micron Optics, bought again by Luna)

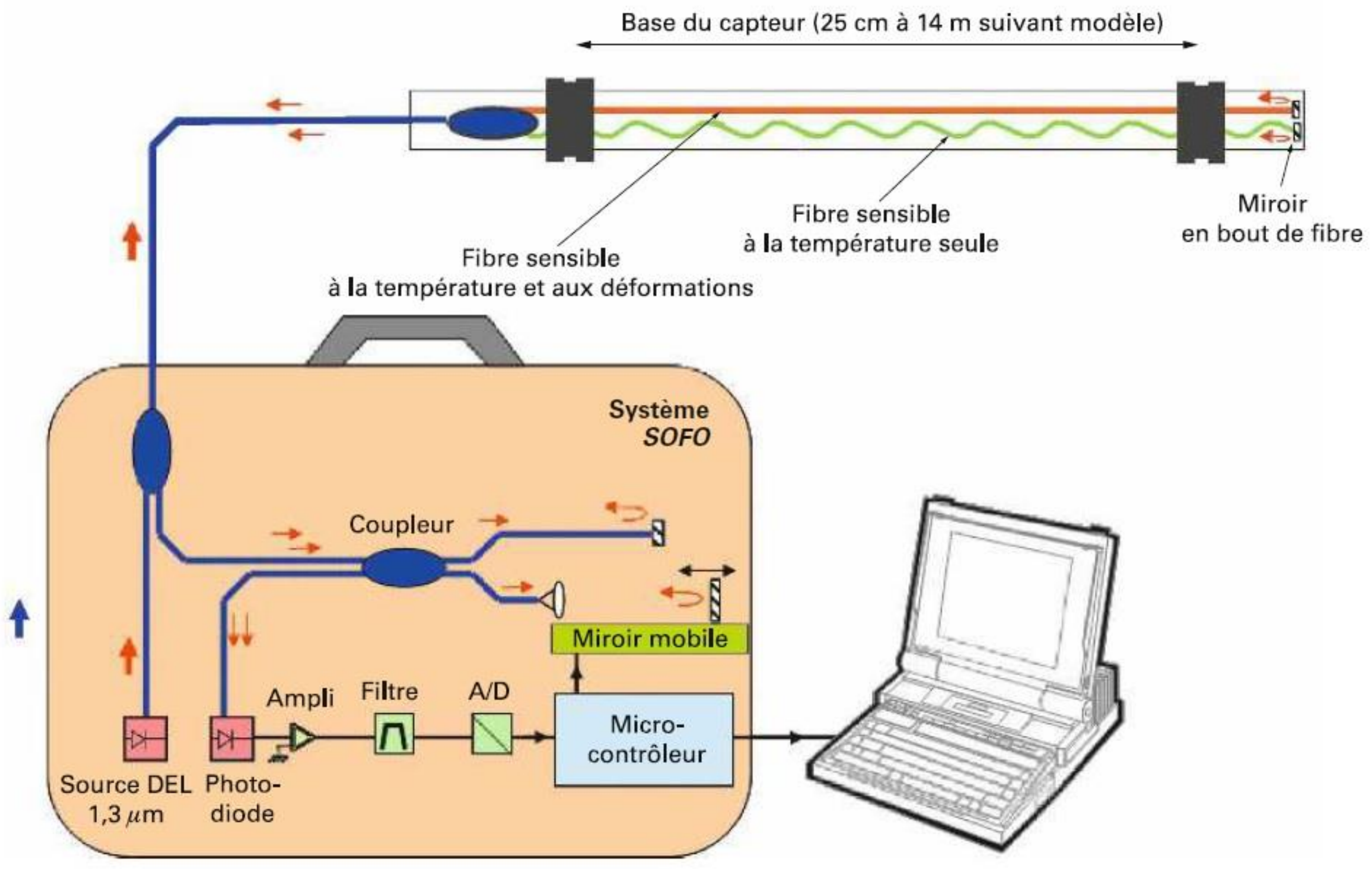

→ Absolute measurement
→ Autocompensated temperature effects

But … usually single point measurement
(coherence multiplexing is strongly limited in capacity …)

D. Inaudi *et al.*, Low-coherence deformation sensors for the monitoring of civil-engineering structures, Sens. & Act. A, 44, 1994, pp. 125-130

SUMMARY

- CEA as a glance
- LIST/DIN/SMCD/LSPM
- Optical fibers : basics
- Optical fibers for telecommunications
- Optical fibers for sensing in harsh environments
- Point sensing : White-Light Interferometry (WLI)
- **Quasi-distributed sensing : Fiber Bragg Gratings (FBGs)**
- **Truly distributed sensing : OTDR DTS, BOTDR/BOTDA, OFDR, FMCW, DAS**
- **MSCA USES2 DC02 : OPTICAL TIME STRETCH (OTS)**

Fiber Bragg Gratings : basics

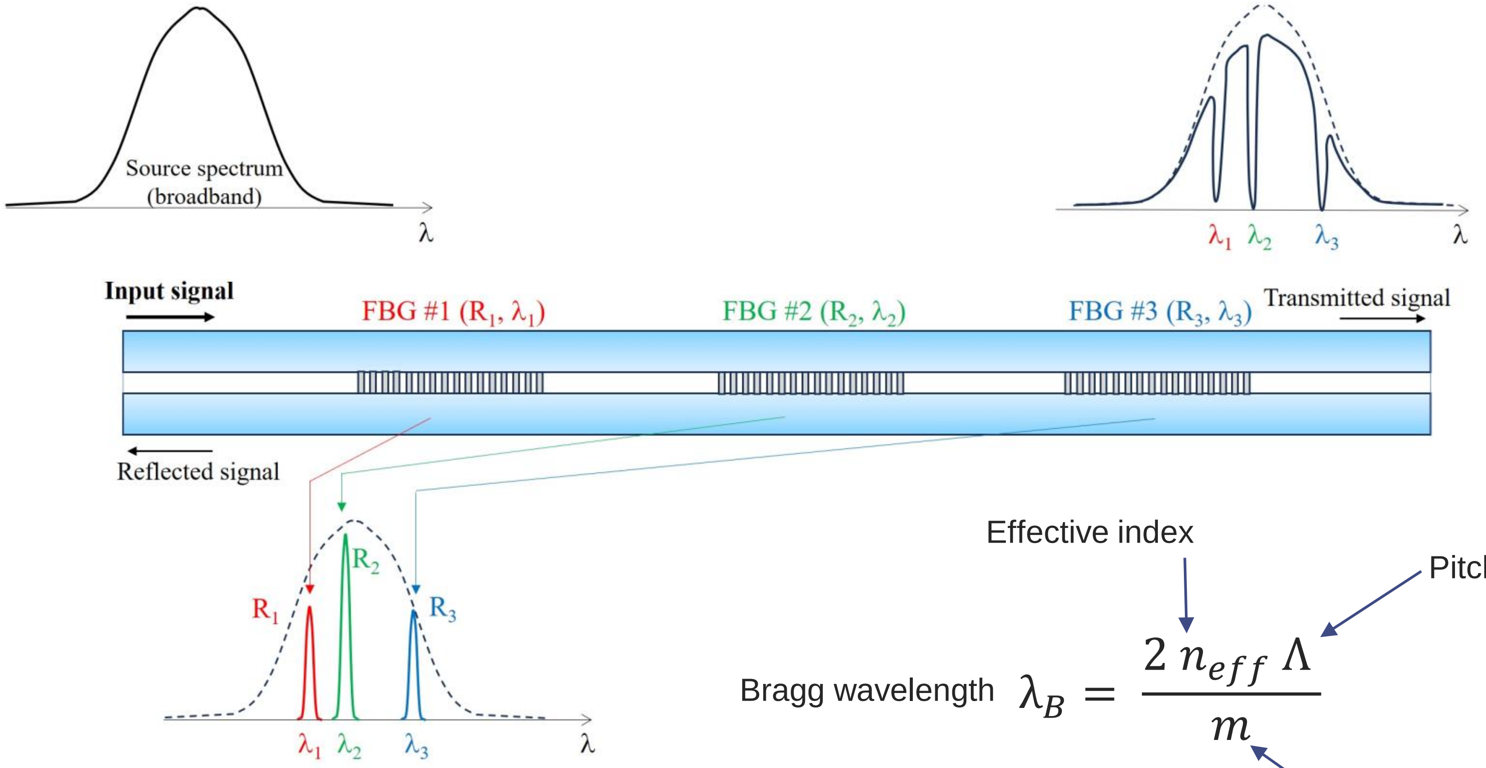

Effective index

Pitch

Bragg wavelength $$\lambda_B = \frac{2\, n_{eff}\, \Lambda}{m}$$

Diffraction order

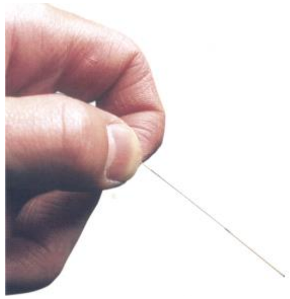

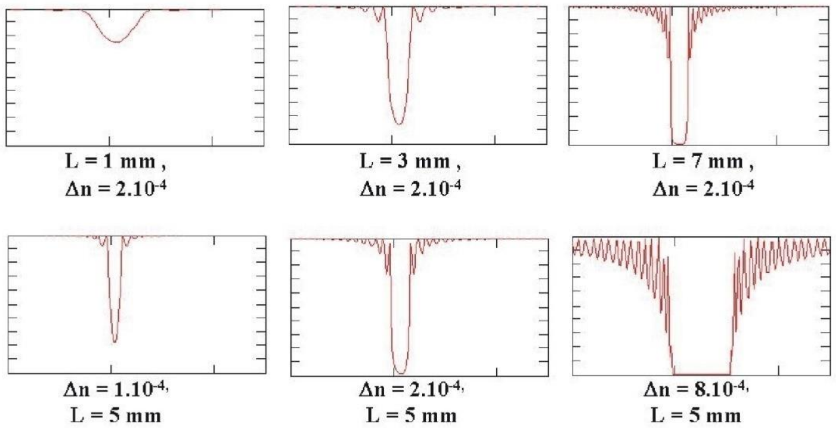

Some FBG examples …

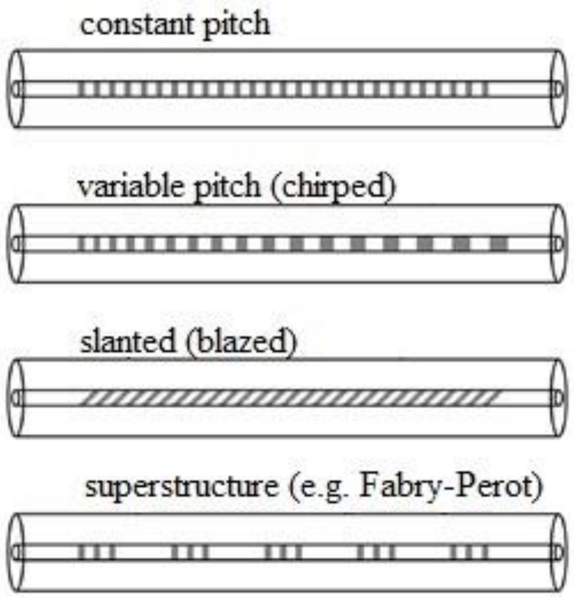

FBG for sensing

Primary parameters : strain, direct pressure, temperature, external refractive index

Secondary parameters : indirect pressure, force, inclinometry, extensometry, displacement, shock/vibration, radiation dose, liquid level, magnetic/electric fields, shape, …

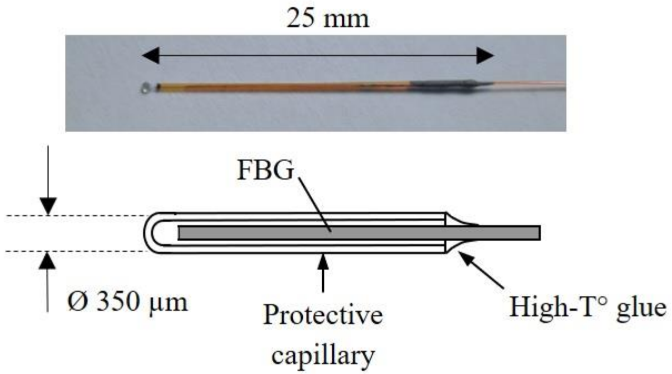

FBG thermal sensor
(for temperature compensation in composite materials)

FBG inclinometer (© CEA)

Short-Gage FBG extensometers (© CEA)

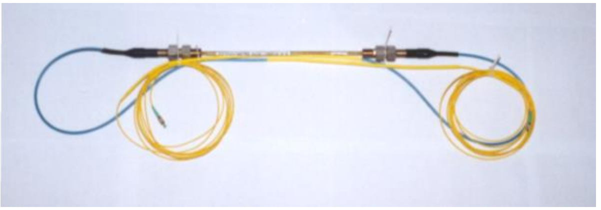

Long-Gage FBG composite extensometers (© CEA)

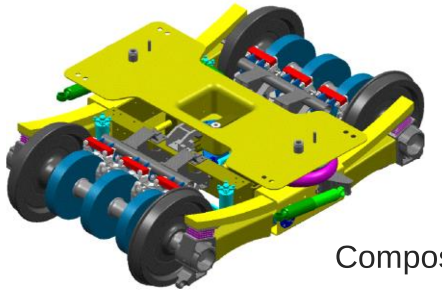

Composite bogie (Alstom)

Pressure sensors (© CEA)

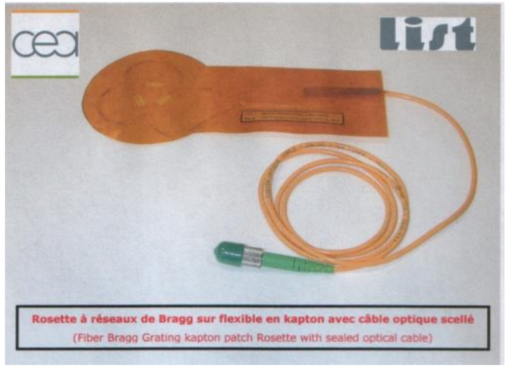

FBG for strain, T° and pressure monitoring

Temperature

$$\frac{\Delta\lambda_B}{\lambda_B} = \left(\alpha_f + \xi\right)\cdot\Delta T$$

$$\xi = \frac{1}{n}\cdot\frac{\partial n}{\partial T}$$

$\alpha_f \sim 5\ 10^{-7}\ K^{-1}$
$\xi \sim 7$ to $8\ 10^{-6}/K^{-1}$

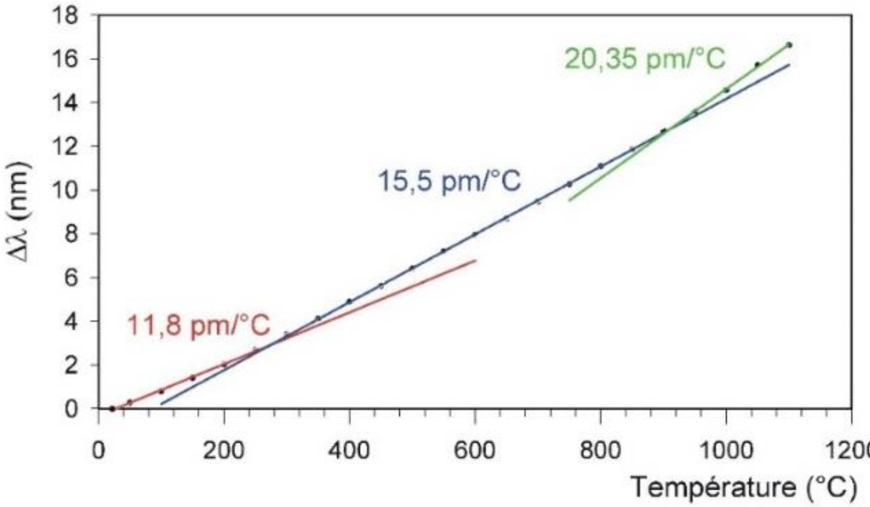

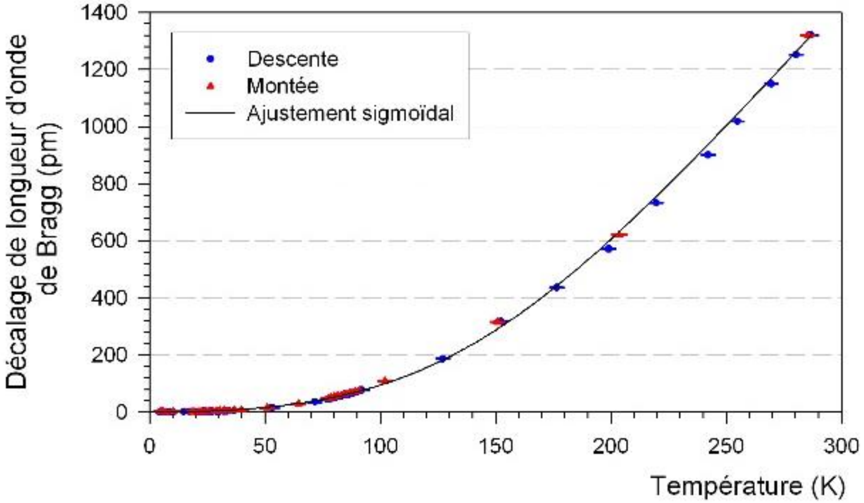

Strain/Pressure

$$\frac{\Delta\lambda_B}{\lambda_B} = (1-p_e)\cdot\Delta\varepsilon_z = \left[1-\frac{1}{2}\cdot {n_r}^2\cdot[p_{12}\cdot(1-\nu)-p_{11}\cdot\nu]\right]\cdot\Delta\varepsilon_z$$

$$\frac{\Delta\lambda_B}{\lambda_B} = -(1-2\nu)\cdot\left[1-\frac{1}{2}\cdot {n_r}^2\cdot[2\cdot p_{12}+p_{11}]\right]\frac{\Delta P}{E}$$

Sensitivities (according to stress application, @1.55 µm)

$K_H \sim$ -3,5 pm/MPa $\quad K_R \sim$ -35 pm/(N.mm^{-1}) $\quad K_L \sim$ 1,2 pm/(µm/m)

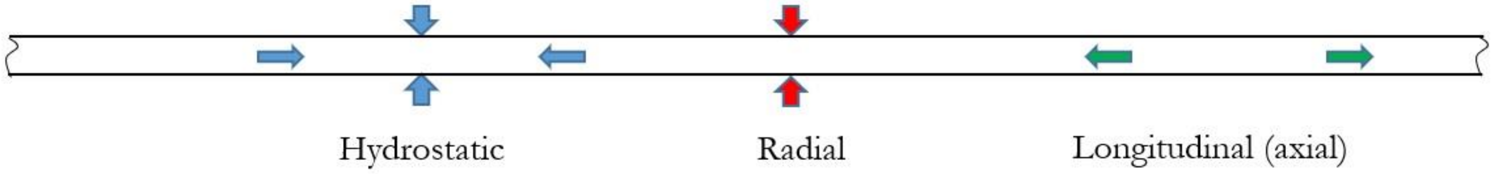

N.B. : Sensitivities are the same for FBG and OFDR monitoring techniques

FBG photo-inscription processes

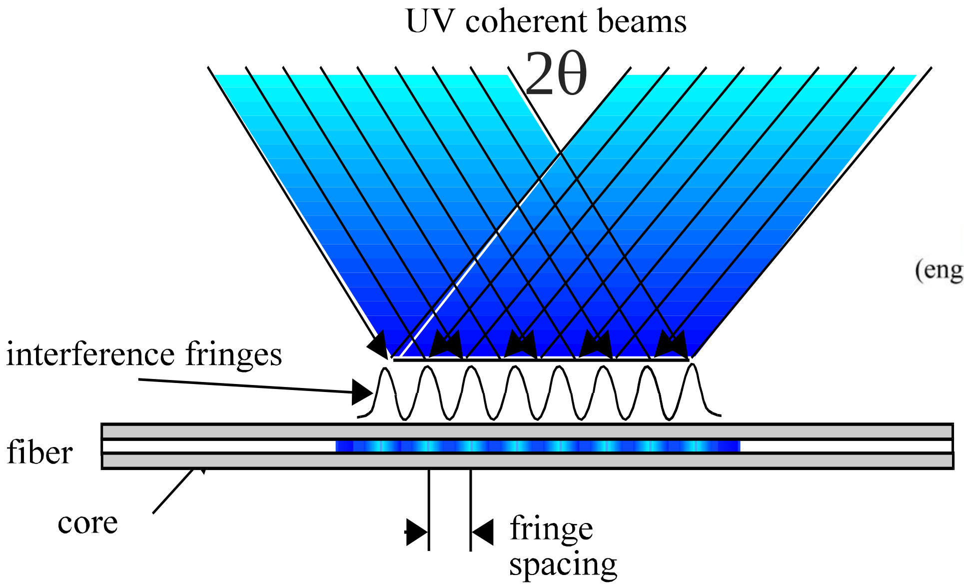

(1) Holographic (Lloyd mirror)

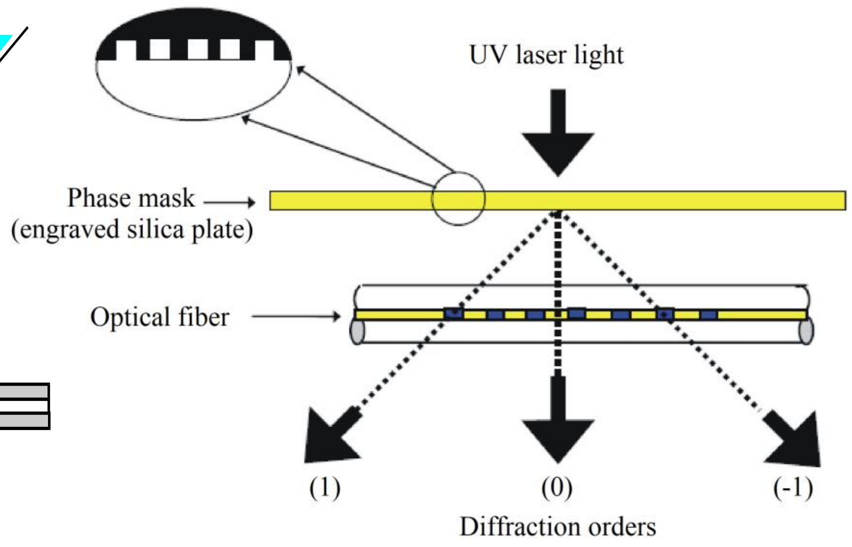

(2) Phase mask

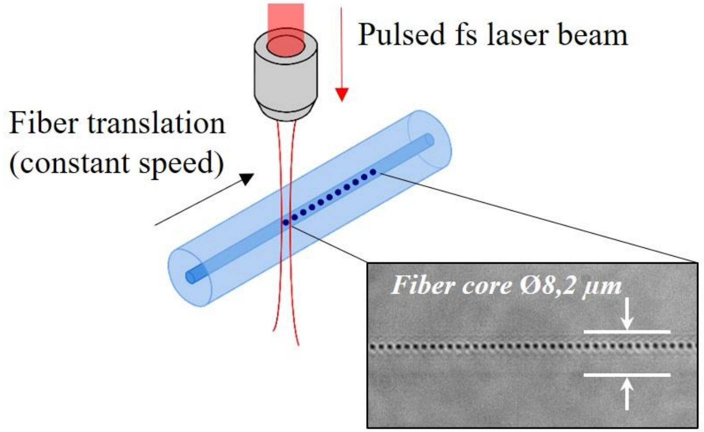

(3) Point-by-point (PbP)
Line-by-Line (LbL)

(4) Talbot setup [hybrid of (1) and (2)]

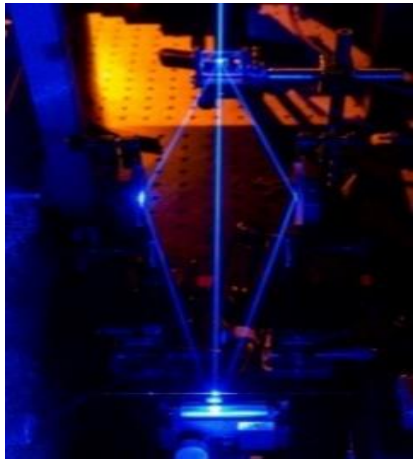

FBG photo-inscription with femtosecond lasers

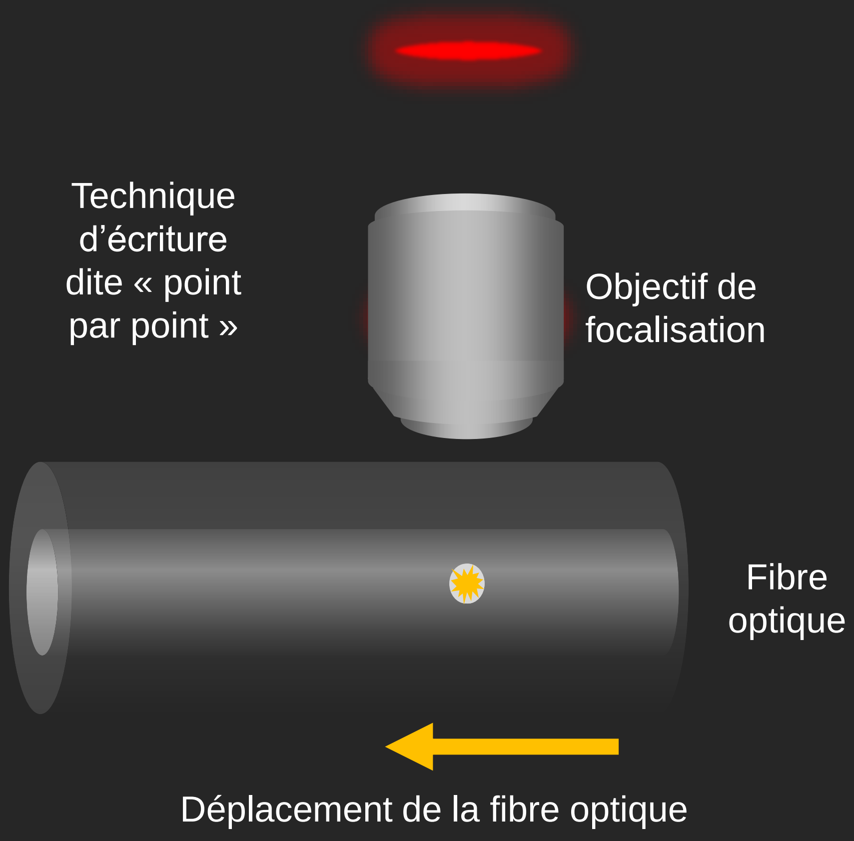

Laser PHAROS
λ_{LASER} = 1030nm / 515nm
$f_{IMPULSION}$ = 1MHz
$E_{IMPULSION}$ = 1mJ@1kHz

Laser LEGEND
λ_{LASER} = 800nm
$f_{IMPULSION}$ = 1kHz
$E_{IMPULSION}$ = 6mJ@1kHz

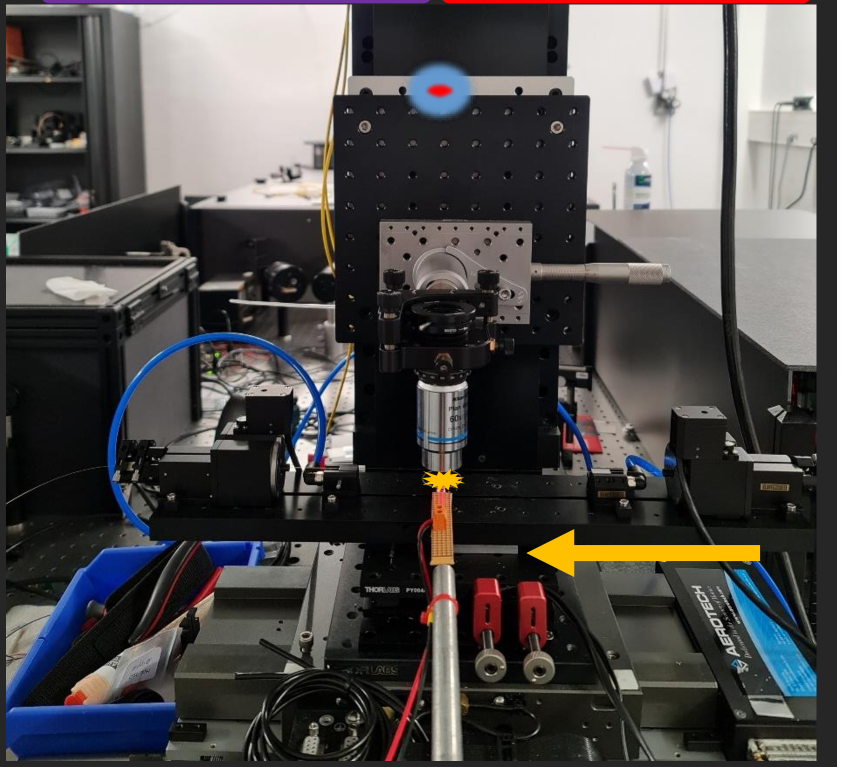

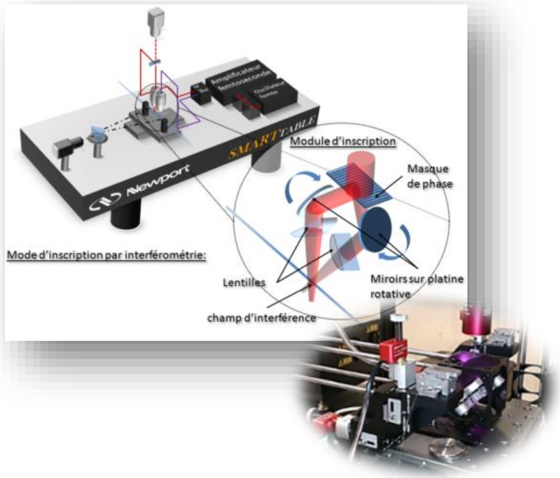

Type-III (femto) FBG photo-inscription (point-by-point)

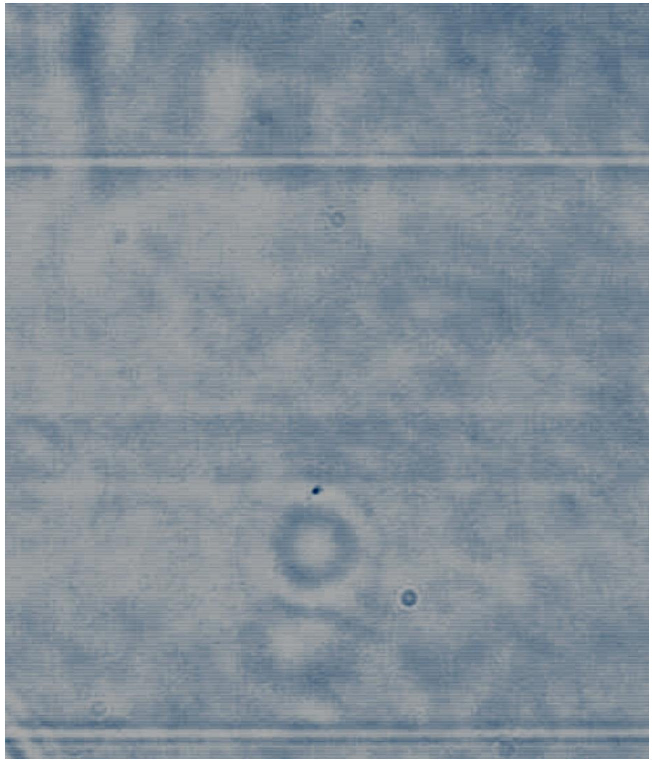

<u>FemtoBragg platform : Nanostructuration and FBG photo-inscription</u>

- ***Inscription through the polymer coating : mechanical reliability +++***
- ***Inscription on many transparent substrates (silica, sapphire, diamond, etc.)***
- ***Extreme temperature stability >> 1000°C***
- ***WDM Multiplexing***
- ***Ultra-short FBG (mm or less)***
- ***Point-by-point engineering of complex structures : apodisation, chirped, etc.***

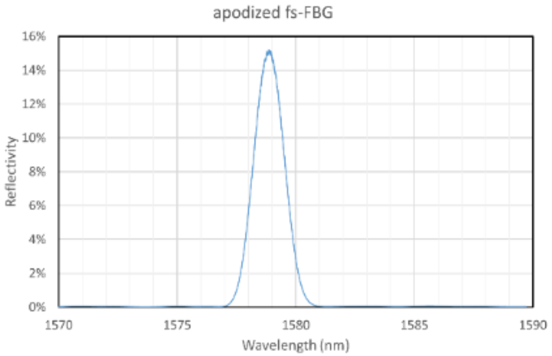

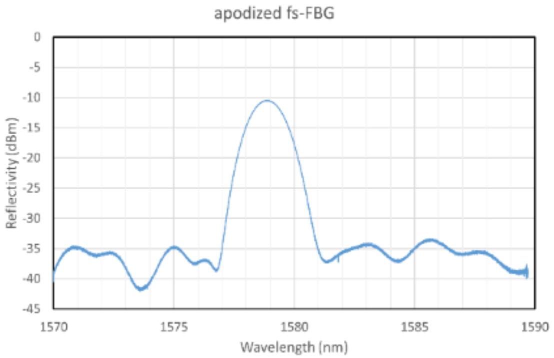

Regenerated FBG (FBG-R)

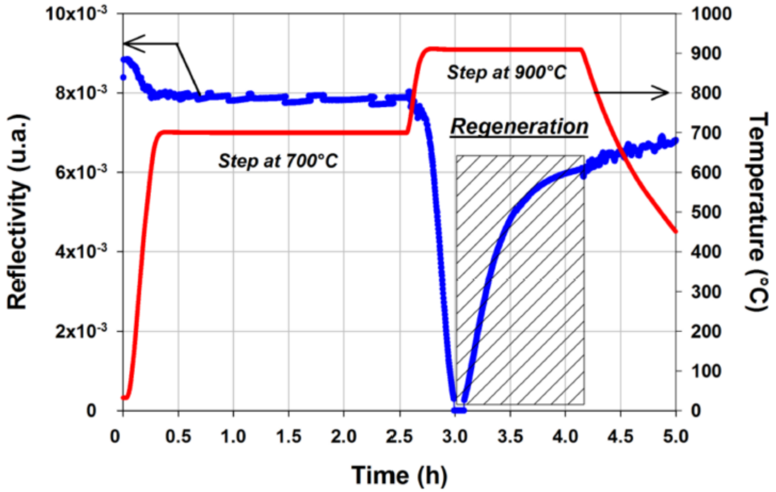

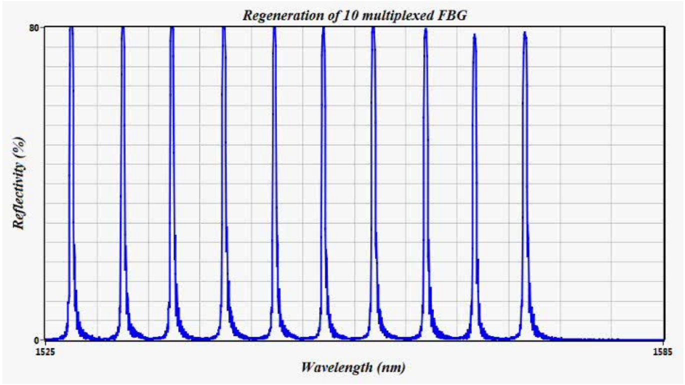

Simultaneous regeneration of 10 FBGs

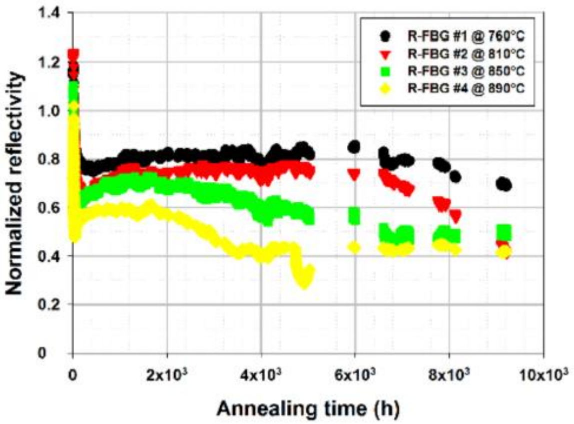

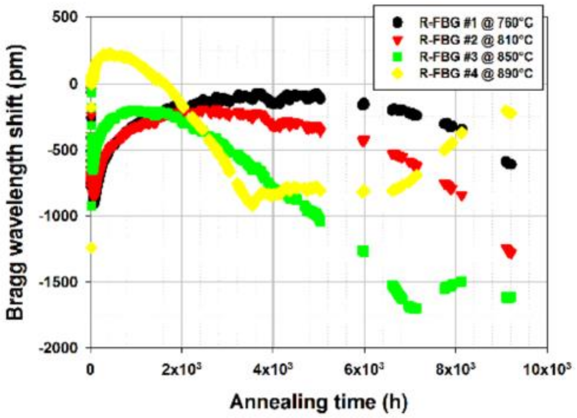

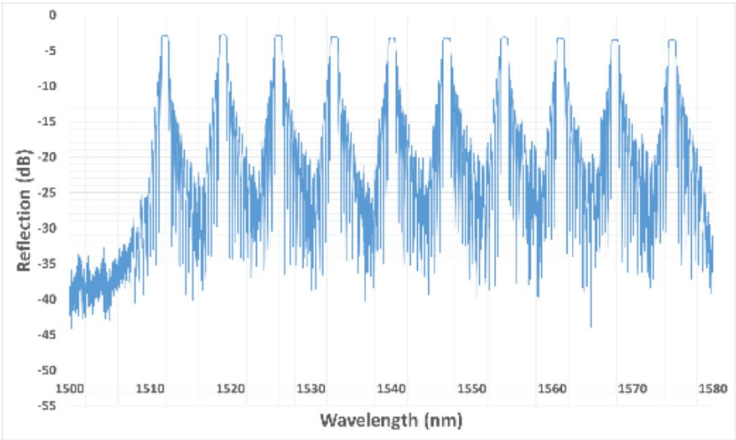

G. Laffont *et al.,* 9000 hours-long high temperature annealing of regenerated Fiber Bragg Gratings, EWOFS, Krakow, Poland, 2013

M. Fokine, Underlying mechanisms, applications, and limitations of chemical composition gratings in silica-based fibres, J. Non-Crystalline Solids 349, 2004, pp. 98–104

Main FBG readout techniques

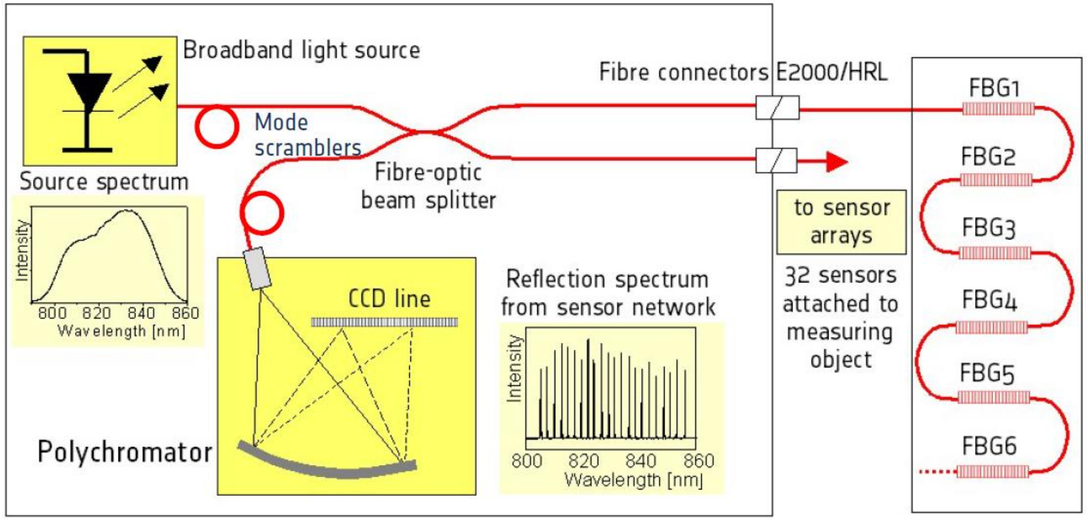

Polychromator & CCD (@800-860 nm) associated with Gaussian fit detection
W. Ecke, IPHT-Jena

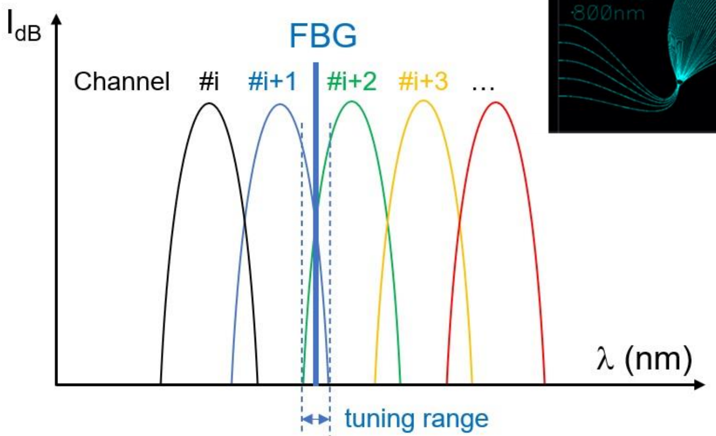

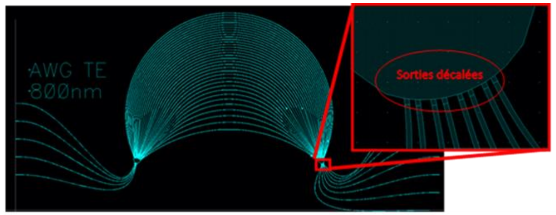

AWG - filter

Tunable laser

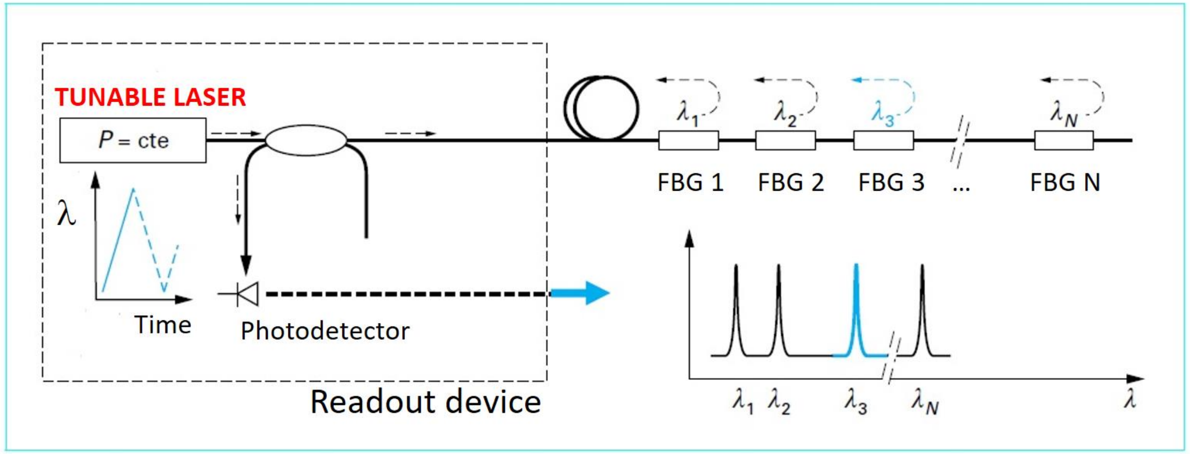

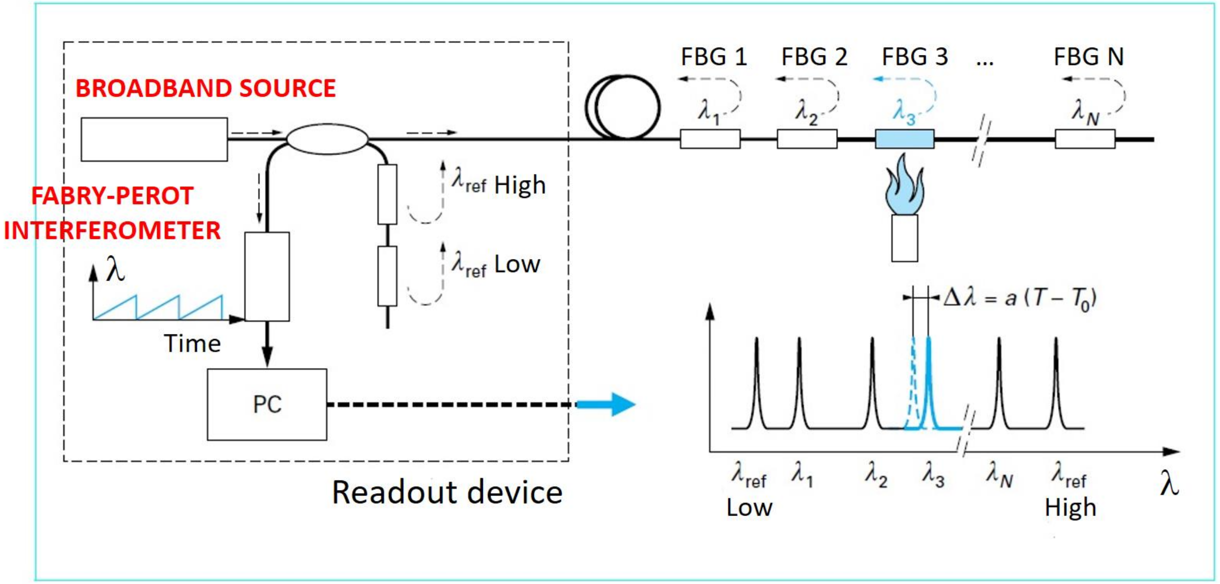

Tunable filter (P. Ferdinand, Tech. De l'Ing., Lavoisier**)**

Main FBG readout techniques : scan rate vs capacity

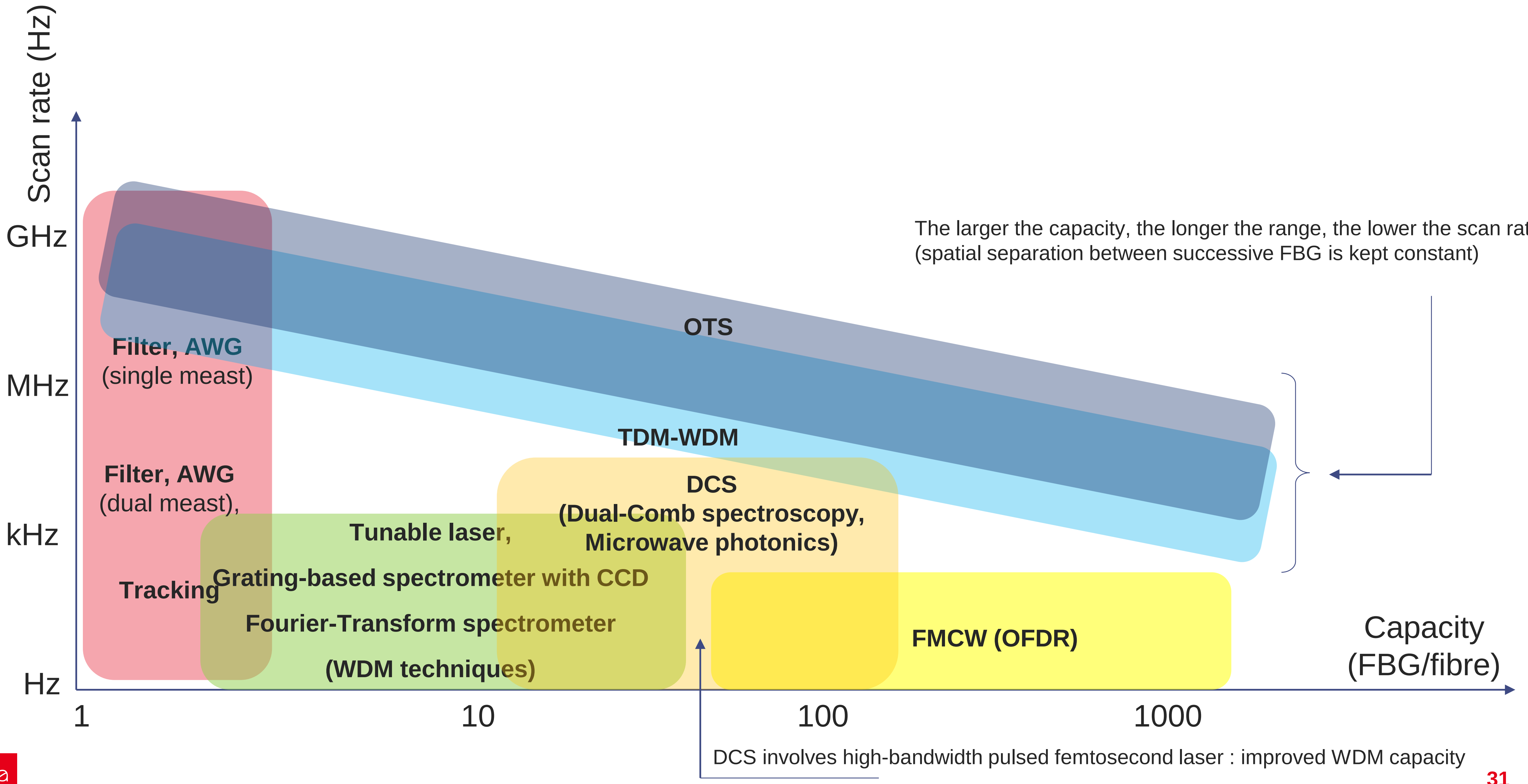

FBG chronology

- Until 1980, Bragg gratings were obtained by Reactive Ion Etching (RIE) onto planar guides (many materials),
→ complex, time-consuming and costly fabrication, fragile device with low reflectivity (evanescent interaction)

- In 1978 : K.O. Hill (CRC Ottawa) incidentally made the first Fiber Bragg Grating (FBG).
He injected an ultra-coherent 488-nm beam (Ar-ion laser) into a single-mode germanosilicate fiber cleaved at both extremities
→ standing-wave pattern inside the core and 2-photon FBG photowriting thanks to SiO_2-GeO_2 photosensitivity
FWHM 20 MHz ! (1-m long fiber)
The Bragg wavelength is identical to the laser wavelength (480 nm).
Preliminary investigations in early 1980's revealed that Hill gratings (« **type-0** ») are not stable with T° : purely photochromic in nature.

- In 1988, G. Meltz and W.W. Morey (UTRC Hartford, CT) photowrite FBGs from the outside : transverse holographic method (Lloyd mirror)
Highly flexible method : arbitrary Bragg wavelength, high efficiency (saturated gratings).
→ **Type-I** grating : erasure at low temperatures (200°C-300 °C). Photo-compaction is mainly involved.

- During the 1990's, other photo-inscription techniques are proposed : phase mask, point-by-point, Talbot interferometer.
Higher powers are delivered (ns- and ps-pulsed laser) → **type-II** gratings : erasure at higher T° (IIa:750 °C, IIb: 1000°C).
Formation of nanogratings (resulting from the interference between the laser field and plasma wave).

- During the 2000's, FBG regeneration was incidentally discovered (Fokine, 2004).
Meanwhile, peak power rises again (femtosecond pulsed laser) → **type-III** gratings : erasure at higher T° (1100°C – 1200°C)
Nanostructuration and local fusion (voids) for local intensities in excess of 10^{14} W/cm^2.

K.O. Hill, Y. Fujji, D.C. Johnson, B.S. Kawasaki, Photosensitivity in optical fibre waveguides: application to reflection filter fabrication, *Appl. Phys. Lett* 32(10), 1978, pp. 647-649.

G. Meltz, W.W.Morey, W.H. Glenn, J.D. Farina, In-fiber Bragg-grating sensors, *5th Conference on Optical Fiber Sensors*, New Orleans (USA), ThBB5-1, 1988

W.W. Morey, G. Meltz, W.H. Glenn, Bragg grating temperature and strain sensors, *6th conference on Optical Fiber Sensor*, Paris (France), 1989, pp. 526-531.

FBG review : further reading

T. Erdogan, Fiber Grating spectra, *J. Lightwave Technol*., 15(8), 1997, pp. 1277-1294.

P. Ferdinand, S. Magne, V. Dewynter-Marty, S. Rougeault, L. Maurin, Applications of FBG Sensors in the composite industry, MRS Bull., 27 (5), 2002, pp. 400-407.

P. Ferdinand, S. Magne, Applications of optical fiber sensors for nuclear power industry, in *Handbook on Optical Fiber Sensing Technology – Principle and Applications*, Wiley & Sons, J.M. Lopez-Higuera Ed., Ch. 6, 2000

K.O. Hill, G. Meltz, FBG technology fundamentals and overview, *J. Lightwave Technol.* 15(8), 1997, pp. 1263-1276.

R. Kashyap, *Fiber Bragg Gratings*, Ac. Press, 1999

A.D. Kersey, M.A. Davis, H.J. Patrick, M. LeBlanc, K.P. Koo, C.G. Askins, M.A. Putnam, E.J. Friebele, Fiber Grating Sensors, *J. Lightwave Technol.* **15**(8), 1997, pp. 1442-1463.

G. Laffont, R. Cotillard, N. Roussel, R. Desmarchelier, S. Rougeault, Temperature-resistant FBGs for on-line SHM of the next-generation of nuclear reactors, Sensors 18, 2018, pp. 1791-1811.

C. Li, J. Tang, C. Cheng, L. Cai, M. Yang, FBG arrays for quasi-distributed sensing: a review, *Photonics Sens.* 11(1), 2021, pp. 91-108.

A. Othonos, Fiber Bragg gratings, *Rev. Sci. Instrum*. 68(12), 1997, pp. 4309-4341.

X. Qiao, Z. Shao, W. Bao, Q. Rong, FBG sensors for the oil industry, *Sensors* 17, 2017, pp. 429-463.

Y.J. Rao, In-fibre Bragg grating sensors, *Meas. Sci. Technol.* 8, 1997, pp. 355-375.

D. Tosi, Review and analysis of peak tracking techniques for FBG Sensors, *Sensors* 17(10), 2017, pp. 2368-2403.

Q. Wu, Y. Okabe, F. Yu, Ultrasonic SHM using FBG, *Sensors* 18, 2018, pp. 3395-3421.

FBG in general : further reading (1990-2005)

A.T. Alavie, S.E. Karr, A. Othonos, R.M. Measures, A multiplexed Bragg grating fiber laser sensor system, *IEEE Phot. Tech. Lett.,* 5(9), 1993, pp. 1112-1114.

J.L. Archambault *et al.,* 100 % reflectivity Bragg reflectors produced in optical fibres by single excimer laser pulses, *Electron. Lett*., 29(5), 1993, pp. 453-455.

C.G. Askins *et al.,* Fiber Bragg reflectors prepared by a single excimer pulse*, Opt. Lett.,* 17(11), 1992, pp. 833-835.

X. Chapeleau, D. Leduc, C. Lupi, R. Le Ny, M. Douay, P. Niay, C. Boisrobert, Experimental synthesis of FBGs using optical low coherence reflectometry, Appl. Phys. Lett., 82(24), 2003, pp. 4227-4229.

S. Chen, Y. Hu,L. Zhang, I. Bennion, Multiplexing of large-scale FBG arrays using a 2D spectrometer, *SPIE* 3330, *Smart Structures and Materials*, San Diego (USA), 1998, pp. 245-252.

D.J.F. Cooper, T. Coroy, P.W.E. Smith, Time-Division Multiplexing of large serial fiber-optic Bragg grating sensor arrays, *Appl. Opt.* 40(16), 2001, pp. 2643-2654.

M.A. Davies, A.D. Kersey, Applications of a Fiber FT Spectrometer to the detection of wavelength-encoded signals from Bragg grating sensors, *J. Lightwave Technol.,* 13(7), 1995, pp. 1289-1295.

M.A. Davies, A.D. Kersey, Matched-filter interrogation technique for FBG arrays, *Electron. Lett.,* 31(10), 1995, pp. 822-823.

W. Ecke, I. Latka, R. Willsch, A. Reutlinger, R. Graue, Fibre optic sensor network for spacecraft health monitoring, *Meas. Sci. Technol.* 12, 2001, pp. 974-980.

M. Froggatt, J. Moore, Distributed measurement of static strain in an optical fiber with multiple FBGs at nominally equal wavelengths, *Appl. Opt.* 37(10), 1998, pp.1741-1746

K.O. Hill, B. Malo, F. Bilodeau, D.C. Johnson, J. Albert, Bragg gratings fabricated in monomode photosensitive optical fiber by UV exposure through a phase mask, *Appl. Phys. Lett.* 62(10), 1993, pp. 1035–1037.

D.A. Jackson, A.B. Lobo Ribeiro, L. Reekie, J.L. Archambault, Simple multiplexing scheme for a fiber-optic grating sensor network, *Opt. Lett.,* 18(14), 1993, pp. 1192-1194.

G. Laffont, P. Ferdinand, Tilted short-period FBG-induced coupling to cladding modes for accurate refractometry, Meas. Sci. Technol. 12, 2001, pp. 765–770.

G.D. Lloyd, L.A. Everall, K. Sugden, I. Bennion, Resonant cavity Time-Division-Multiplexed FBG sensor interrogator, *IEEE Phot. Tech. Lett.* 16(10), 2004, pp. 2323-2325.

S. Magne, S. Rougeault, M. Vilela, P. Ferdinand, State-of-strain evaluation using FBG rosettes - Application to discrimination between strain and temperature effects in fiber sensors, *Appl. Opt.* 36(36), 1997, pp. 9437-9447.

B. Malo, K.O. Hill, F. Bilodeau, D.C Johnson, J. Albert, Point-by-point fabrication of micro-Bragg gratings in photosensitive fibre using single excimer pulse refractive index modification techniques, *Electron. Lett.* 29, 1993, pp. 1668–1669.

Ch. Martinez, S. Magne, P. Ferdinand, Apodized FBGs manufactured with the phase plate process, *Appl. Opt.* 41(9), 2002, pp. 1733-1740.

S. Melle, K. Liu, R.M. Measures, A passive wavelength demodulation system for guided-wave Bragg grating sensors, *IEEE Phot. Tech. Lett.* 4, 1992, pp. 516-518.

N. Roussel, S., Magne, Ch. Martinez, P. Ferdinand, Measurement of index modulation along FBGs by side scattering and local heating methods, *Opt. Fiber. Tech.* 5, 1999, pp. 119-132.

Y. Sano, T. Yoshino, Fast optical wavelength interrogator employing Arrayed Waveguide Grating for Distributed FBG sensors, *J. Lightwave Technol.* 21(1), 2003, pp. 132-139.

FBG in general : further reading (2005-2020)

M. Cavillon, M. Lancry, B., Poumellec, Y. Wang, J. Canning, K. Cook, T. Hawkins, P.D. Dragic, J. Ballato, Overview of high temperature FBGs and potential improvement using highly-doped aluminosilicate glass optical fibres, *J. Phys. Photonics,* 1, 2019, pp. 042001-042013.

M. Busch, W. Ecke, I. Latka, D. Fischer, R. Willsch, H. Bartelt, Inscription and characterization of Bragg gratings in single-crystal sapphire optical fibers for high-temperature sensor applications, Meas. Sci. Technol. 20, 2009, pp. 115301-115307.

C. Chojetzki *et al.,* High-reflectivity draw-tower FBGs array and single gratings of type II, *Opt. Eng.* **44**(6), 2005, pp. 060503-060504.

G.A. Cranch, G.M.H. Flockhart, C.K. Kirkendall, Distributed feedback fiber laser strain sensors, *IEEE Sensors J.,* 8(7), 2008, pp. 1161-1178.

B. Culshaw, G. Thursby, D. Betz, B. Sorazu, The detection of ultrasound using Fiber-optic sensors, *IEEE Sensors J.,* 8(7), 2008, pp. 1360-1367.

M. Gotten, S. Lochmann, A. Ahrens, E. Lindner, J. Van Roosbroeck, 2000 serial FBG sensors Interrogated with a hybrid CDM-WDM scheme, *J. Lightwave Technol.* 38(8), 2020, pp. 2493–2503.

D. Grobnic, S.J. Mihailov, C.W. Smelser, R.T. Ramos, Ultrafast IR laser writing of strong Bragg gratings through the coating of high Ge-doped optical fibers, IEEE Phot. Tech. Lett., 20(12), 2008, pp. 973-975.

J. Guo, Y. Ding, X. Xiao, L. Kong, C. Yang, Multiplexed static FBG strain sensors by dual-comb spectroscopy with a free running laser, *Opt. Express* 26(13), 2018, pp.16147-16154.

G. Laffont, R. Cotillard, P. Ferdinand, Multiplexed regenerated FBGs for high-temperature measurement, Meas. Sci. Technol. 24(9), 2013, pp. 094010-094015.

L. Ma, C. Ma, Y. Wang, D.Y. Wang, A. Wang, High-Speed Distributed Sensing Based on Ultra Weak FBGs and Chromatic Dispersion, IEEE Phot. Tech. Lett. 28(12), 2016, pp. 1344-1346.

S. Magne, Y. Barbarin, A. Lefrançois, M. Balbarie, F. Sinatti, A. Osmont, J. Luc, K. Woirin, Real-time distributed monitoring of pressure and shock velocity by ultrafast spectrometry with CFBG: Experimental vs calculated wavelength-to-pressure sensitivities in the range [0-4 GPa], J. Appl. Phys. 124, 2018, pp. 145902

S. Magne, N. Legrand, S. Ertz, G. Jouvin, V. André, G. Laffont, L. Boissonnet, New shapemeter roll technology based on FBG technology for on-line flatness monitoring of thin cold rolled metal sheets, J. Appl. Phys. 131, 2022, pp. 224502-30.

A. Martinez, I.Y. Khrushschev, I. Bennion, Direct inscription of Bragg gratings in coated fibers by an infrared femtosecond laser, *Opt. Lett.* 31(11), 2006, pp. 1603-1605.

J.P. Moore, M.D. Rogge, Shape sensing using multi-core fiber optic cable and parametric curve solutions, Opt. Express 20(3), 2012, pp. 2967-2973.

B. Qui, F. Ye, L. Qian, H.K. Lo, Reflectometry based on a frequency-shifted interferometric using sideband interference, *Opt. Lett.* 38(7), 2013, pp. 1083-1085.

F. Ye, L. Qian, Y. Liu, B. Qi, Using Frequency-shifted interferometry for multiplexing a FBG array, *IEEE Phot. Tech. Lett.* 20(17), 2008, pp. 1488-1490

In situ temperature monitoring in PFU (TOKAMAK Fusion WEST)

PFU = Plasma Facing Unit (graphite/tungsten)

Divertor = target for high E particles, surface T° up to 2000°C

Arrays of high T° resistant FBGs (FBG-R and FBG-III) to monitor sub-surface temperature

WEST Tokamak at CEA Cadarache

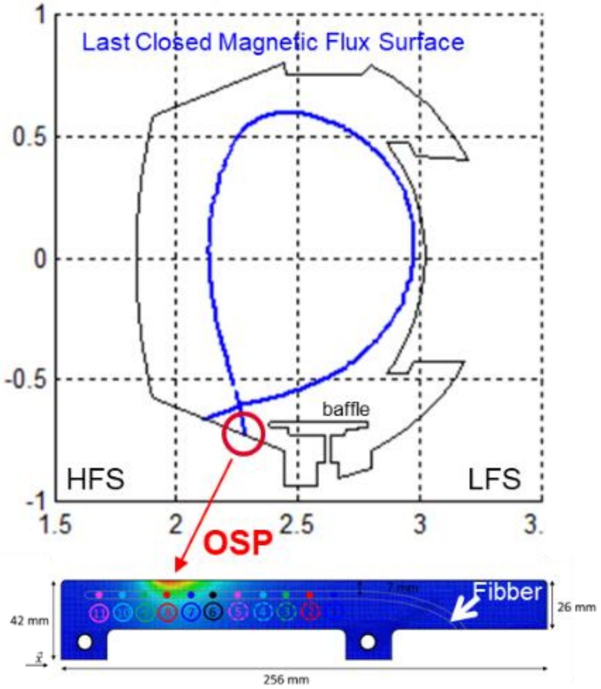

PFU instrumented with FBG probes

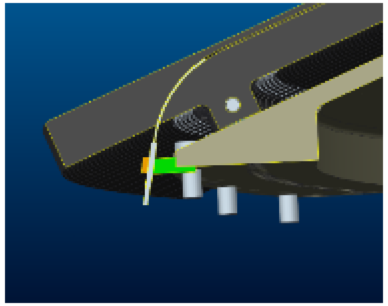

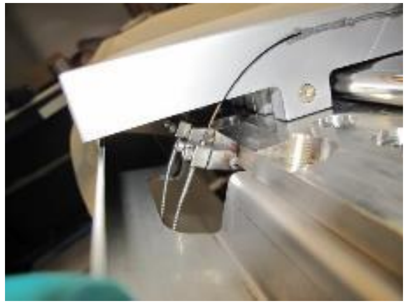

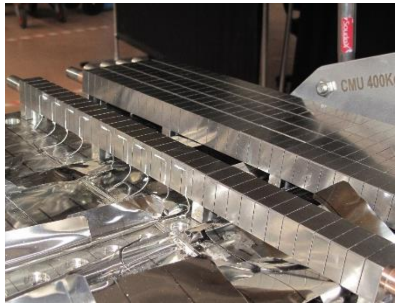

Y. Corre, G. Laffont, C. Pocheau, R. Cotillard, J. Gaspar, N. Roussel, M., Firdaouss, J.L. Gardarein, D. Guilhem, M. Missirlian,
Integration of FBG temperature sensors in plasma facing components of the WEST Tokamak,
Rev. Sci. Instrum. 89, 063508-10, 2018

Fusion WEST

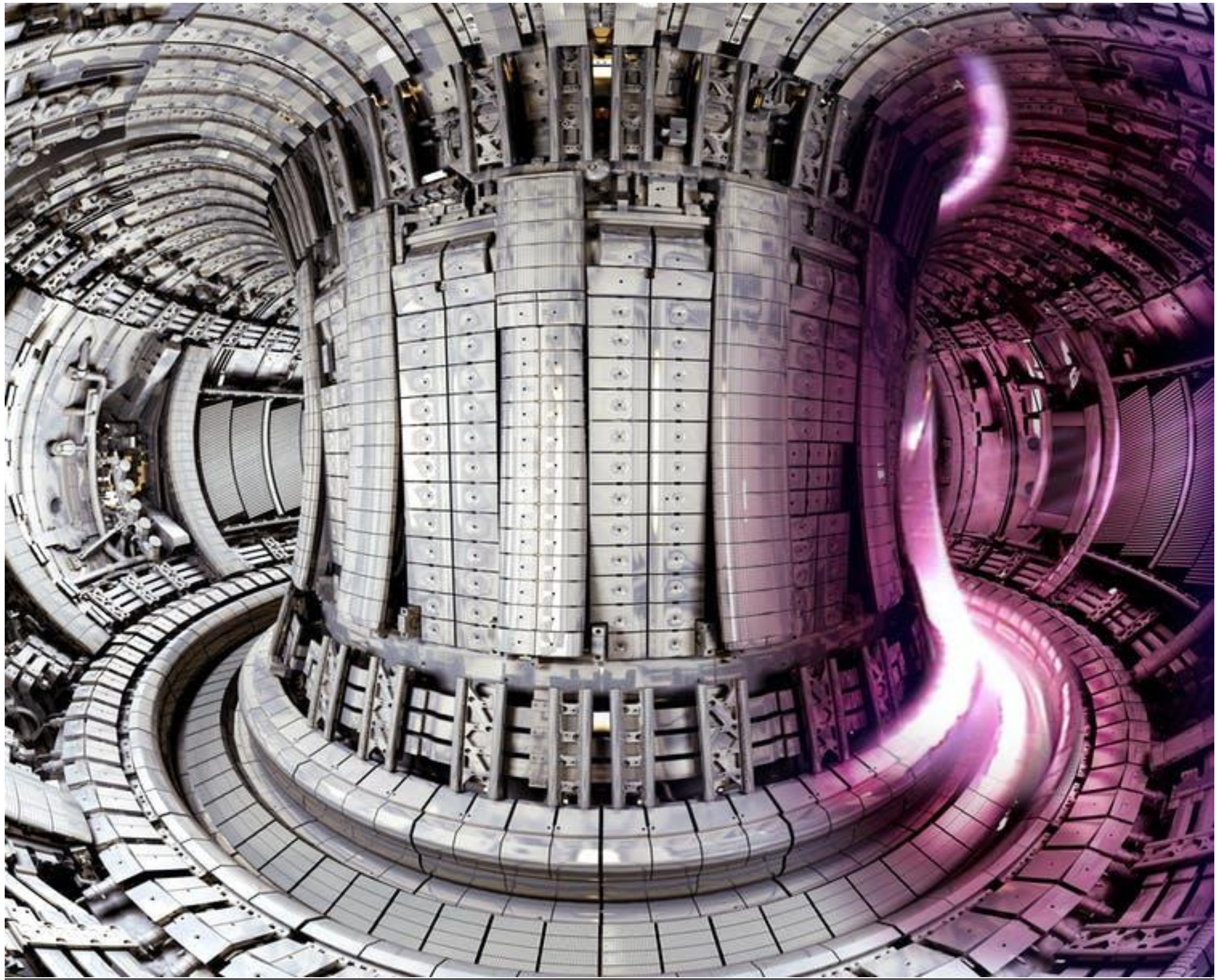

Tokamak WEST (Cadarache, France)

THERMAL DIAGNOSTIC IN A TOKAMAK >800°C

INSTRUMENTED W-BLOCKS OF A DIVERTOR'S SECTOR

Heat flux 5 MW/m2, Sun surface ~60 MW/m2, On the beach 0.001 MW/m2

FULL INSTRUMENTATION

Packaged FBGs, Feedthrough, Remote line, System/Soft to the control room

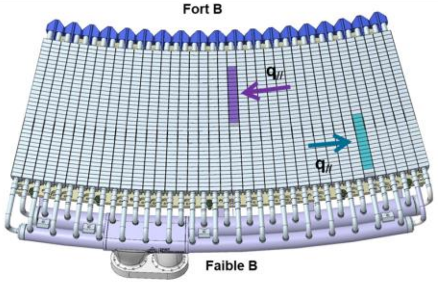

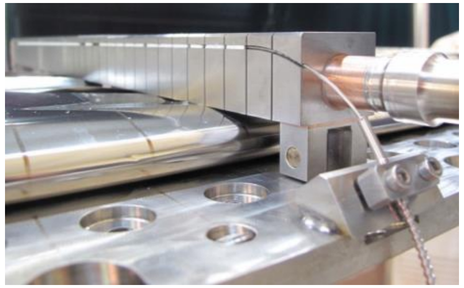

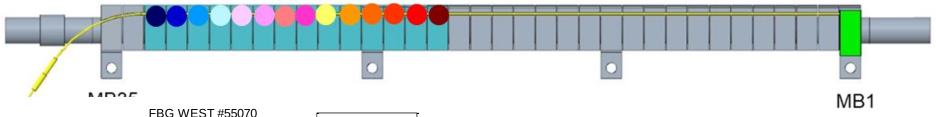

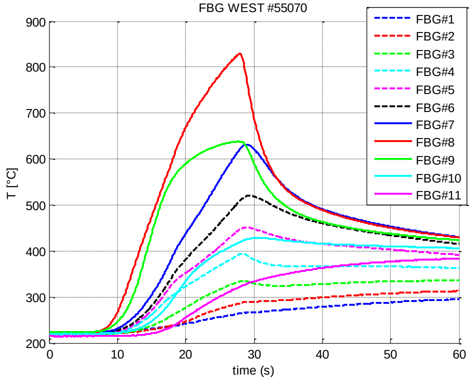

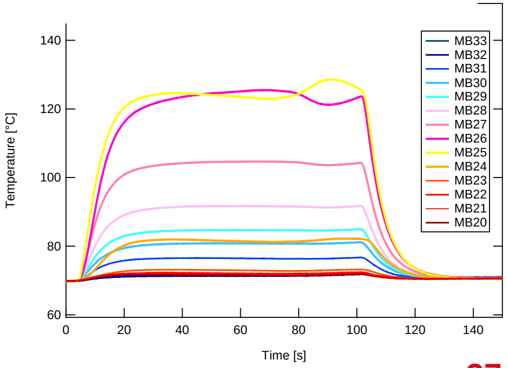

Acoustic sensing with FBG

Compact monitoring system for λ-mux FBG acoustic receivers in SHM systems

- Array Waveguide Grating customized for sensing needs (edge filtering)
- AWG Si/SiN developed through a collaboration between CEA List and Leti

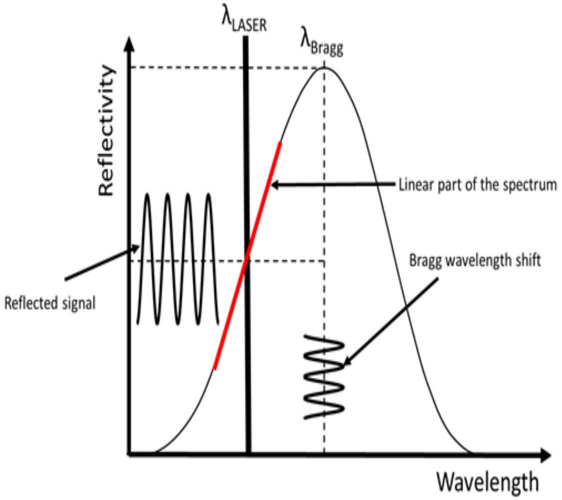

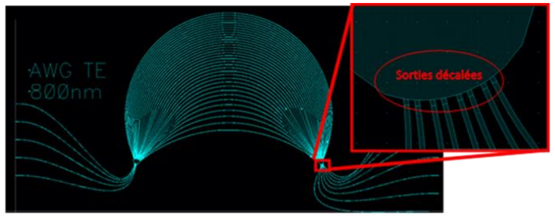

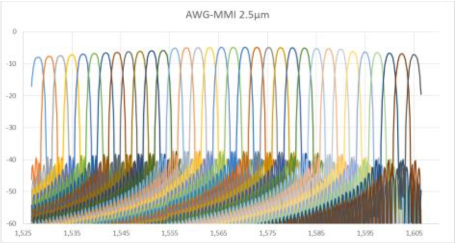

Demux *Telecom*

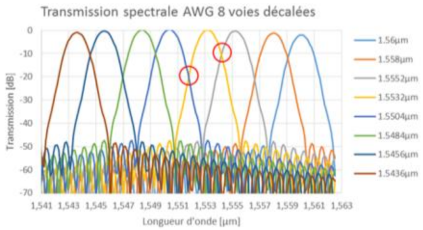

Demux *Sensing*

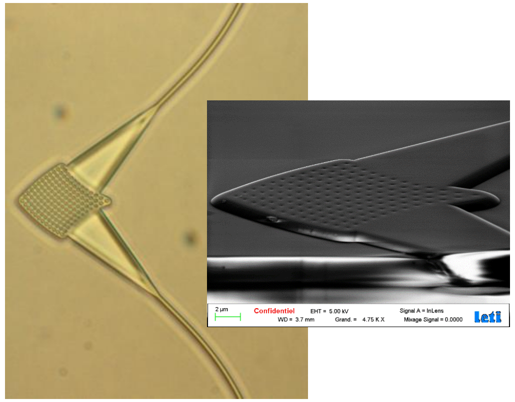

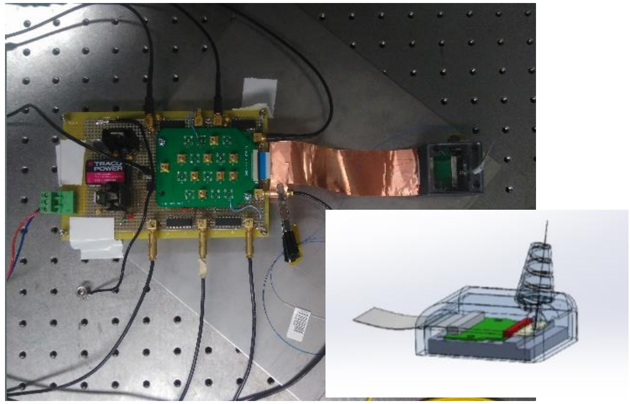

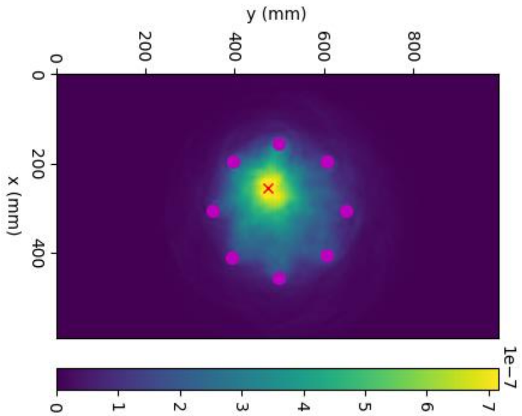

Active/Passive Tomography for damage detection in composite panels

FBGs = acoustic receivers

and PZT = emitters

A. Recoquillay, T. Druet, S. Nehr, M. Horpin, O. Mesnil, B. Chapuis, G. Laffont, O. D’Almeida,
Guided-wave imaging of composite plates using passive acquisitions by FBG,
J. Acoust. Soc. Am. 147, 2020, pp. 3565-3574

FBG sensing applied to shock monitoring (1/2)

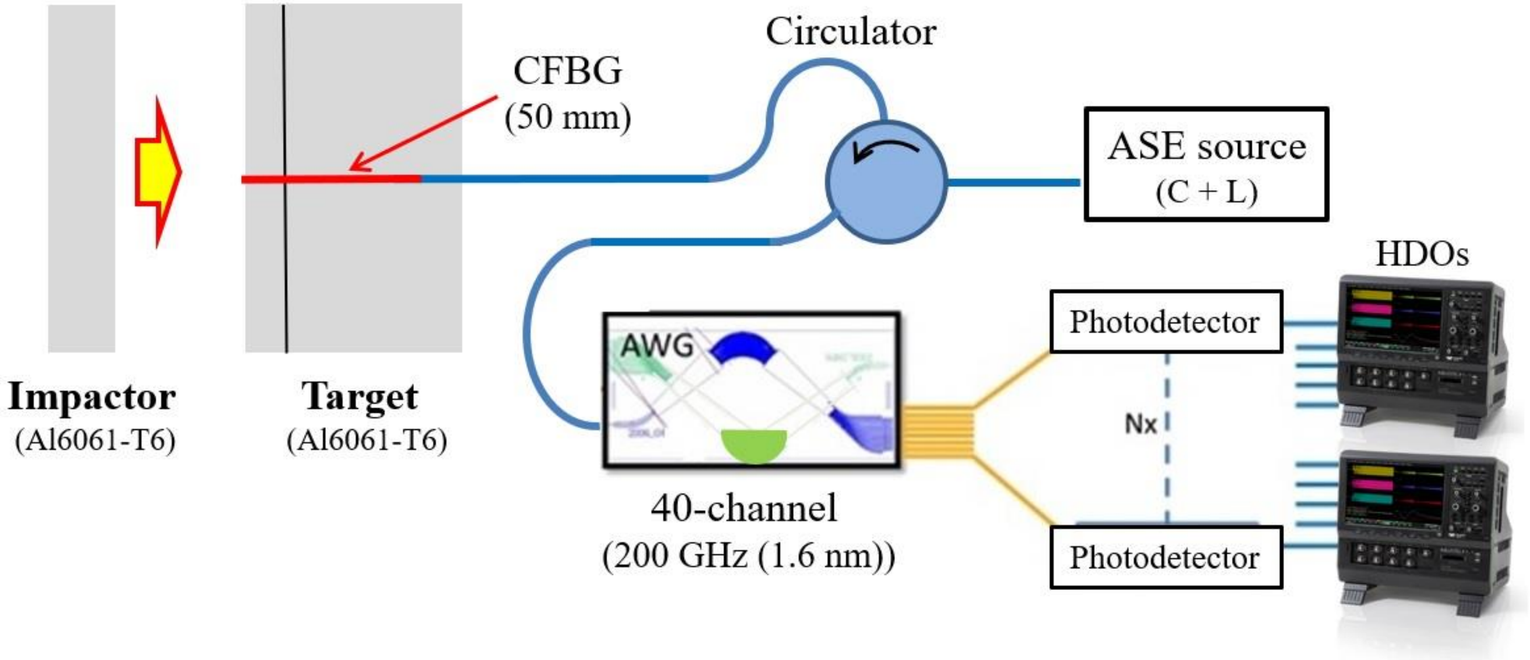

Launcher (CEA/Gramat)

- Plane impact
- Impact stress dependent on impactor speed and impactor-target materials
- **Sustained shock during several microseconds** (geometry-dependent).

FBG sensing applied to shock monitoring (2/2)

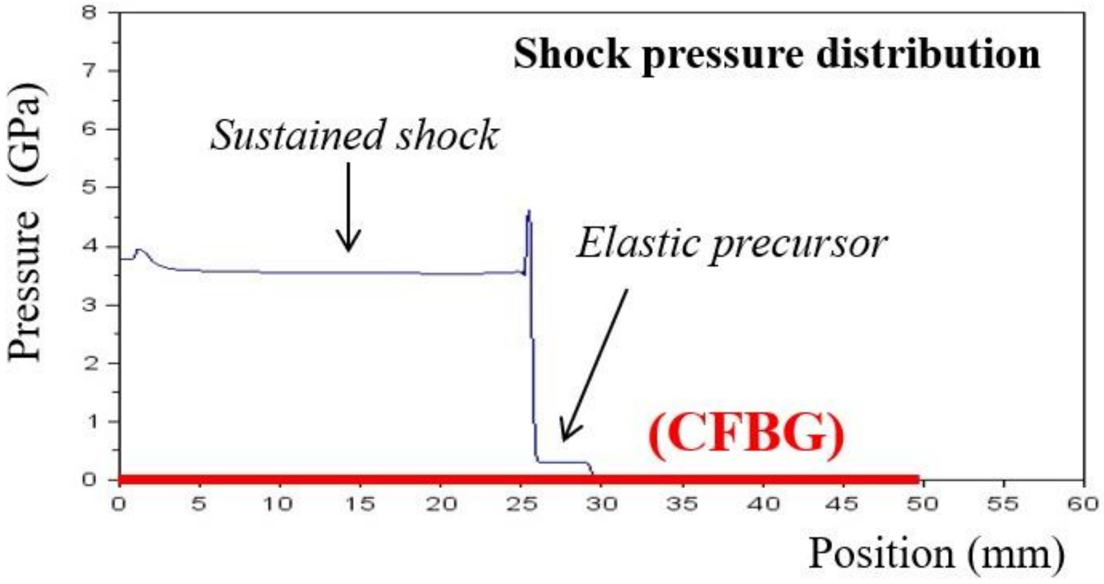

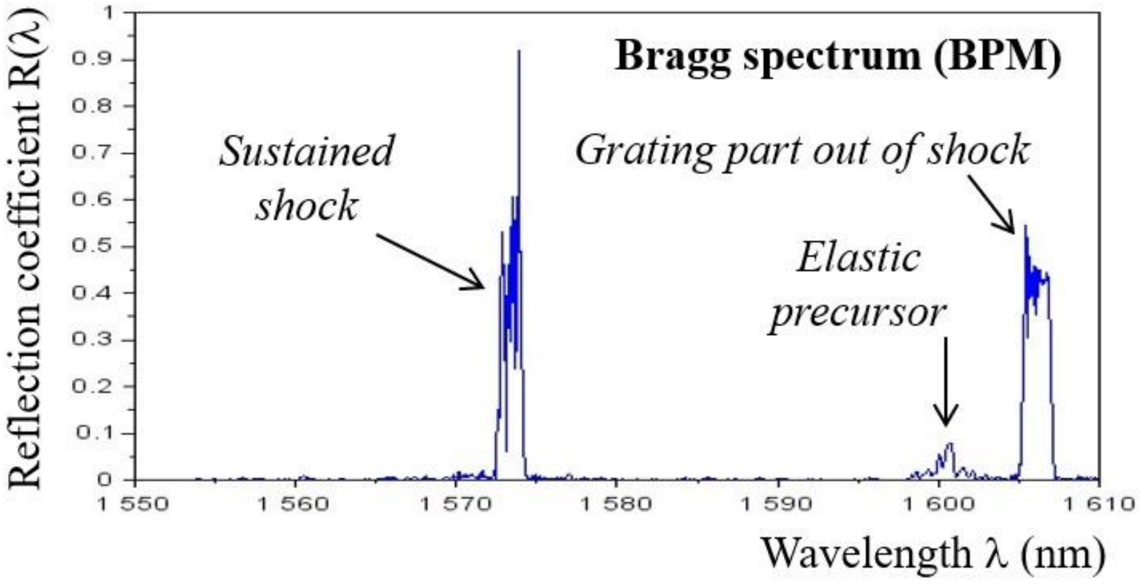

S. Magne, A. Lefrançois, J. Luc, G. Laffont, P. Ferdinand,
Real-time, Distributed measurement of detonation velocities inside High Explosives with the help of CFBG,
European Workshop on Optical Fiber Sensors (EWOFS), Krakow (Poland), *Proc. SPIE* 8794, 2013, 87942K.

S. Magne, Y. Barbarin, A. Lefrançois, M. Balbarie, F. Sinatti, A. Osmont, J. Luc, K. Woirin,
Real-time distributed monitoring of pressure and shock velocity by ultrafast spectrometry with CFBG:
Experimental vs calculated wavelength-to-pressure sensitivities in the range [0-4 GPa], J. Appl. Phys. 124, 145902, 2018

OTS is now used for intense shock sensing

C-band, pulse 90 fs, 13 km SMF28 (220 ps/nm),
PRF = 100 MHz,
High-speed PhD (23 GHz) and oscilloscope (25 GHz)
Capacity = 1 [CFBG 10 mm, FWHM 30 nm]

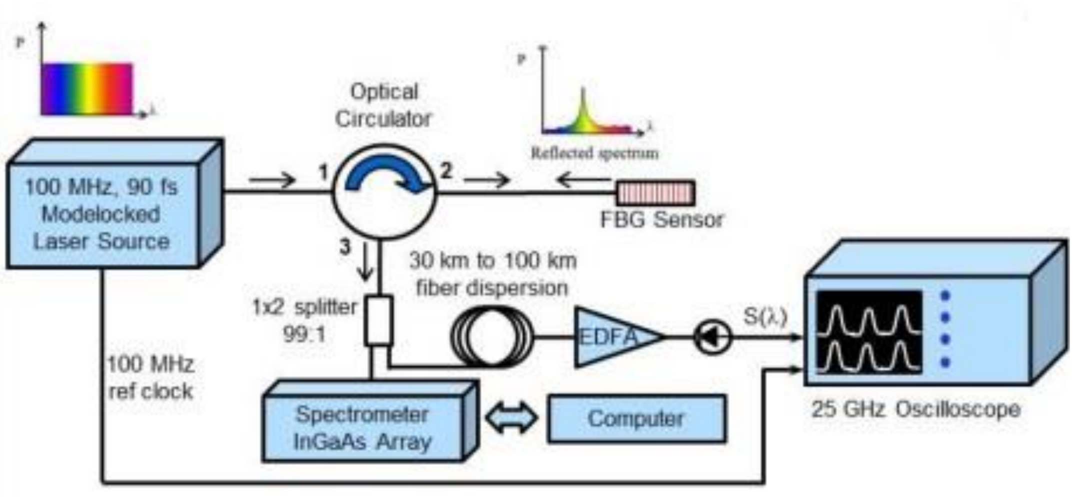

G. Rodriguez and S.M. Gilbertson, Ultrafast FBG interrogation for sensing in detonation and shock wave experiments, Sensors, 17, 248, 2017
[Los Alamos, National Lab. (LANL, USA)]

18 km SMF28 (306 ps/nm),
PRF = 100 MHz
High-speed PhD (38 GHz) and oscilloscope (33 GHz)
Capacity = 3 FBGs

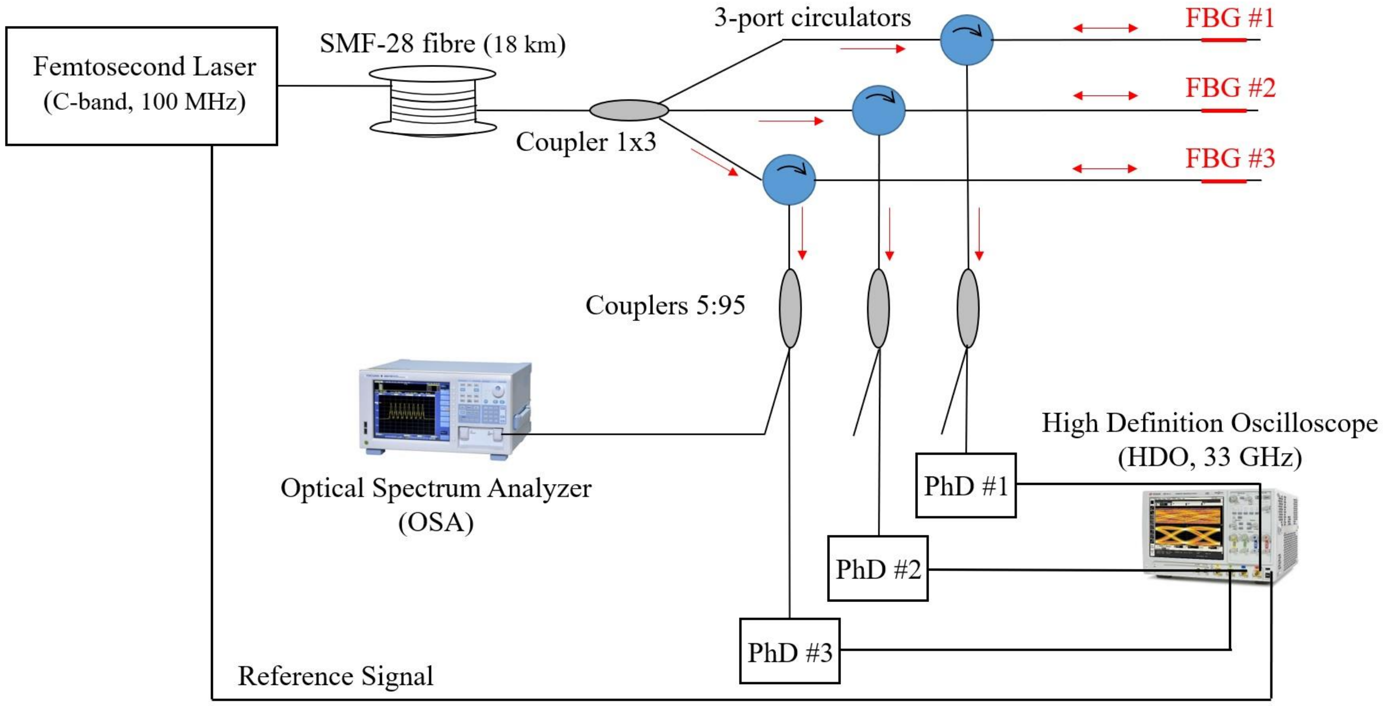

Y. Barbarin et al., IEEE RAPID Conference (Orlando, USA), 2018
[CEA/Gramat, FR]

OTS basic principle

- Pulse laser (typ. ps to 100 fs), Pulse Repetition Frequency (PRF) ~ 1 MHz to 100 MHz
- PRF = readout rate,
- Temporal delay of Bragg reflected pulse is proportional to Bragg shift,
- Pure TDM or combined TDM-WDM approach,
- Propagation delay must be taken into account (FBG location along fiber),
- Several trade-offs to consider : Capacity *vs* scan rate, distance range *vs* PRF, spatial separation between FBGs *vs* measurand range (ε/T°C).

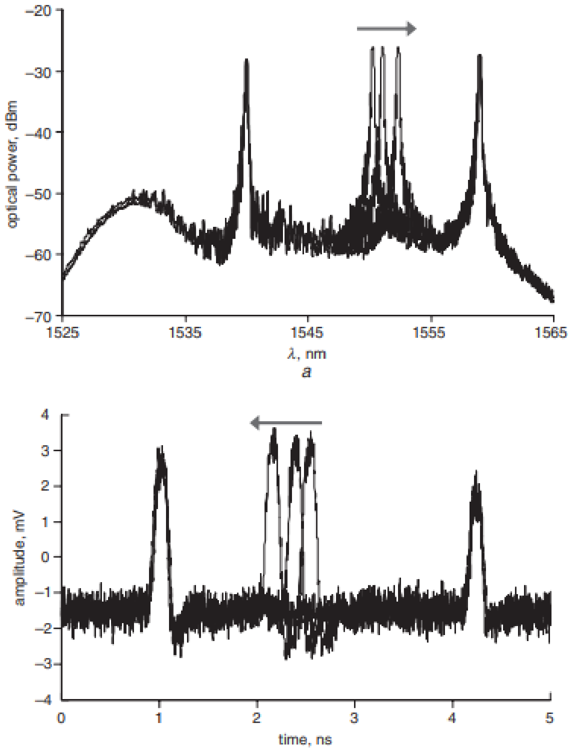

$$\Delta\lambda = D \cdot L \cdot \Delta_t$$

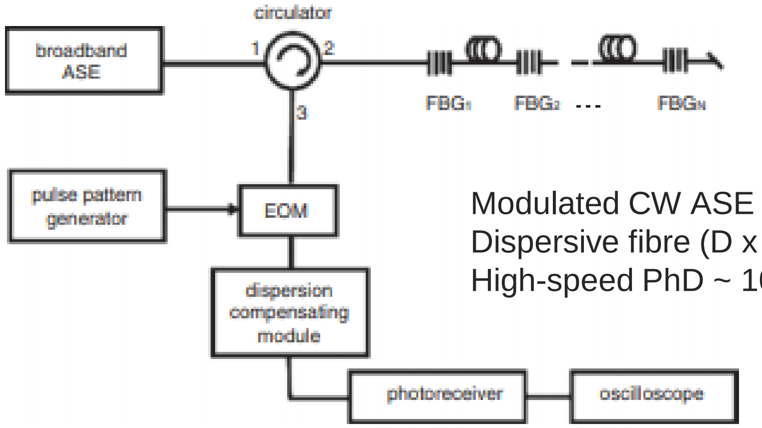

Modulated CW ASE source (EOM),
Dispersive fibre (D x L = -170 ps/nm),
High-speed PhD ~ 10 GHz

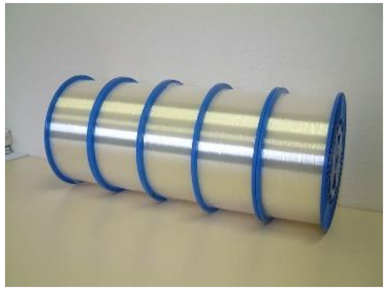

H.Y. Fu *et al.*,
High-speed FBG sensor interrogation using dispersion-compensation fibre,
Electron. Lett., 44 (10), 2008, pp. 618-620

FBG sensing used in High Pulse Power (HPP)

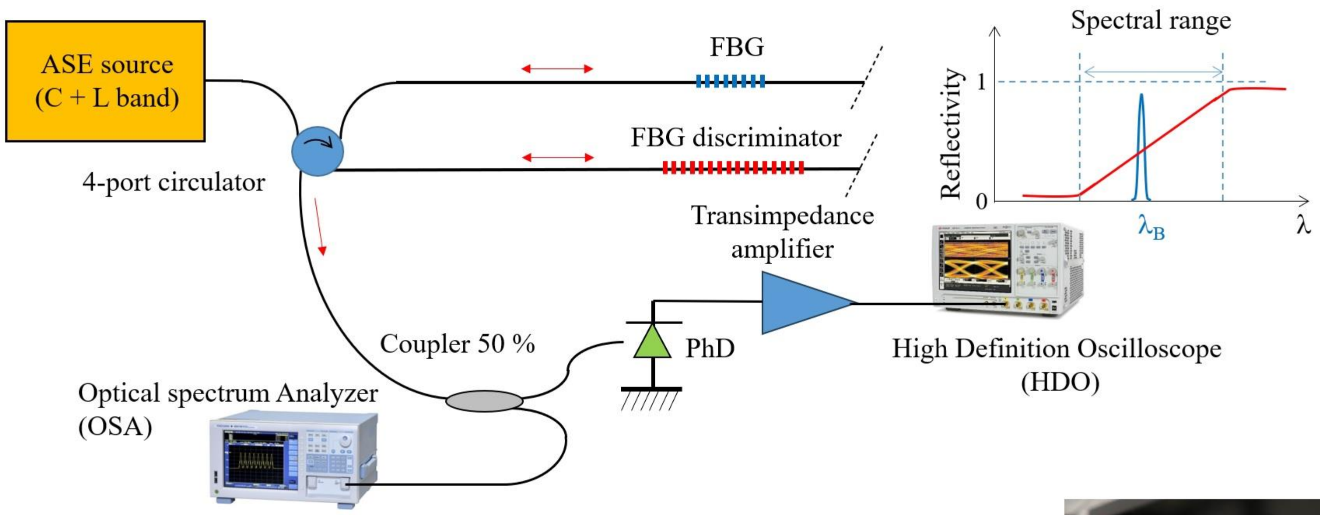

Linear discriminator

$\Delta\varepsilon$ (microstrain) $\leftrightarrow$ $\Delta\lambda$ (pm) $\leftrightarrow$ ΔV (µV)

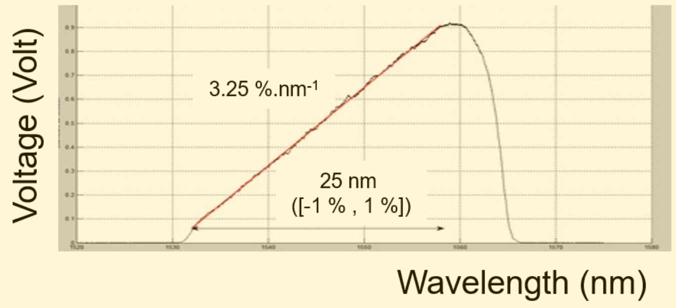

Chirped Fiber Bragg Grating (CFBG)
mounted in thermal compensator

Specifications

- Strain range : [-1 %, 1 %]
- Uncertainty ± 0,5 % (k=2)
- Accuracy < ± 2 % (k=2)
- Spatial resolution < 2 mm
- Bandpass [DC, 10 MHz]

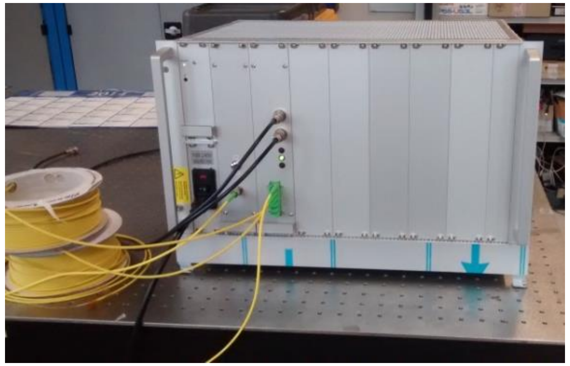

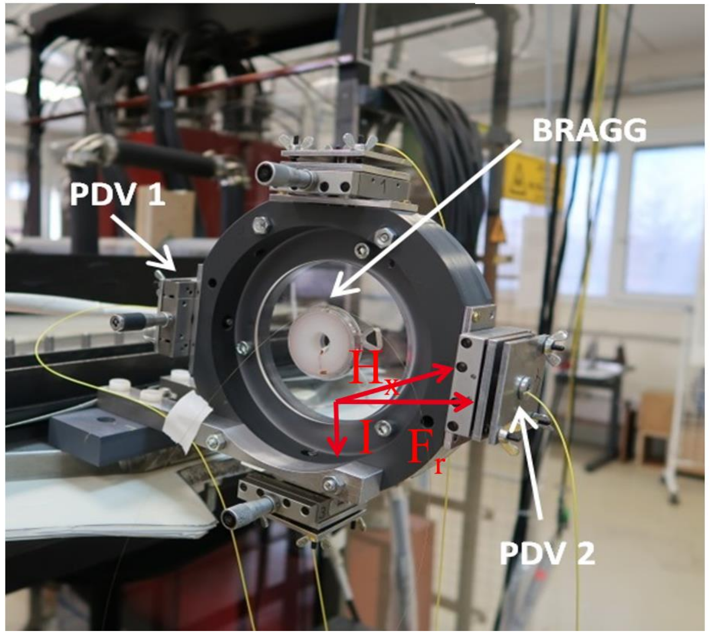

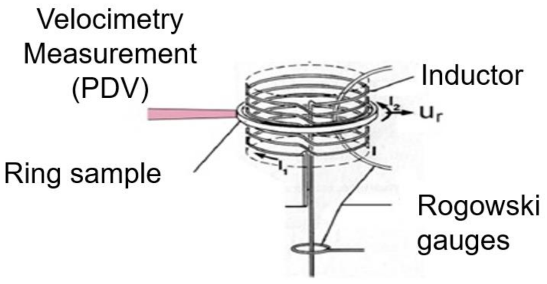

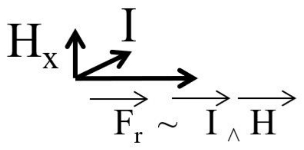

Generation of magnetic pressure pulses (Lorentz force)
Capacity discharge : ~ 5 MA (~ kT)
High-frequency ~ 50 – 500 kHz
Max pressure ~ 100 GPa
Pulse lapse ~ microsecond
Energy ~150 kJ

S. Magne *et al.*, Fiber Bragg Grating Dynamic Extensometry on metallic samples submitted to High Pulse Power Magnetic Fields, OSA Advanced Photonics Congress, BGPP, Zurich (Switzerland), 2-5 July 2018

SUMMARY

- CEA as a glance
- LIST/DIN/SMCD/LSPM
- Optical fibers : basics
- Optical fibers for telecommunications
- Optical fibers for sensing in harsh environments
- Point sensing : White-Light Interferometry (WLI)
- Quasi-distributed sensing : Fiber Bragg Gratings (FBGs)
- **Truly distributed sensing : OTDR DTS, BOTDR/BOTDA, OFDR, FMCW, DAS**
- **MSCA USES2 DC02 : OPTICAL TIME STRETCH (OTS)**

Reflectometry schemes in optical fibers

Measurements relying on scattering phenomena in optical fibres

- Raman scattering ⇨ Distributed Temperature Sensing **DTS Raman**
- Brillouin scattering ⇨ Distributed Temperature and Strain Sensing **DTSS Brillouin**
- Rayleigh scattering ⇨ Distributed Temperature and Strain Sensing : **OFDR Rayleigh**

The optical fibre is the sensor

- From µm/m and 0.1°C (OFDR Rayleigh) to typ. 30 µm/m and several °C (Brillouin)
- Up to several tens of km (Brillouin, Raman)
- Application to remote Long-range/High-capacity monitoring
- Distance resolved in the Time-Domain or in the Frequency-Domain

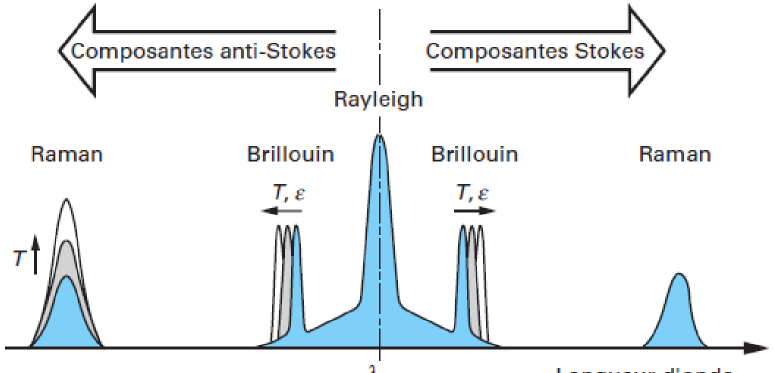

source : Techniques de l'Ingénieur

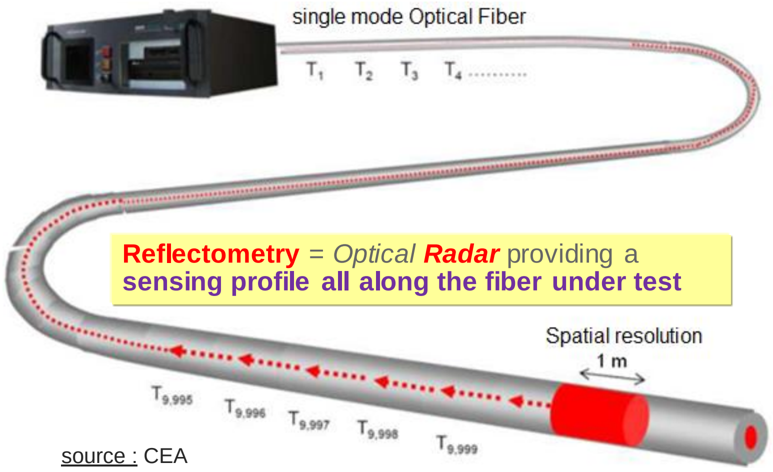

source : CEA

Reflectometry units available at CEA List

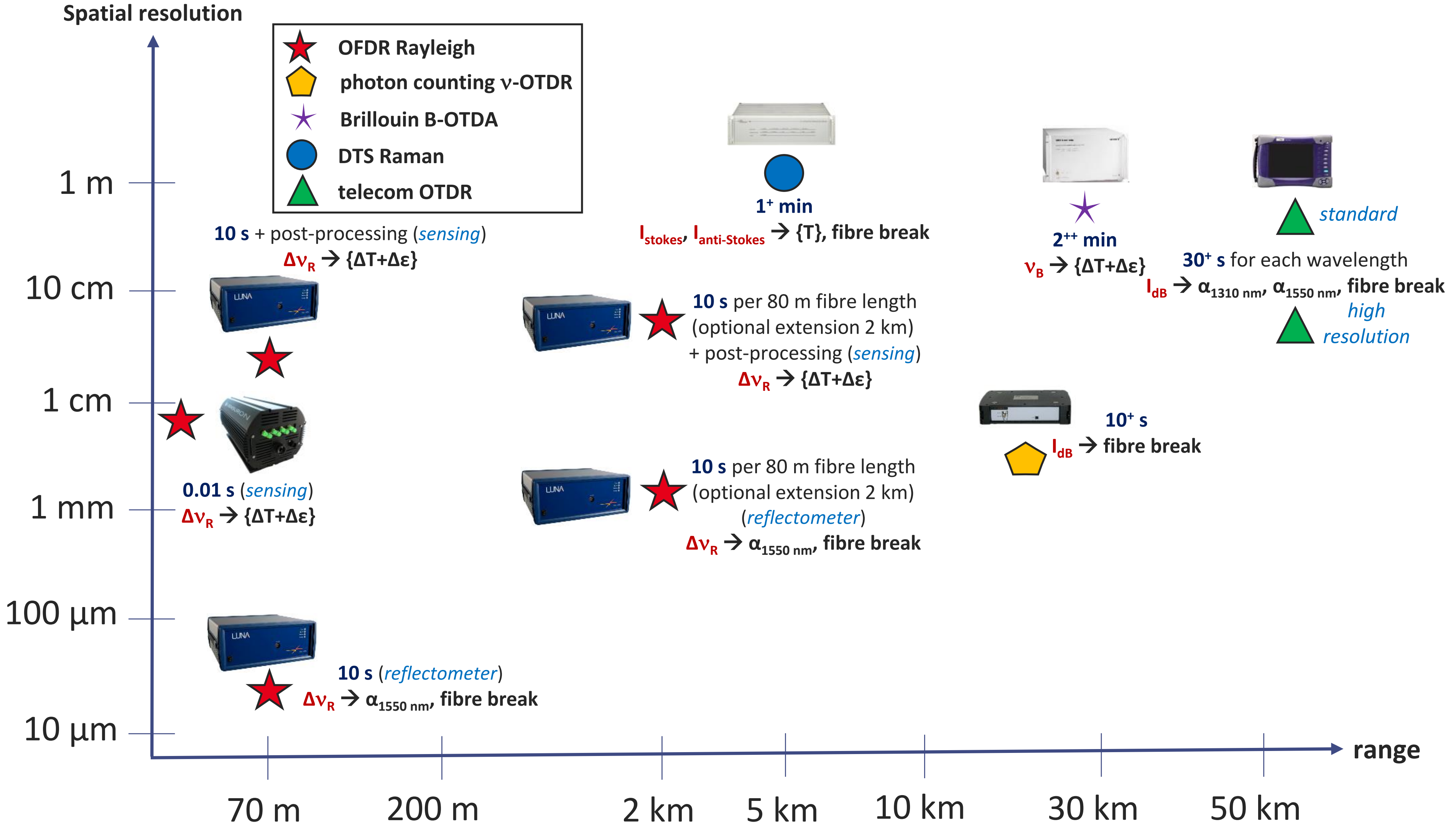

Optical Time-Domain Reflectometry (OTDR)

Time-resolved Rayleigh scattering (« optical radar »)

Time delay converted into distance

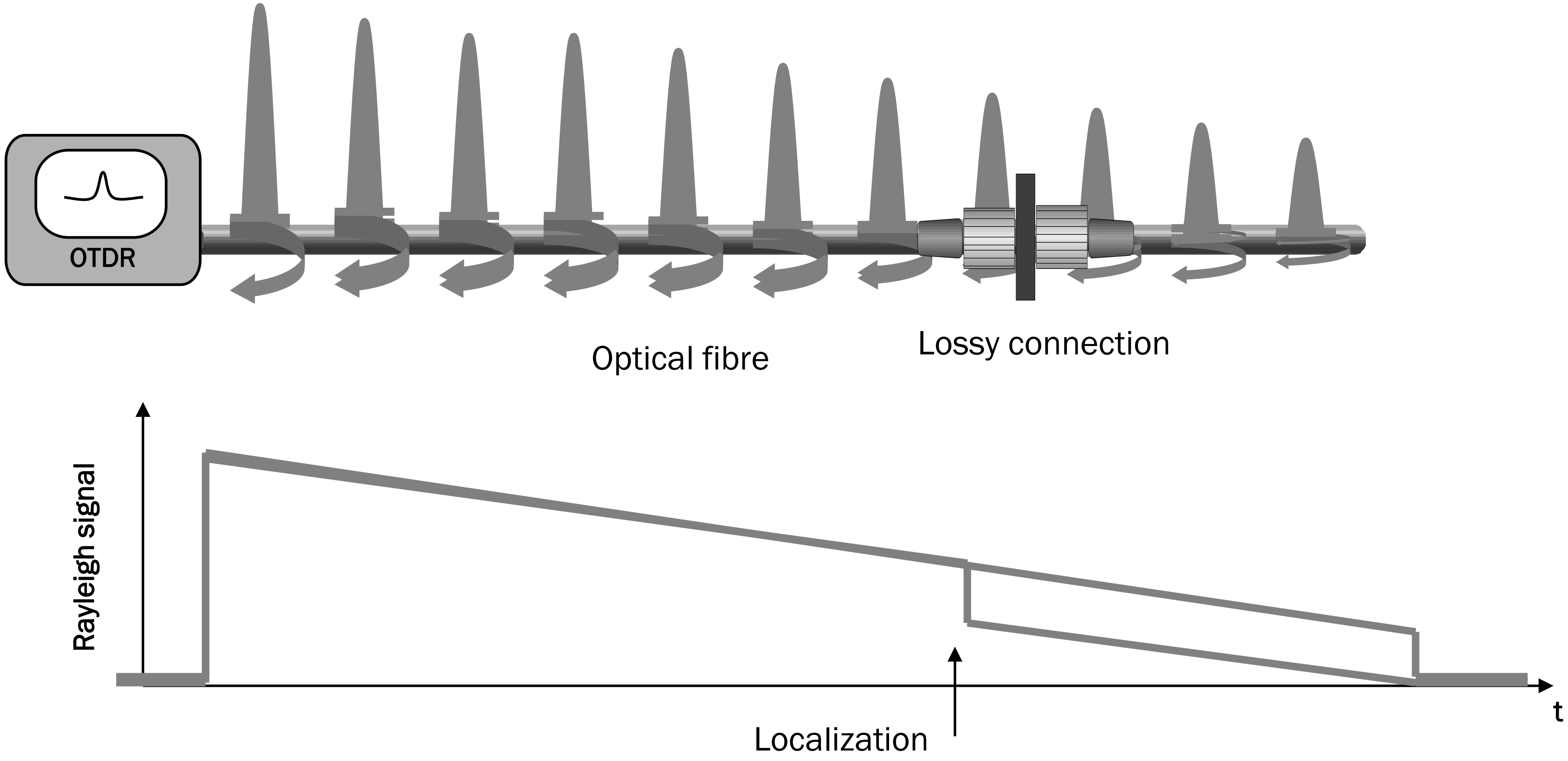

OTDR is heavily used in telecommunications

Main use : Fault detection and localization

Main wavelengths : 1550 nm, 1300 nmm, sometimes 850 nm or 1064 nm (YAG)

Commercial OTDR devices (*e.g.* JDSU™ MTS 6000)

Wavelengths : 1300 nm et 1550 nm

Measurement dynamic ~ 15 dB (@1550 nm),

Range ~ some tens km

Spatial resolution : meter (10-ns pulse width)

Scan rate ~ several minutes (range-dependent).

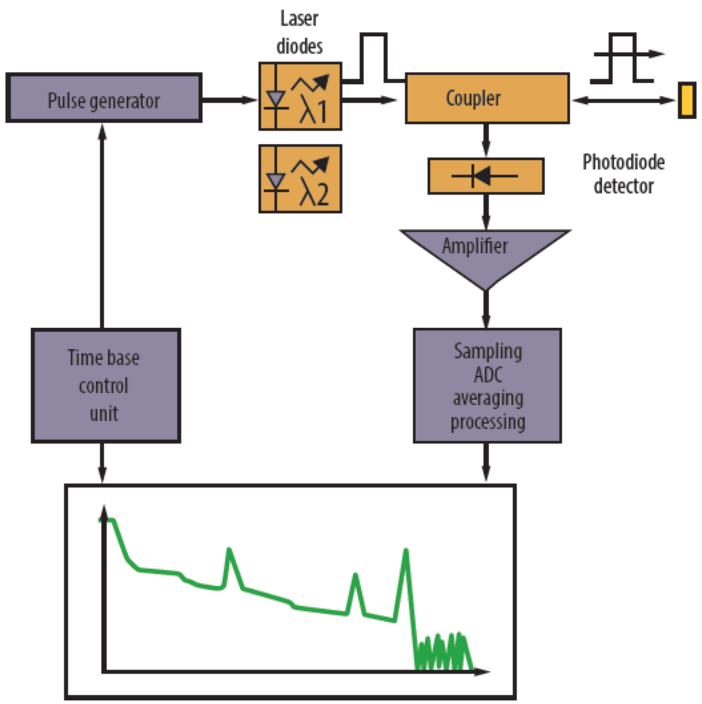

OTDR block diagram

Raman-OTDR

✦ **DTS (Distributed Temperature Sensor)**

- Collection of Rayleigh or Stokes AND AntiStokes backscattered light,
- AntiStokes light is temperature-dependent
- The temperature profile is obtained through the ratio of both AS/S or AS/R ratios

$$\frac{I_{anti-Stokes}}{I_{Stokes}} = \left(\frac{\nu_0 + \Delta\nu_{Raman}}{\nu_0 - \Delta\nu_{Raman}}\right)^4 \exp\left(-\frac{hc\Delta\nu_{Raman}}{k_B T}\right)$$

Typical perf: ✦ *Resolutions ~ 1 m , < 0,1 °C, scan rate ~ minutes.*
✦ *Range depends on fibre type and wavelength : from 5 km up to 30 km*

$$R(T) = \frac{I_{AS}}{I_S} = \left(\frac{\lambda_s}{\lambda_{as}}\right)^4 \cdot \exp\left(-\frac{hc\upsilon'}{kT}\right) \cdot \exp(-\Delta\alpha z)$$

(Raman scattering) *(Boltzmann)* *(DAF)*

(Temperature-dependent)

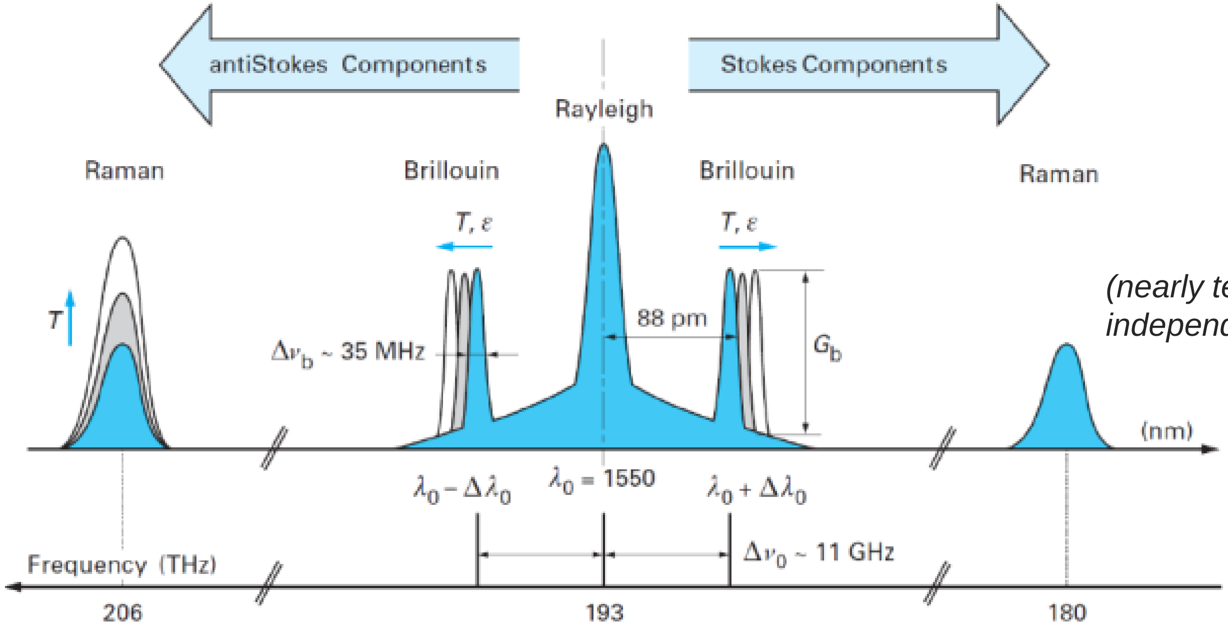

(nearly temperature-independent)

A.H. Hartog, A.P. Leach and M.P. Gold, Distributed temperature sensing in solid-core fibres, Electron. Lett., 21 (23), 1061-1062, 1985

Applications of Raman-DTS

Hot spot on HV lines

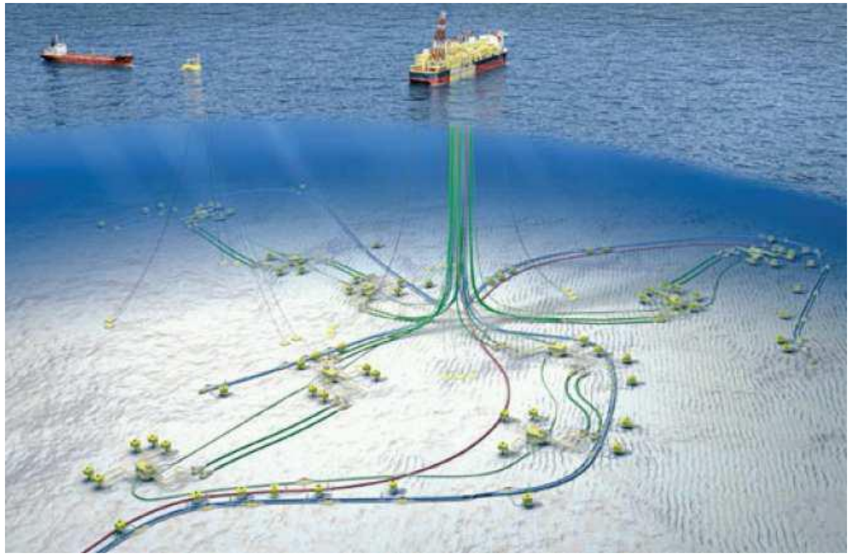

Oil & Gas (offshore, onshore)

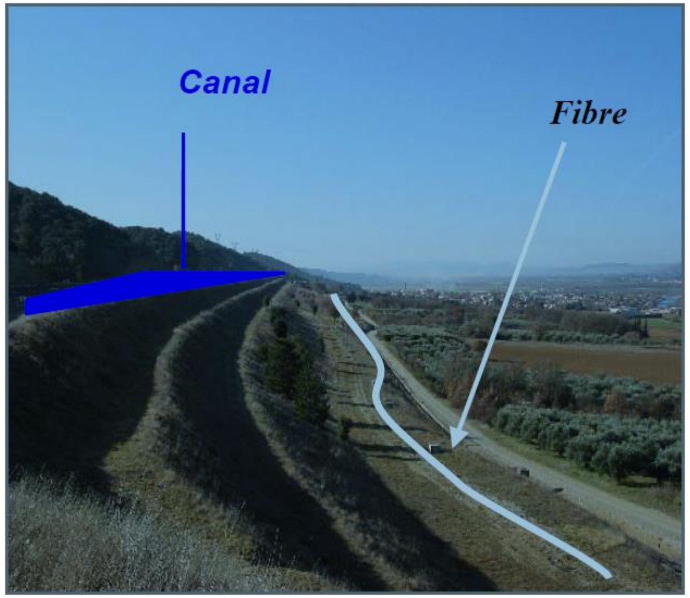

Leak detection

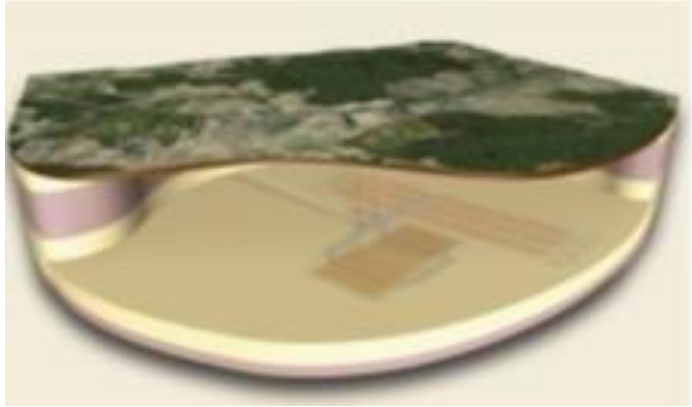

Underground storage monitoring

Brillouin-OTDA (1/2)

Mesure du décalage de la raie Brillouin
en fonction de la déformation ou de la température

Acquisition de profils de T° / déformations
(résolution spatiale métrique)

$$\Delta\nu_{Brillouin}(\varepsilon,T)=\frac{2.n_e(\varepsilon,T).V_a(\varepsilon,T)}{\lambda}$$

<u>Brillouin sensitivities:</u>

In strain: → 50 kHz/microstrain
(20 microstrain/MHz),

In temperature: → ~ 1 MHz/°C

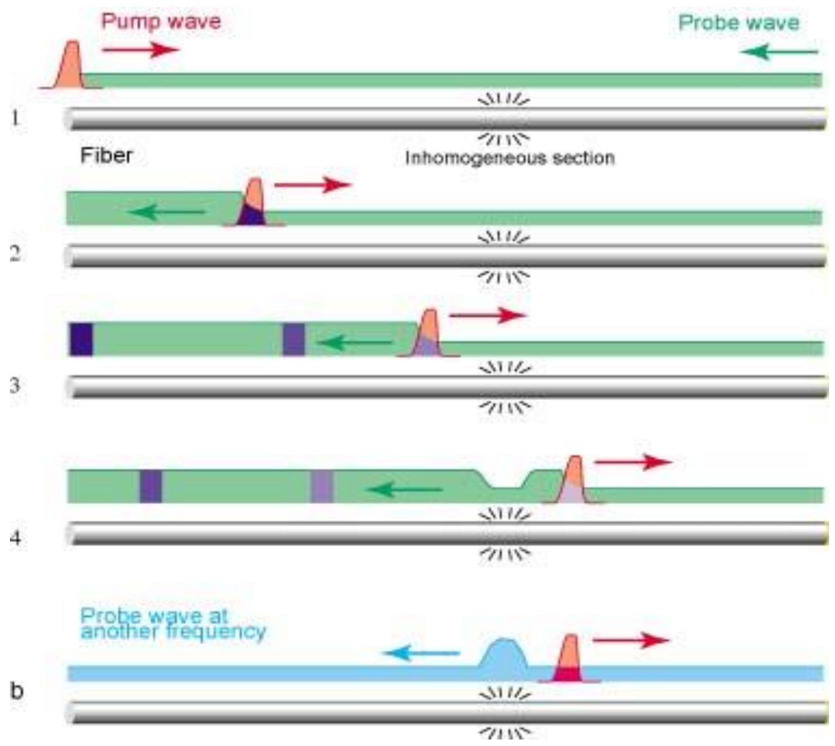

No amplification for this stretch (figure 4).
Amplification occurs at another Brillouin shift (b),
(depending on strain or temperature applied.)

(Picture from Omnisens)

M. Nikles, L. Thevenaz, P.A. Robert, Simple distributed fiber sensor based on Brillouin gain spectrum analysis, Opt. Lett., 21 (10), 1996, pp. 758-760

Brillouin-OTDA (2/2)

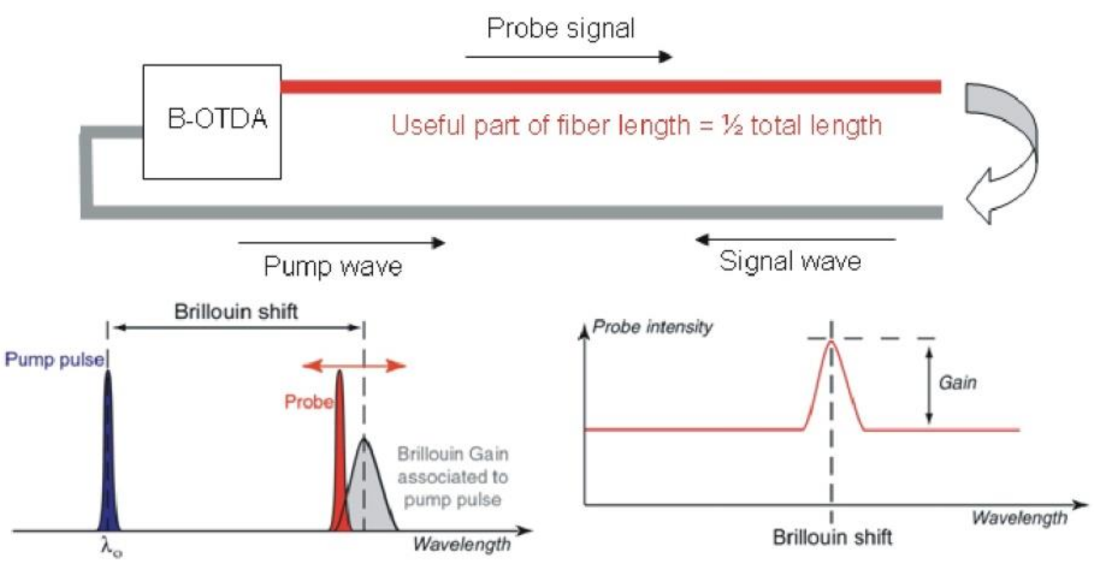

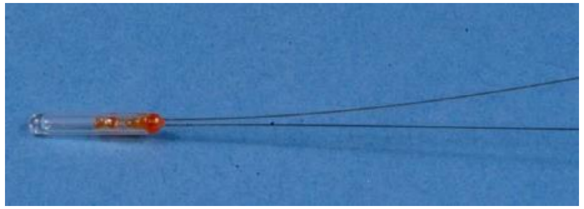

End loop (« optical U-turn »)

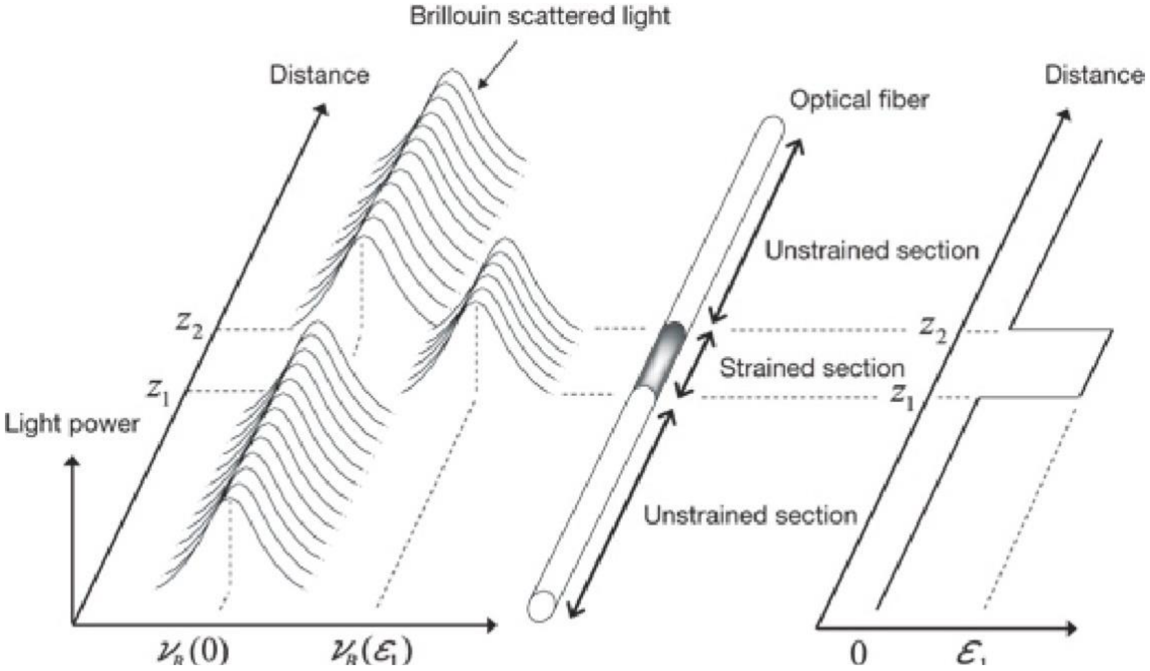

(picture from Advantest)

Stimulated Brillouin Scattering (SBS): 2 lasers are used

✓ Contra-propagative pump (CW),

✓ Co-propagative probe (pulsed),

→ B-OTDA devices **require end-loop.**

Acquisition protocol

1/ **Acquisition** of Brillouin traces at several $\Delta\nu_B$

2/ **Transposition** of Brillouin gain spectra/location table

BOTDA vs BOTDR

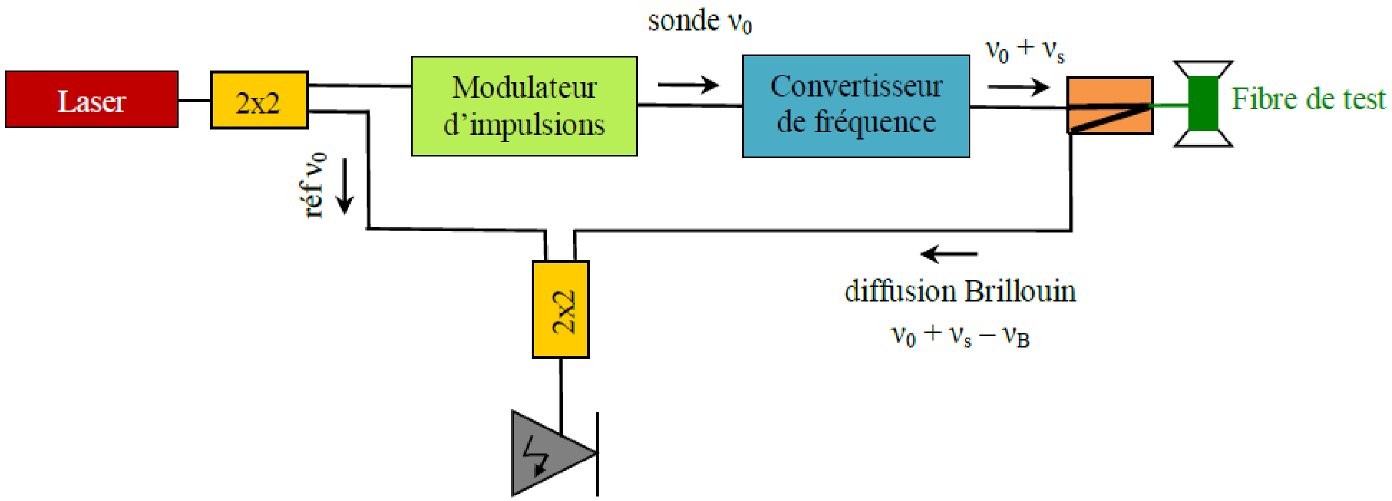

Brillouin B-OTDR
Spontaneous Brillouin Scattering

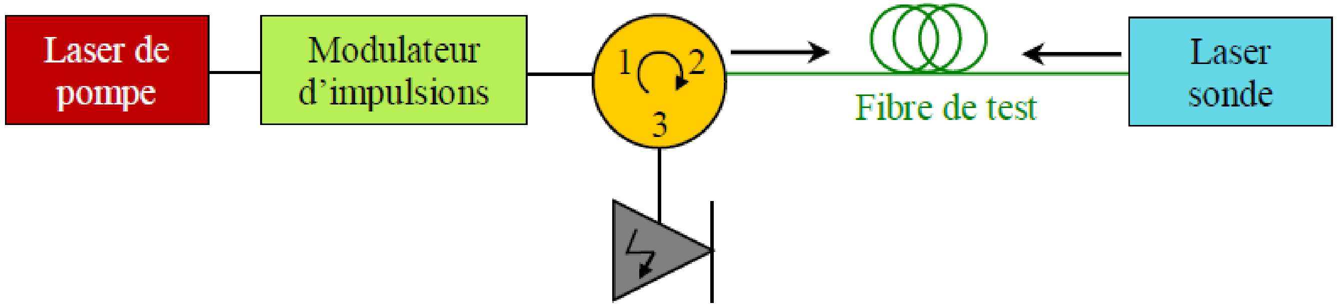

Brillouin B-OTDA
Stimulated Brillouin Scattering - SBS

Applications of BOTDA

Monitoring of ground pipelines

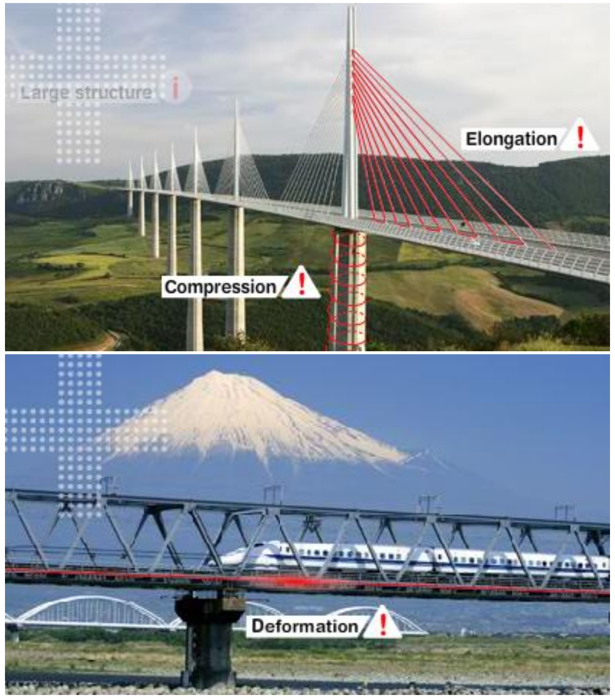

Civil engineering structures

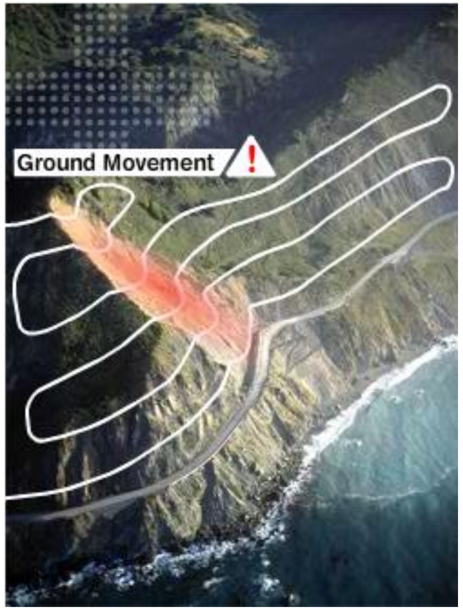

Monitoring of soil movement


Traction control during deployment, storage and during service life of telecommunication cables


Monitoring of high voltage lines

Level/leak monitoring


Process control of cable manufacturing

Rayleigh – OFDR (1/2)


Luna OBR 4600

- Signal = Rayleigh backscattering
- Highly coherent laser (200 kHz, L_c = 1,5 km), frequency-modulated : $\nu(t)= \nu_0 + \gamma.\Delta t$
- Interference between the reference signal and the frequency-shifted backscatted signal
- Both polarization states (TE, TM) are separated (PBS)
- For each polarization state, interferograms are recorded as a function of laser frequency (module = $\sqrt{|S|^2+|P|^2}$)
- Interferogram = TF of susceptibility distribution ($\Delta\varepsilon$)
- Susceptibility profile along the guide is then retrieved by inverse TF $\Psi(\beta) \sim \frac{\beta}{2i}\int_0^L \Delta\varepsilon(z)\cdot\exp(2i\beta z)\,dz$

- Distributed strain/T° measurement is done by intercorrelation along gaugelength (~ 5 mm to 20 mm).
- Frequency shift : $\Delta\nu$ (GHz) = - 0,151 x $\Delta\varepsilon$ (µm/m)

$$\Delta\varepsilon\left(z_0 + {}^{x}/_{2}\right) \sim \frac{i}{\beta}\int_{-\Delta\beta}^{\Delta\beta} \mathrm{I}(\beta-\beta_0)\cdot\exp(-i\beta x)\,d\beta \qquad \beta = \frac{2\pi n}{\lambda} \qquad \mathrm{I}(\beta) \sim |\Psi(\beta)|^2$$

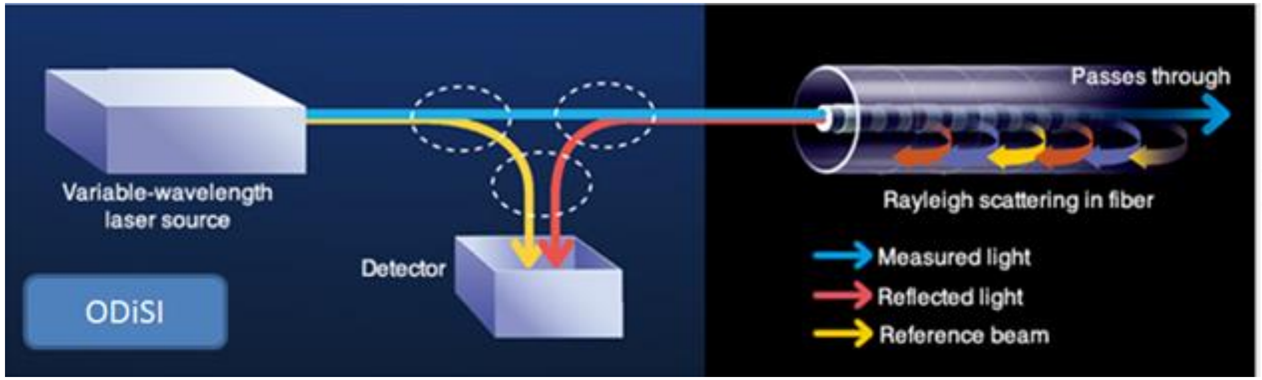

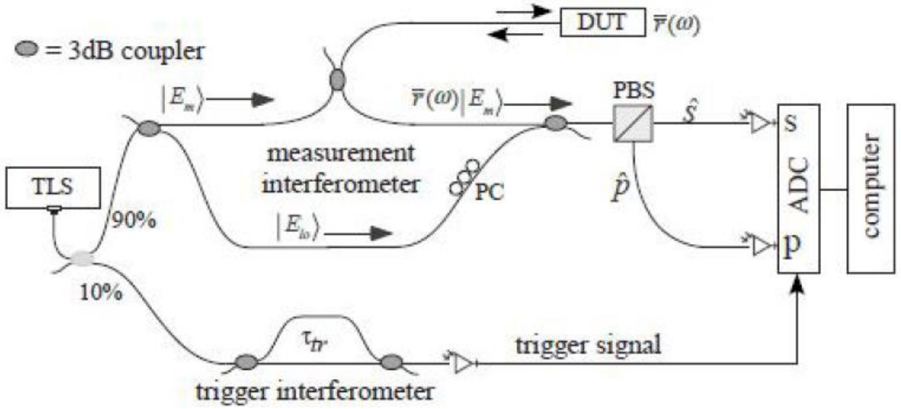

source : Luna™

Rayleigh – OFDR (2/2)

$$\Delta z = \frac{\lambda^2}{2n\Delta\lambda}$$ *(TF property)*

Δz ~ **10 µm** for $\Delta\lambda$ = 88 nm

N = number of data points (several millions)

$\Delta\lambda$ = wavelength range, typ. between 0.8 nm and 88 nm,

Δz = Spatial resolution (m), typically 10 µm up to 250 µm

L_{max} = Measurement range (m), ~ 70 m (extended version : 2 km)

γ = tunable rate (in GHz/s or nm/s), typ. 10 nm/s (2500 GHz/s) at 200 nm/s

Δt = scan time ~ several seconds

R = scan rate (MS/s) ~ typically **3.5 MS/s**

Dynamic > 70 dB (10^7)

$$\gamma = {}^{\delta\nu}/_{\delta t}$$

$$L_{max} = \mathrm{N}.\frac{\Delta z}{2} = \frac{N\lambda^2}{4n\Delta\lambda} = \frac{Nc}{4n\Delta\nu} = \frac{Nc}{4n}\cdot\frac{1}{\gamma\Delta t} = \frac{c}{4n\gamma}\cdot R$$

$$\mathrm{R} = {}^{N}/_{\Delta t}$$

Further reading

W. Eickhoff, R. Ulrich, Appl. Phys. Lett. 39 (9), 1981, p. 693

R.I. Mc Donald, Appl. Opt., 20 (10), 1981, p. 1840

U. Glombitza, E. Brinkmeyer, J. Lightwave Technol. 11 (8), 1993, p. 1377

M. Froggatt et al., Appl. Opt. 37 (10), 1998, p. 1735 and 1741

B.J. Soller et al., Opt. Exp. 13 (2), 2005, p. 666

A.K. Sang et al., IEEE Sensors J., 8 (7), 2008, p. 1375

Frequency-Modulated Continuous-Wave (FMCW)

Beat frequency f_b is proportional to distance L
→ frequency-to-distance conversion
Very commonly used in RADAR, LIDAR, etc …
First transposed to fiber sensing in 1985.

Sensors are demultiplexed in the spectral domain (Fourier-Transform)

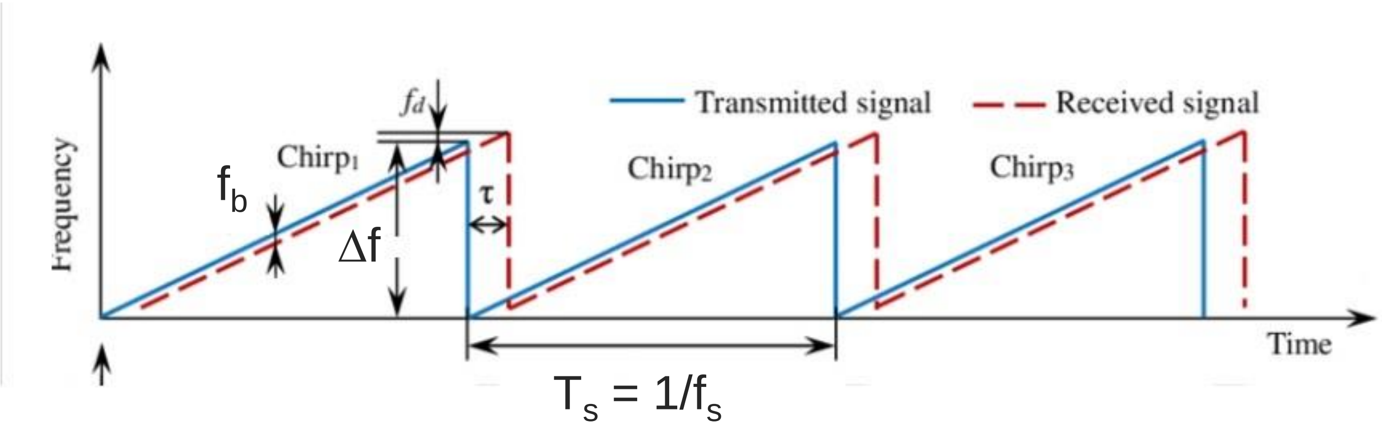

<u>Example</u>
Δf = 120 GHz (960 pm @ 1,55 µm)
f_s = 1 kHz
L = 13 m
→ f_b max = 15.6 MHz

$$f_b = \frac{2 \cdot n_{eff} \cdot L}{c} \cdot \gamma = \frac{2 \cdot n_{eff} \cdot L}{c} \cdot \underbrace{\Delta f \cdot f_s}_{\gamma \text{ = chirp (Hz/s)}}$$

Spatial resolution depends on frequency excursion Δf
(ΔL = 0.8 mm with above values)

$$\Delta L = \frac{c}{2 \cdot n_{eff} . \Delta f}$$

D. Uttam, B. Culshaw, Precision time domain reflectometry in optical fiber systems using a frequency modulated continuous wave ranging technique, *J. Lightwave Technol.* 3(5), 971-977, 1985

FMCW

Features

- Ruggedized
- 8 simultaneously monitored fiber optic sensing channels
- 2048 equally spaced sensors per fiber
- Software selectable spatial resolution down to 6.3mm.
- Real time strain and temperature measurements through FBGs
- Up to 100 Hz refresh rate
- Deflection sensing capability
- 3D shape sensing capability
- Immune to EMI/RFI and radiation for reliable operation in demanding environments.
- Networking capability via Ethernet

www.sensuron.com/rts125

CFG (*Continuous-Fiber Grating*)

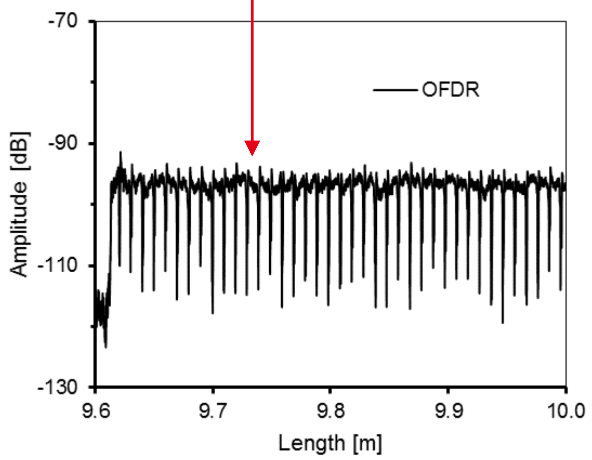

Reflectivity ~ 0,1 %
Same Bragg wavelength
Pitch ~ between 25.4 mm et 6.3 mm

Reflection spectra (500 DTGs)

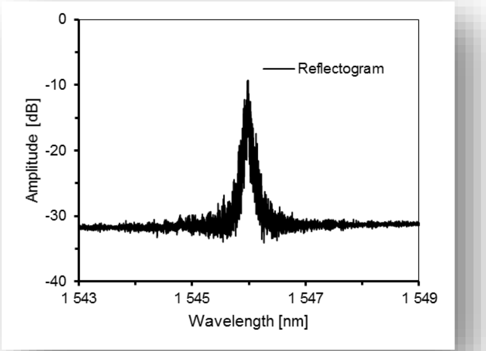

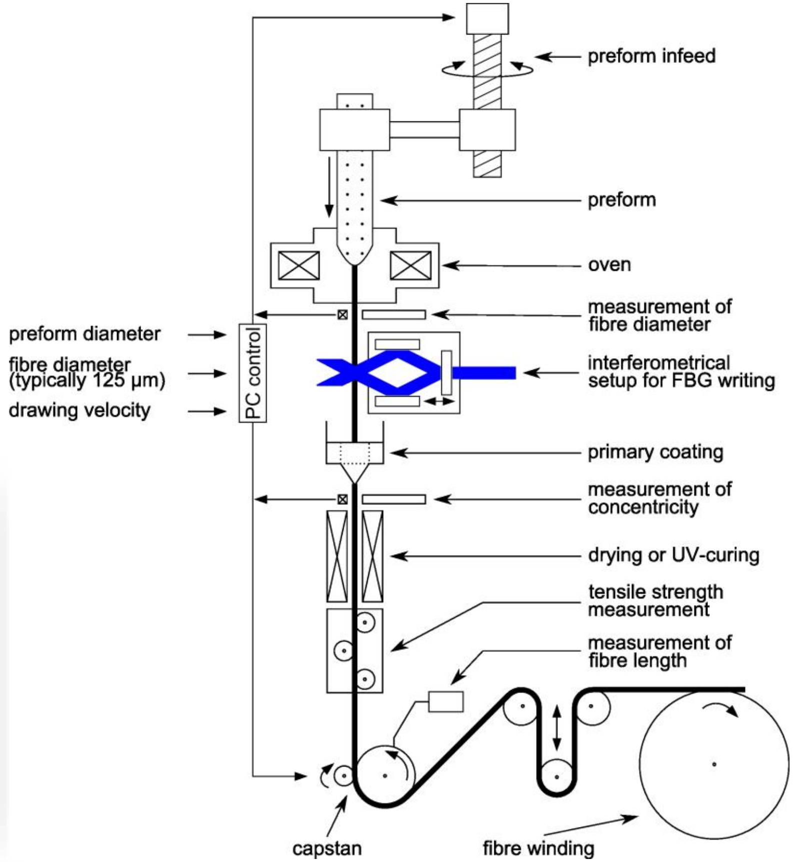

Leak detection/localization with the OFDR technique

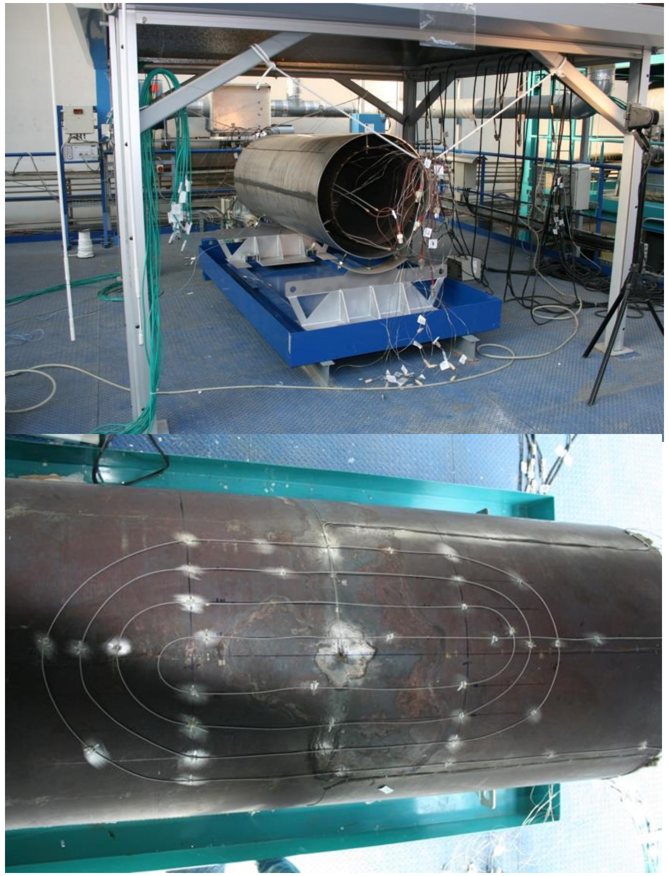

Installation FUTUNA (CEA/CAD)

- Sodium leak detected and localized as hot spot
- metal-coated silica fiber (gold or copper) wounded as spiral form onto the structure surface
- Metal packaging and point soldering.

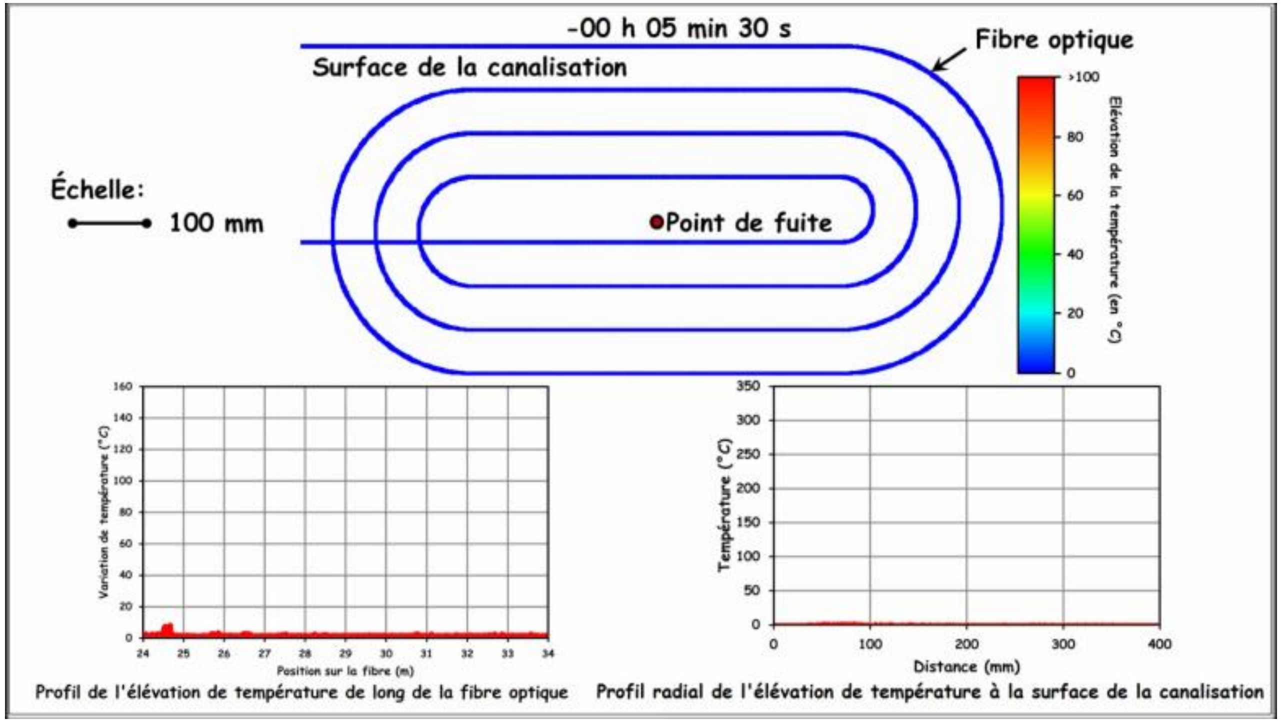

Sodium leak detection/localization onto the 2D surface

SHM of concrete structures with the OFDR technique

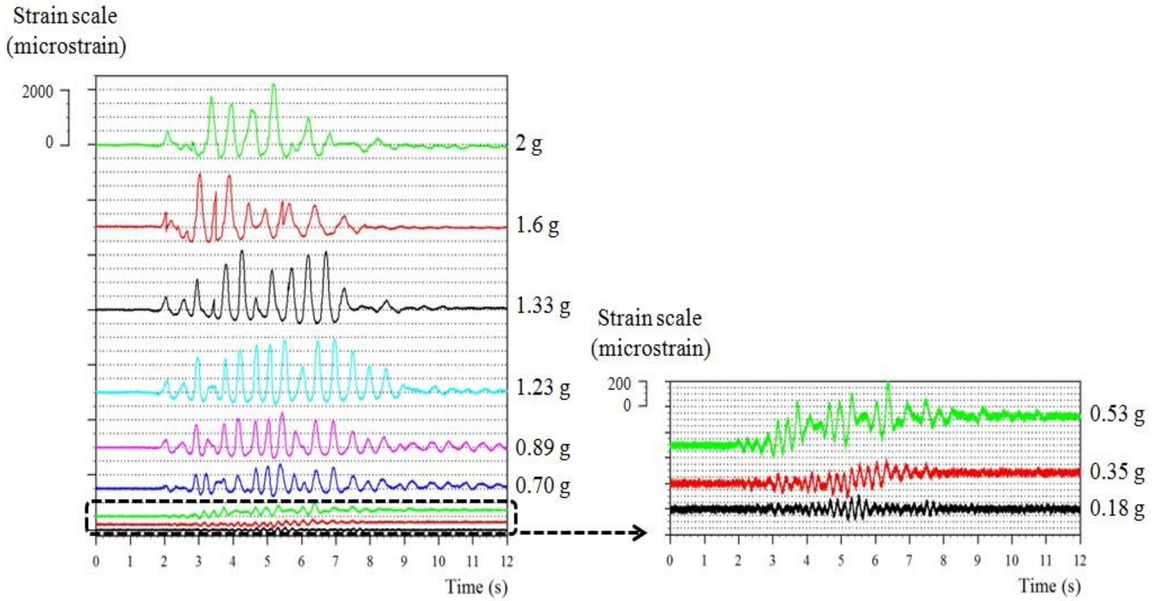

Wall center

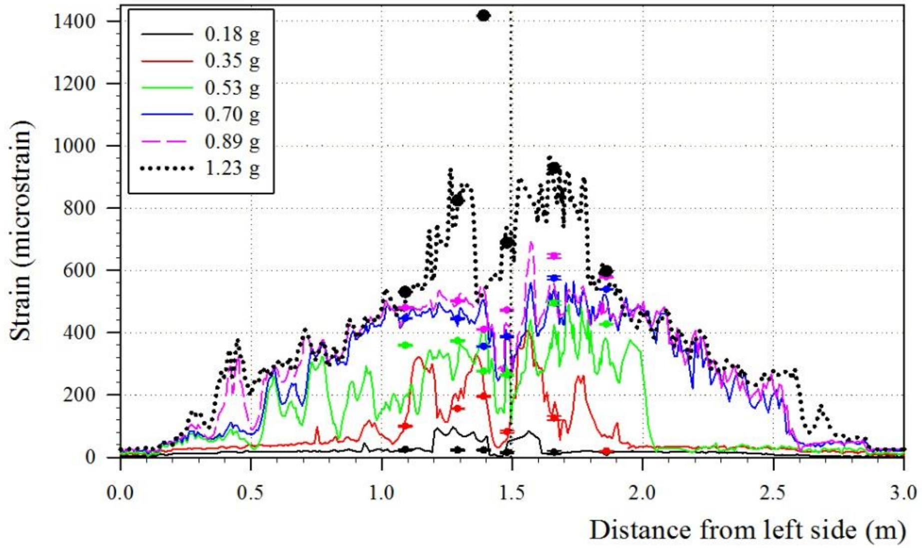

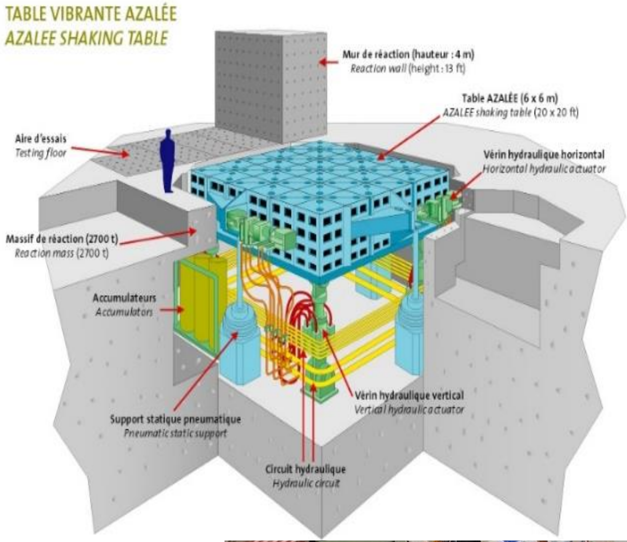

S. Magne *et al.*, IWSHM 2019

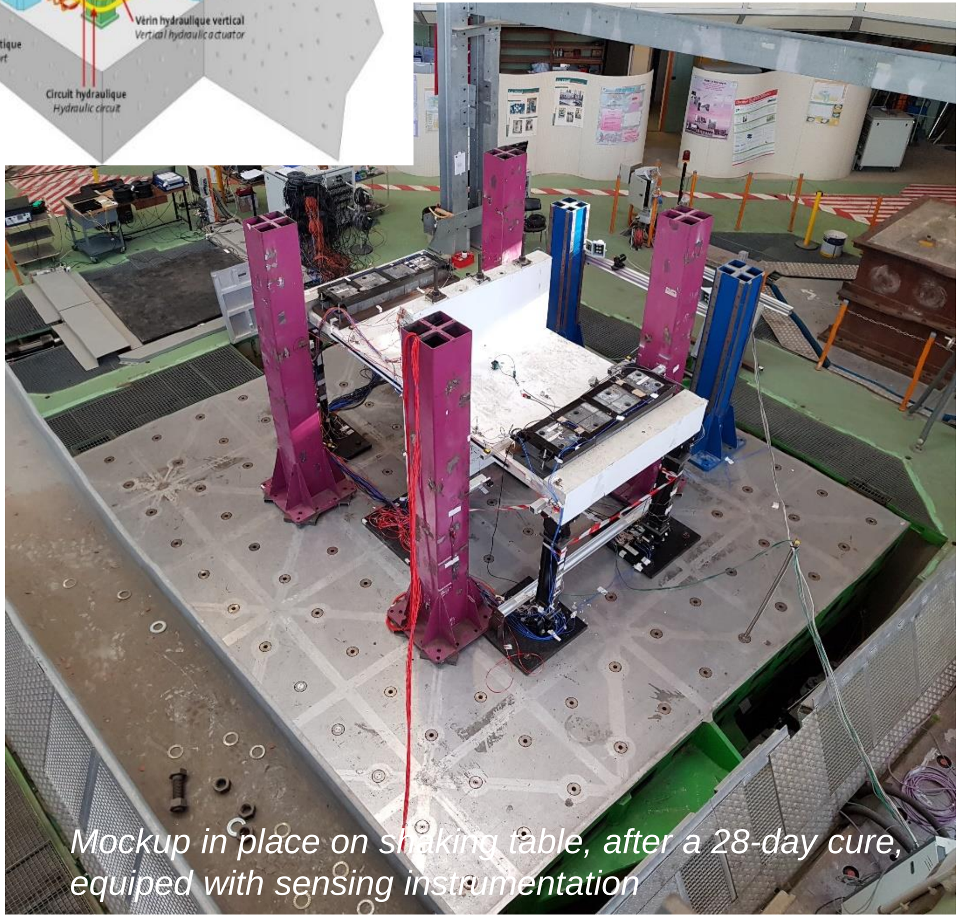

Mockup in place on shaking table, after a 28-day cure, equiped with sensing instrumentation

Corrosion detection/localization with the OFDR technique

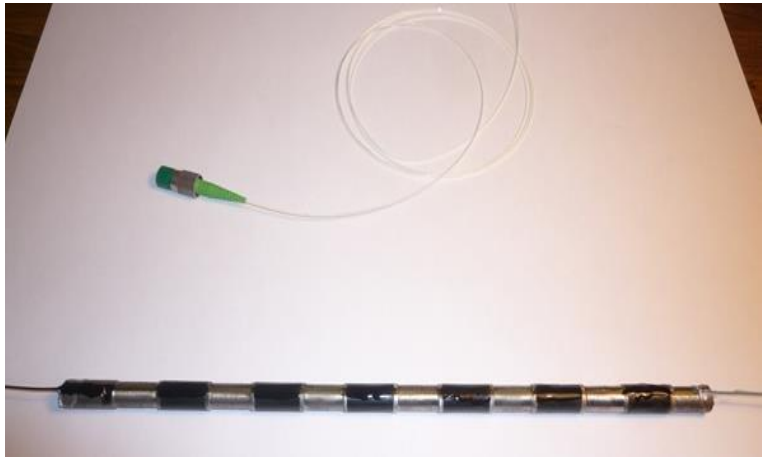

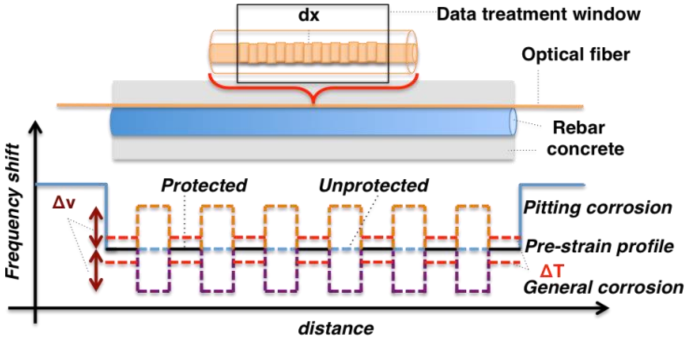

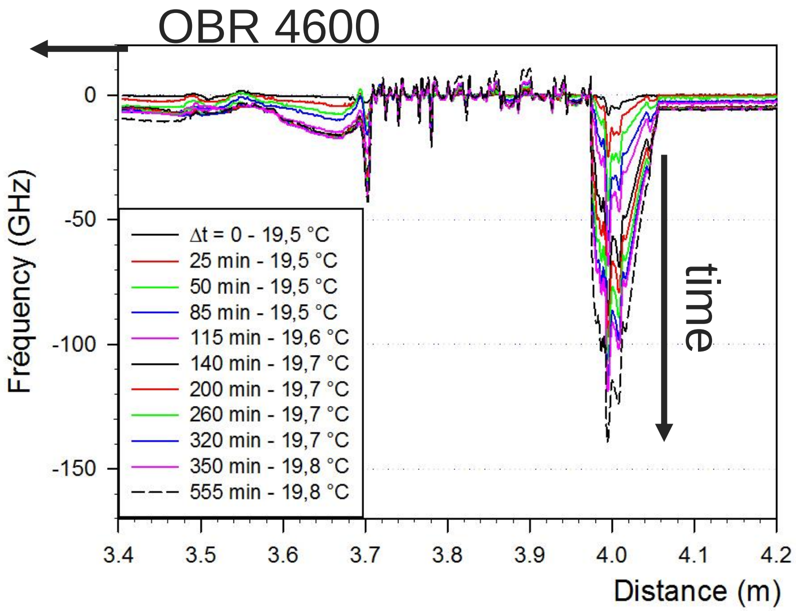

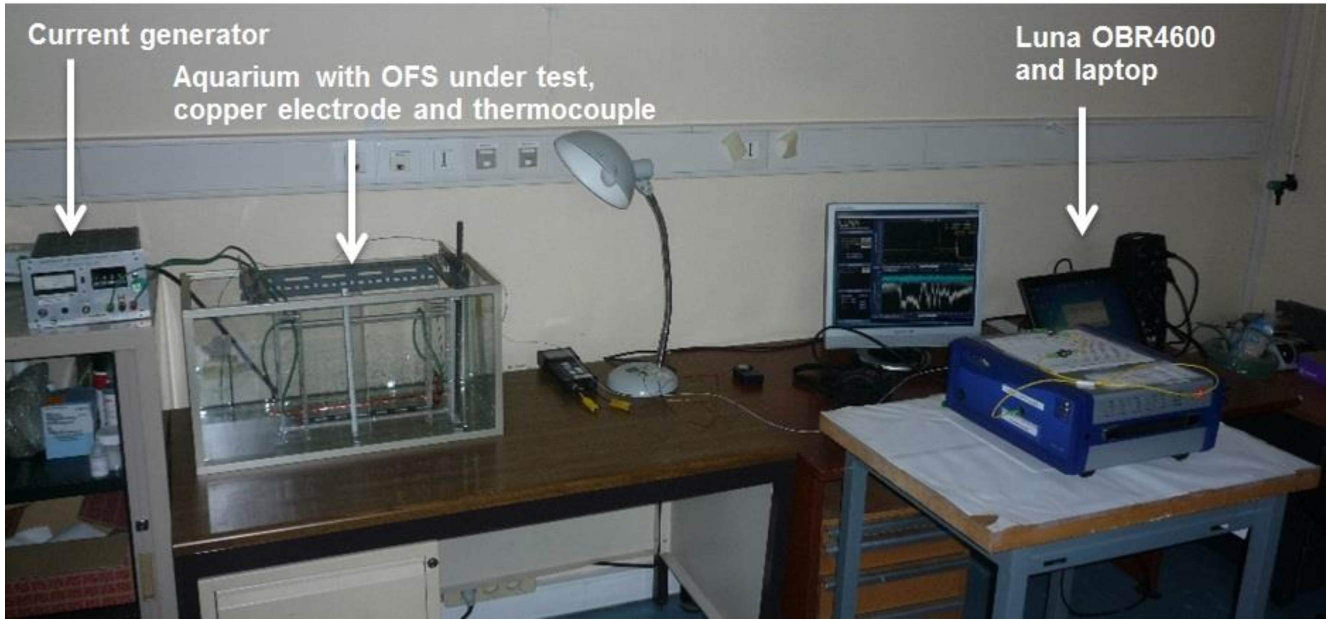

$$F_2(GHz) = -4.9.\sqrt{t(min) - 590\ min}$$

$$F(GHz) = -3.85.\sqrt{t(min) - 4900\ min}$$

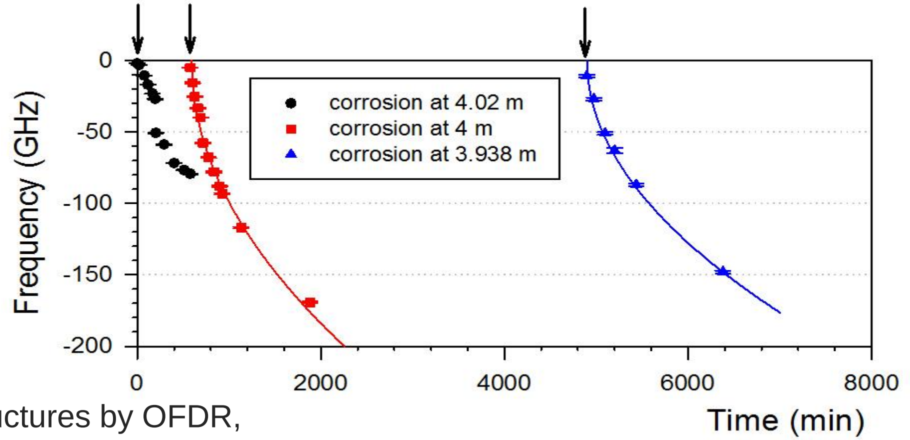

S. Magne, S. Ali-Alvarez, S. Rougeault,
Distributed corrosion detection and dedicated OFS based rebar within reinforced concrete structures by OFDR,
EWSHM 9, Manchester (UK), 2018

Sensing Specification	Quasi-distributed Fiber Bragg Grating	Distributed Rayleigh OTDR	Distributed Raman DTS	Distributed Brillouin BOTDR/A	Distributed Rayleigh OFDR
Spatial resolution	2 mm (Bragg length)	1 m (ν–OTDR: 1.3 cm)	1 m	50 cm (to 5 cm)	3 cm (OTDR mode: 2 mm)
Spatial Range (L)	up to ~ 10 km	50 km (ν–OTDR: 20 km)	30 km	30 km and more	70 m (N*80 m up to 2 km)
Measur^t. speed	DC-10 kHz up to GHz	10 sec. typ.	10 s to hours	2-3 s up to 10 min	10 s (L<70 m) + post process N*10 s (N=L/80m) + post pro.
Dynamic (budget)	> 20 dB	50 dB (ν–OTDR: 35 dB)	20 dB typ.	10 dB (loop 20 dB)	(OTDR mode: 70 dB)
Temp. resolution	0.01°C (0.1 pm resol.)	---	0.1°C @ 2 σ (1 h averaging)	1°C @ 2 σ (minutes averaging)	+/- 0.1°C
Temp. accuracy	0.1°C (with abs. ref.)	---	+/- 1°C	°C (with calibration)	5µm/m(<70m); 25µm/m(>70m)
Temp. range	1000°C *(limited by fiber specifications)*	---	- 200°C; 700°C *(fiber specif.)*	700°C *(fiber specif.)*	relative +/-175°C (L>70 m)
Strain resolution	0.1 µm/m (0.1 pm)	---	---	+/-10 µm/m (+/- 10^{-5})	+/- 1 µm/m (+/- 10^{-6})
Strain accuracy	---	---	---		< 10 µm/m (L < 70 m) +/- 25 µm/m (L > 70 m)
Strain range	1% to 4% on-line FBG	---	---	> 2% (20 000 µm/m)	+/- 0.425% (L < 70 m) +/- 0.13% (L > 70 m)

P. Ferdinand, EWSHM 2014, Nantes, France

Rayleigh – incoherent OFDR

→ *Not interferometry-based : SMF or MMF may be used*
→ *Amplitude modulation (fixed frequency) and lock-in detection*
→ *Fourier-Transfom of demultiplexed signals*
→ *Only applied to Raman-based temperature monitoring*

Advantages of IOFDR-Raman compared to OTDR-Raman (Conventional DTS)

✦ *Improved SNR (CW light instead of pulsed),*
✦ *Improved range : typ. 30 km, without amplifier*
✦ *No dead zone,*
✦ *Spatial resolution ~ 30 cm,*
✦ *Readout device insensitive to vibrations (onboard use).*

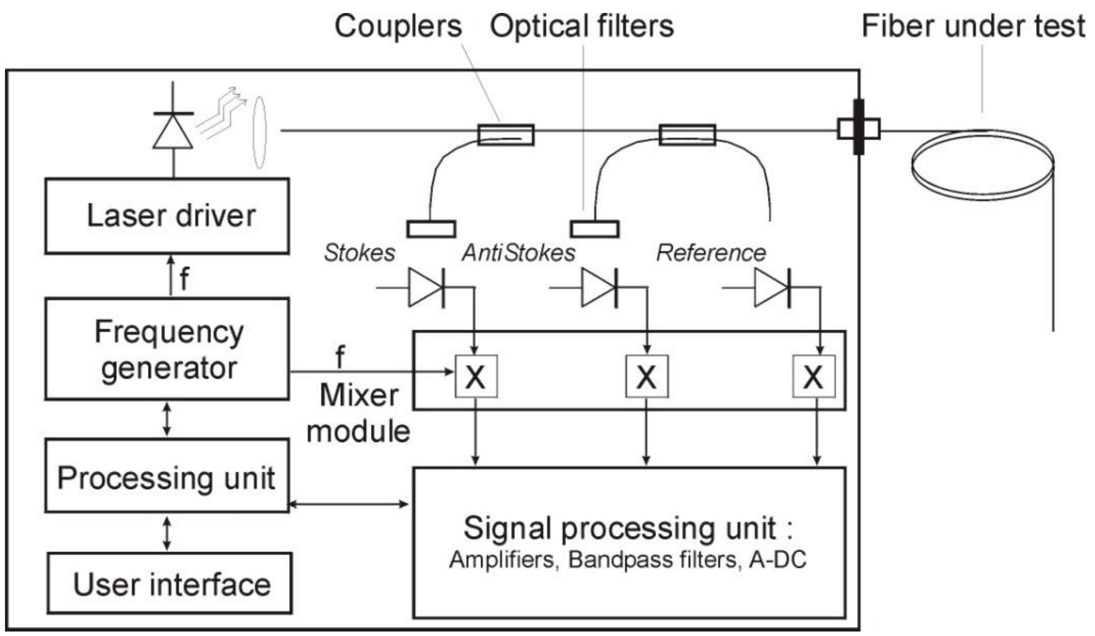

Incoherent OFDR-Raman design (LIOS "Well.Done DTS")

N.B. Also exists in Brillouin version (Fibristerre)

E. Karamehmedovic, Fiber Optic DTS using incoherent OFDR, SPIE 5363, 2004

Distributed Acoustic Sensing (DAS)

Principle

Coherent Rayleigh Noise (CRN) in high coherence OTDR

→ Highly undesirable in OTDR *(low coherence sources are prefered ..)*

→ Highly interesting for DAS *(high coherence lasers (1 km – Lc) are advocated : e.g. DFB laser)*

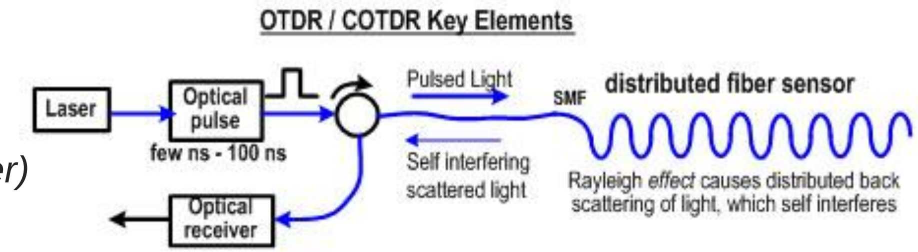

- Several schemes are proposed :
  - Heterodyne (2-pulse COTDR),
  - Single pulse (*actually the most used one*),
  - FMCW, etc.
- Two detection processes:
  - DASI (optical-**I**ntensity-based) : OTDR trace, non-linear
  - DASP (optical-**P**hase-based) : interferométry, linear but more complex.
- DAS with or without FBG,
- DAS with or without « Enhanced Rayleigh ».

Improved SNR

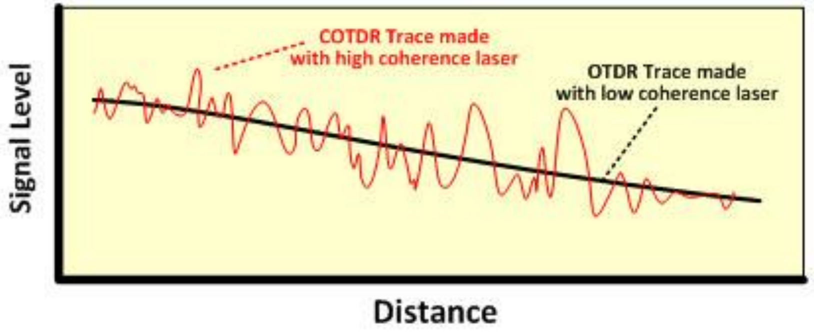

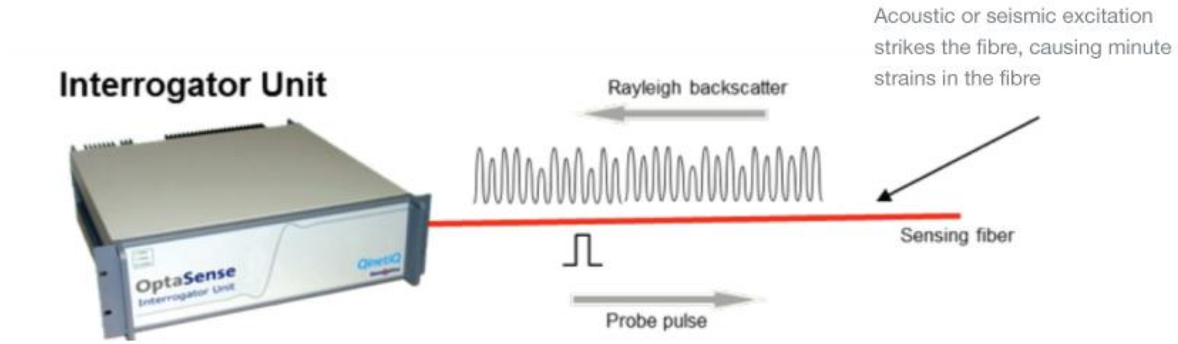

Z. He, optical fiber DAS : a review, J. Lightwave Technol. 39 (12), 2021, pp. 3671-3686

B. Gorshkov et al., Scientific ,applicationbs of DAS : state-of-the-art review and perspective, Sensors MDPI, 22, 2022, pp. 1033

Distributed Acoustic Sensing (DAS)

Performance and limitations

Typical parameters of Rayleigh-based DAS

- Spatial resolution ~ 1-10 m (some demonstrations as low as 10 cm),
- Phase sensitivity ~ mrad/rac(Hz),
- Range (typical) : 10 m – 50 km,
- Acoustic bandpass [20 Hz, 20 kHz] (*a minima*), may reach 500 kHz (DVS : Distributed Vibration Sensing).

Rayleigh-based DAS limitations

- Spatial resolution,
- High directivity : along fiber axis,
- Acoustic sensitivity trades with spatial resolution and range (*distributed monitoring*),
- Fibre birefringence requires *polarization-diversity receiver*,
- Laser phase noise has a major impact over SNR
- Laser pulse power limited by nonlinear effects (XPM, 4WM, SBS, etc.),
- Heavy computational power required (high data flow) : Compressed sensing ?

Applications/Markets

- Oil & gas,
- Process control,
- Perimeter security (border/harbour control)
- Geophysics,
- Structural Health Monitoring.

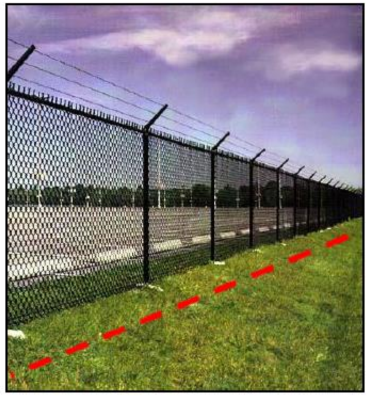

(Inventec)

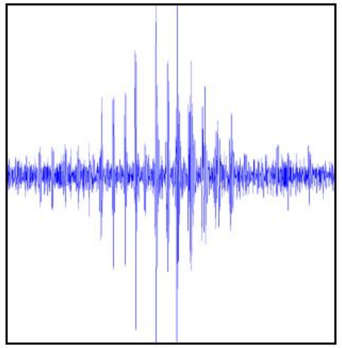

Footstep audio wave form

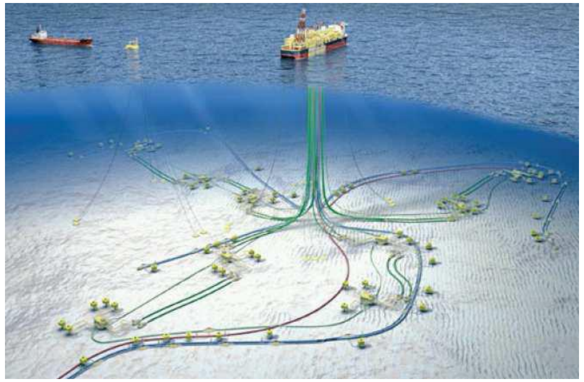

(Technip)

SUMMARY

- CEA as a glance
- LIST/DIN/SMCD/LSPM
- Optical fibers : basics
- Optical fibers for telecommunications
- Optical fibers for sensing in harsh environments
- Point sensing : White-Light Interferometry (WLI)
- Quasi-distributed sensing : Fiber Bragg Gratings (FBGs)
- Truly distributed sensing : OTDR DTS, BOTDR/BOTDA, OFDR, FMCW, DAS
- **MSCA USES2 DC02 : OPTICAL TIME STRETCH (OTS)**

MSCA USES DC02 – State of the art in OTS

HIGH CAPACITY : 2014 FBGs/fibre
C-band, pulse 2 ns, 22 km DCF (2.7 ns/nm),
PRF = 20 kHz,
High-speed APD (0.25 GHz) and oscilloscope (2.5 GHz)

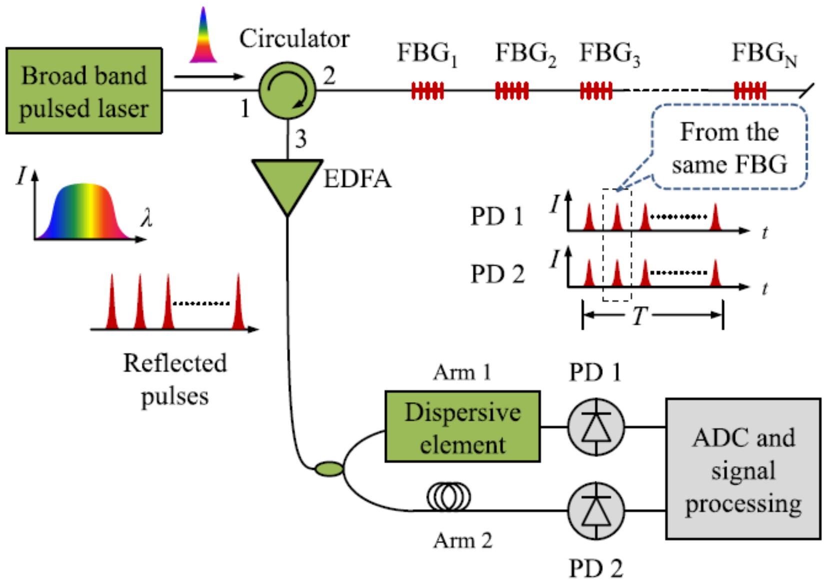

L. Ma *et al., High speed distributed sensing based on ultra weak FBGs and chromatic dispersion,* IEEE Phot. Tech. Lett., 28 (12), 2016, pp. 1344-1347
[Virginia Polytechnic Institute and State Univ. (USA)]

Distributed monitoring along CFBG length
(« *Interferometric Temporal Spectroscopy* »)
Distribution of the Free-Spectral Range (FSR) along the CFBG length (Inverse Fourier-Transform).

C-band, pulse 0.8 ps, D ~ 1.4 ns/nm
PRF = 50 MHz,
High-speed PhD (53 GHz) and oscilloscope (20 GHz)
CFBG ~ 2.5 cm, FWHM ~ 7 nm

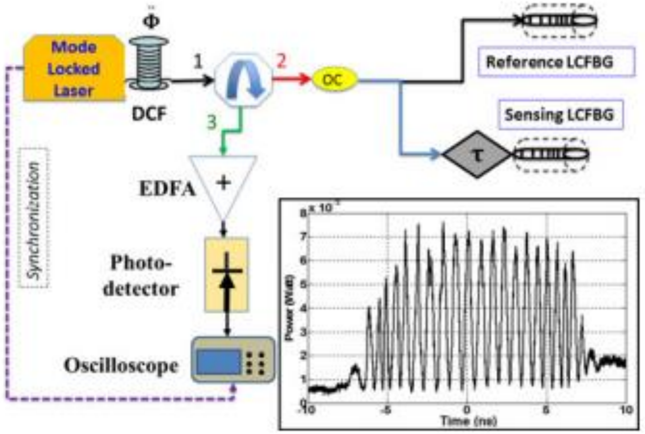

E.J. Ahmad *et al.,* High temporal and spatial resolution distributed FBG sensors using time-stretch frequency-domain reflectometry, J. Lightwave Technol., 35 (16), 2017, pp. 3289-3295
[Kent & Aston Universities, UK]

MSCA USES DC02 - Rationale

Limitation of state-of-the-art for SHM purposes

FBG sensing for SHM purposes : mainly based upon WDM or OFDR approaches.
WDM : High scan rates (> 10 MHz, up to GHz) but limited capacity (~ several sensors/fibre),
OFDR : Low scan rates (typ. some tens Hz, max. 100 Hz) but high capacity (several thousands sensors/fibre).

Problem : Tomographic reconstructions simultaneously require **high scan rates** (MHz) and **high capacity** (typ. tens to hundreds of sensors/fibre).
Time-Division Multiplexing (TDM) associated with Wavelength-to-Time Mapping (WTM) may solve the issue.

Optical Time Stretch (OTS) technique uses highly dispersive media providing WTM of pulse Bragg signals.

→ **Optical Time-Stretch (OTS) provides both high scan rates and high capacity**.

Challenges for SHM applications

- **Improve strain resolution (µstrain or < µstrain)** → **Increase dispersion,**
- **High-bandwidth HDO are economically prohibitive** → **New time measuring techniques** *(under investigation)*

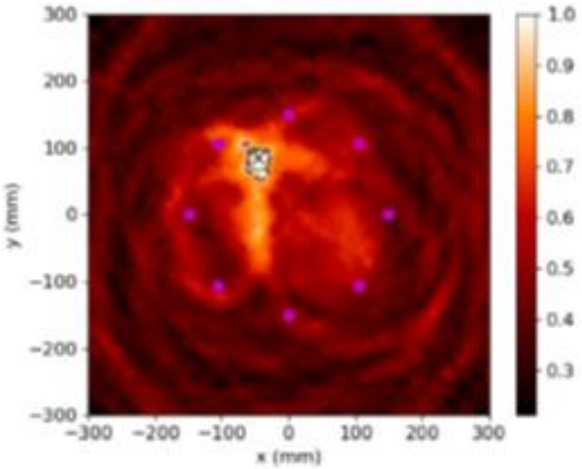

Example of 2D tomographic reconstruction (cross-correlation of ambient noise) with FBG US transducers:
A. Recoquillay, T. Druet, S. Nehr, M. Horpin, O. Mesnil, B. Chapuis, G. Laffont, O. D'Almeida,
Guided-wave imaging of composite plates using passive acquisitions by FBG,
J. Acoust. Soc. Am. 147, 2020, pp. 3565-3574

Thank you for your attention

Any questions ?